PROPERTIES OF AND FACTORS INFLUENCING INFILTRATION RATES AT A RECLAIMED LIGNITE MINE, FREESTONE COUNTY, TEXAS

by

Karen E. Jarocki, B.S.

Thesis

Presented to the Faculty of the Graduate School
of the University of Texas at Austin
in Partial Fulfillment
of the Requirements
for the Degree of

Master Of Arts
The University Of Texas At Austin
December 1994

PROPERTIES OF AND FACTORS INFLUENCING INFILTRATION RATES AT A RECLAIMED LIGNITE MINE, FREESTONE COUNTY, TEXAS

Approved by

Supervising Committee:

Supervisor: 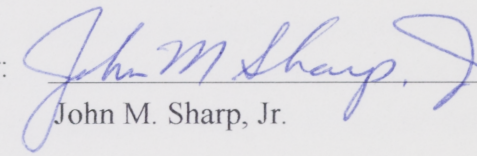

John M. Sharp, Jr.

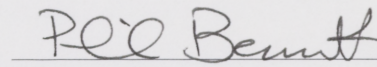

Philip C. Bennett

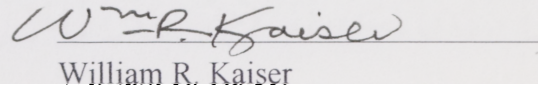

William R. Kaiser

To my husband John for all your help,
support, and love throughout this endeavor.
To my parents for your love and support
throughout the years.

Acknowledgments

There are a great many people who deserve thanks for their help with this project and their support of me. This research was made possible through the generous financial support of the Texas Utilities Environmental Research Program. I am particularly grateful to Dick White for his encouragement throughout this project. Thanks also to Sharon Everett for always being available to answer questions and help solve problems when they occurred.

The staff at the Big Brown Mine was very supportive of my work there. Dave Morris, Jerry Richards, and Richard Hart provided information about the mine and were always glad to provide me with equipment when needed. Thanks also to Zella and Sherry at the Big Brown Research Center for making sure I had everything I needed for my stays there. Steve Barton and Craig Jackson served as field assistants during the summer. Both proved invaluable in installing equipment and never complained about all the holes I made them dig.

Dr. Jack Sharp supervised this thesis and provided both insight and encouragement for this project. I am grateful to Dr. Phil Bennett for his help in working out the best method for tracer experiments and his comments on this thesis. Dr. Bill Kaiser served as a reader for this thesis providing me with a critical review of the project.

Special thanks go to Joyce Best, Kimberly Kurtz, and Scott Schroder in the Geology Foundation office. Joyce and Kimberly managed the finances for the grant, always making sure I was paid on time. Scott was instrumental in ordering equipment at the last minute. Thanks also to Betty Kurtz for her help in arranging transportation to the field.

A final thank you to my husband, friends, and parents. You, most of all made this work, without your help, love, and support this would have been very difficult. Becky Smith served as student editor for this thesis. Carlotta Chernoff provided help late into the night and was always willing to talk over problems scientific in nature in addition to other numerous subjects. Thanks to my parents for instilling in me my ambitious nature and thank you John, for everything. You made a great field assistant.

Abstract

PROPERTIES OF AND FACTORS INFLUENCING INFILTRATION RATES AT A RECLAIMED LIGNITE MINE, FREESTONE COUNTY, TEXAS

by

Karen E. Jarocki, M.A.

The University of Texas at Austin, 1994

Supervisor: John M. Sharp, Jr.

Over the last 30 years, lignite has become an important energy resource for the State of Texas. Production of lignite involves strip mining large areas of land in the Texas Gulf Coast region. Lignite at the Big Brown Mine, Freestone County, Texas, is produced from fluvial-deltaic sediments of the Calvert Bluff Formation of the Paleocene-Eocene Wilcox Group. Mining processes mix overburden material resulting in a spoil that is more homogeneous than the original unmined material over the area of the mine. The effects of mining on the environment are wide and varied, but mining is especially disruptive to the groundwater system. Groundwater recovery begins immediately after the spoil is placed, but occurs at highly variable rates. Hydrogeologic properties change rapidly in the first few years after mining and much of the groundwater recovery is dependent on the infiltration capacity of the spoil material. Resaturation of shallow spoil aquifers at the Big Brown Mine occurs at rates ranging from 0.6 to 3.0 m/yr (2-10 ft/yr). Recharge to the groundwater system is principally from direct infiltration of precipitation with variable resaturation rates attributed to variations in infiltration.

For this study, four sites at the Big Brown mine were chosen for characterization. Three sites, designated fields C-13, C-24 and C-32, are located in reclaimed areas of the mine and range in age from 9 to 14 years old, while the

fourth site is located in an unmined area (UM) between the two active mining pits. Infiltration rates were quantified using a drip infiltrometer to simulate rainfall. Results show that mining and reclamation processes can reduce infiltration rates by as much as 53 percent from the unmined values. Unmined areas show infiltration rates ranging from 12 to 30 cm/hr (4.7-11.8 in/hr) with a mean value of 20 cm/hr (7.9 in/hr). Mined areas show infiltration rates ranging from 3 to 22 cm/hr (1.2-8.7 in/hr) with a mean value of 9 cm/hr (3.5 in/hr). These rates vary significantly over the area of a single field resulting in high standard deviations, but a comparison of mean infiltration rates between the three mined areas show much less variation. It is unlikely that the small variations seen in the infiltration rates of fields C-13 and C-24 can, by themselves, account for the large variations in resaturation rates for these fields.

Infiltration rates vary in response to changes in soil moisture content, spoil heterogeneity, soil mineralogy, and method of spoil placement. Higher values of infiltration occur when the soils are dry, generally from late spring to early fall. Differences in soil texture had less effect on infiltration rates than was hypothesized, with both coarse and fine grained soils showing similar values.

Tracer tests, using sodium bromide as a conservative tracer and the red dye Rhodamine WT, were performed to determine if channeling of water occurs in the reclaimed soils. Trenches, cut in the dyed areas, were inspected for fractures and macropores and sampled at regular intervals for analysis of bromide concentration. Rhodamine WT showed some fractures in the soil structure, but due to a chemical reaction, sorbed strongly to the soil surface with little movement into the soil column. Concentration plots of bromide proved much more useful in determining mechanisms of flow and showed good vertical flow paths in fields C-13 and C-32. Lateral flow dominates in field C-24. Differences in flow mechanisms may best account for the variable resaturation rates seen in these fields.

Table of Contents

List of Tables

List of Figures

Introduction

Over the last 30 years, lignite has become an important source of energy due, in part, to the rising cost and availability of natural gas. Texas is the leading producer of lignite in the United States, with an estimated production of 51 million metric tons (56 million short tons) in 1993 (Railroad Commission of Texas, personal communication). Near surface lignite resources are estimated at 19.2 billion metric tons (21.1 billion short tons) for the state (Kaiser, *et al*, 1980). Near surface lignite is defined as lignite seams 0.9 m (3 ft) or greater in thickness and located under less than 61 m (200 feet) of overburden. These resources are often utilized on site at mine-mouth electric generating plants.

In East Texas, strip mining is used to recover lignite, which greatly disturbs nearby shallow aquifers. Mining of deeper seams requires aquifers to be dewatered and depressured for mining to proceed. During mining overburden sands and muds are mixed randomly creating a chaotic texture, resulting in a spoil material that is considered homogeneous over the area of the mine, but highly heterogeneous on the scale of a few meters (tens of feet).

Near-surface lignite mining at the Big Brown Mine in Freestone County, Texas significantly affects shallow unconfined aquifers. This mine has been the site of study for over a decade of research involving the effects of mining and reclamation on these shallow aquifers. When the disturbed land is reclaimed, the mine spoil is replaced to reflect the pre-mine topographic relief. This presumably helps reestablish pre-mine groundwater flow systems. Groundwater recovery begins immediately, but at highly variable rates. As aquifer resaturation continues, hydrogeologic properties of the spoil become increasingly significant. The mining process alters the pre-mine groundwater system and different methods of spoil placement during mining likely have different effects on the recovery of shallow aquifer systems.

The ultimate goal of reclamation at a mine site is to restore the land to its previous productivity. One of the most important aspects of this land restoration is the groundwater system. It is often the controlling factor in the return of

vegetation and wildlife to an area. Studies in other reclaimed strip mines indicate that the hydrogeologic character and response of disturbed land is controlled to a large degree by the infiltration capacity of surface soils (Jorgensen and Gardner, 1987). Holzmer (1992) found resaturation rates to be highly variable over relatively small areas of the Big Brown Mine. Understanding how to predict and control infiltration and its effect on resaturation could improve reclamation processes and reduce the time necessary for groundwater systems to approach pre-mine conditions.

Objectives

The purpose of this study is to extend hydrogeological research at the Big Brown Mine and examine characteristics of infiltration influencing the variable resaturation rates documented in area C of the mine. Specific objectives include:

- Determine if variations in infiltration control variations resaturation.
- Quantify infiltration rates in different soil types found in the reclaimed areas.
- Quantify the following factors and determine their influence on infiltration:
    1) surface spoil heterogeneity, including soil texture and soil mineralogy,
    2) surface spoil saturated hydraulic conductivity, and
    3) seasonal variations in soil moisture content.
- Compare hydrogeologic characteristics of spoil placed with the cross-pit spreader with spoil placed with the draglines.
- Determine if flow along soil structures exists in the reclaimed soils and how it might enhance infiltration.

Previous Work

Hydrologic and environmental studies have been carried out at the Big Brown Mine and other areas of East Texas effected by surface mining. Included among these previous studies are pre-mining assessments of the geology and

hydrogeology to fulfill pre-mining regulations, during and post mining studies focusing on the groundwater chemistry and acid mine drainage, and studies of hydrogeologic characteristics of both the unsaturated and saturated zones, often comparing mined areas with unmined areas. Examples of recent work on understanding the effects of surface mining on sediments and groundwater systems in East Texas follow.

Spoil settlement and redensification rates were studied by Schneider (1977) at the Alcoa (Sandow) Lignite Mine in Milam County, Texas. His study found that spoil material settles rapidly shortly after mining with most settling occurring within the first few years. Ten years after mining, virtually all settling has occurred.

French (1979) evaluated the hydraulic conductivity, water chemistry, and infiltration capacity in the unsaturated zone of areas A and B of the Big Brown Mine (Figure 1). He estimated hydraulic conductivities of areas A and B to be 10^{-4} cm/sec and 2.6×10^{-3} cm/sec, respectively, and surmised that Area A was less permeable because of post-reclamation redensification. Water chemistry was affected by pyrite oxidation, but no acid mine drainage was present.

Henry and Basciano (1979) studied the environmental geology of the Wilcox Group lignite belt. They mapped 22 geologic units within this belt in an inventory of land resources. They outlined flood-prone areas, land use, soil types, and groundwater resources. Detailed maps were drawn to help assess problems associated with the development of surface mining. Henry *et al.* (1980) also studied the hydrology and water quality of the Wilcox Group to determine the impact of lignite development in East Texas.

Dutton (1982) studied the water chemistry of the unsaturated zone at the Big Brown Mine. He specifically looked at pre-mine sand and mud facies and reclaimed mud facies. He studied the water chemistry of these different facies and found little water quality degradation of the underlying sandstone aquifers when compared to pre-mine chemistry. He found the chemistry of the spoil material to be dominated by Ca^{2+}, Mg^{2+}, Na^{+}, and Cl^{-} ions. Recharge to the

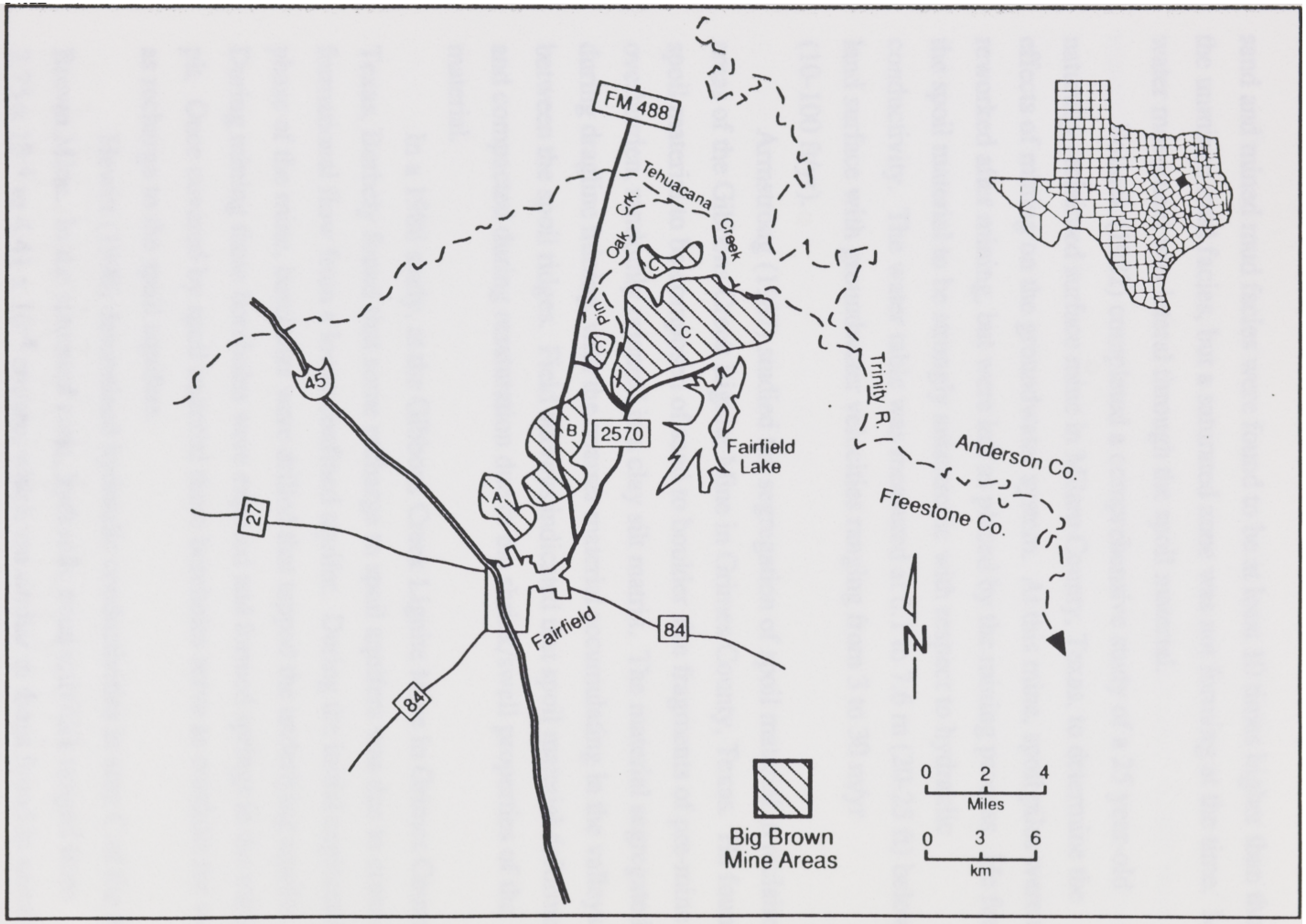

Figure 1. Location of the Big Brown Mine, Freestone County, Texas (Holzmer, 1992).

sand and mined mud facies were found to be at least 10 times higher than those in the unmined mud facies, but a saturated zone was not forming at the time. Most water movement was lateral through the spoil material.

Pollock (1982) completed a comprehensive study of a 25 year-old naturally reclaimed surface mine in Milam County, Texas, to determine the effects of mining on the groundwater system. At this mine, spoil piles were not reworked after mining, but were left as placed by the mining process. He found the spoil material to be strongly anisotropic with respect to hydraulic conductivity. The water table was measured at 6.1 to 7.6 m (20-25 ft) below the land surface with groundwater velocities ranging from 3 to 30 m/yr (10-100 ft/yr).

Armstrong (1987) studied the segregation of spoil material in reclaimed areas of the Gibbons Creek Lignite Mine in Grimes County, Texas. He found spoil material to be composed of sand to boulder size fragments of pre-mine overburden, randomly oriented in a clay silt matrix. The material segregated during dragline mining, with the coarser material accumulating in the valleys between the spoil ridges. Field surveys indicated that spoil material deformed and compacted during resaturation due to the shrink/swell properties of the material.

In a 1988 study, at the Gibbons Creek Lignite Mine in Grimes County, Texas, Borbely found that some recharge to spoil aquifers was due to cross-formational flow from a lower confined aquifer. During the initial exploration phase of the mine, boreholes were drilled that tapped the underlying aquifer. During mining these boreholes were exposed and formed springs in the mining pit. Once covered by spoil material these boreholes serve as conduits for water as recharge to the spoil aquifers.

Hewitt (1990) determined hydraulic conductivities in area C of the Big Brown Mine. In the saturated zone, hydraulic conductivities ranged from 2.75×10^{-4} to 4.41×10^{-4} cm/sec, which are similar to those found in unmined silty sand aquifers. Resistivity surveys were conducted to delineate the water table, but did not provide conclusive results.

The most recent hydrogeologic investigation of the Big Brown Mine is the study by Holzmer (1992) which examines resaturation rates, sources of recharge, and the groundwater chemistry of the saturated zone. In this study, resaturation rates were found to vary from 0.6 to 3.0 m/yr (2-10 ft/yr) across the reclaimed portion of the mine. Recharge to the system is thought to be dominantly from direct infiltration of precipitation. Groundwater chemical processes are dominated by pyrite oxidation, with water salinity ranging from 1,200 to 4,000 mg/L (milligrams/liter).

The Big Brown Mine Setting

Location and Climate

The Big Brown Mine, located in Freestone County, Texas, approximately 16 km (10 miles) northeast of the town of Fairfield, is operated by Texas Utilities Mining Company (TUMCO). The mine lies within the Trinity River Valley watershed, with the permit area bounded by Pin Oak Creek on the west and Tehuacana Creek on the northeast. Tehuacana Creek, which drains into the Trinity River approximately 4.8 km (3.0 miles) east of the mine, serves as the major drainage system for the mine area. The mine is divided into three areas, "A", "B", and "C" (Figure 1). Today, areas B and C are actively mined while production in area A ceased in the mid 1970's and was reclaimed by 1977. Kaiser (1974) estimates lignite reserves at the Big Brown Mine near 249 million metric tons (275 million short tons), with more than 90% of these reserves found in Area C. The mine supplies lignite to the Big Brown Steam Electric Station, located at the southeast end of the mine. Lake Fairfield was built to serve as the cooling reservoir for this power plant which consists of two 575 megawatt electric power generating units.

The mine is part of the lignite belt of the Gulf Coast Plain, which is characterized by gently rolling to hilly countryside. The topography is controlled by the geology, where sands form the topographic highs and mud deposits form the low areas. Within the mine permit area sands form highs with slopes of 3% to 10%, while mud deposits have slopes less than 3% (Henry and Basciano, 1979). Topographic relief across the area is approximately 30 m (100 ft). The habitat of Freestone County is dominated by Post Oak Savannah with a small area of Blackland Prairie. Soils of the Post Oak Savannah are characterized by thin sandy loams over dense clay B horizons. Areas with a sandy substrate have little clay accumulation in either the A or B horizons (Henry and Basciano, 1979). Land use is primarily pasture land for cattle ranching.

The climate in Freestone County is classified as humid sub-tropical. Rainfall data, collected by TUMCO, gives an annual average of 41.87 in/yr

(106.34 cm/yr) since 1971 (Figure 2). The heaviest rains occur in the late spring and early summer, but late fall to early spring is considered the rainy season with lower intensity rainfall events and lower evapotranspiration rates. Temperatures for the area can be extreme, with highs in the summer reaching 37.8° C (100° F). Winters are mild with generally fewer than 14 days reaching below the freezing point (0°C, 32° F).

Geology

The Big Brown Mine is located in the outcrop area of the Paleocene-Eocene Wilcox Group. Structurally, the mine lies along the edge of the East Texas Basin, which trends north-south, with strata that dip inward toward the axis. Areas within the basin are locally deformed by salt dome structures. Two major fault systems occur in the area; the Mexia-Talco fault system to the west and the Mount Enterprise fault system to the south (Hall *et al.*, 1985). Strata in the mine area generally parallel the coast and dip south-east less than 1 degree. Lignite in the Gulf Coast Plain occurs in the Wilcox Group, Jackson Group, and Yequa Formation. Wilcox Group lignite is most important north of the Colorado River and is the best grade of lignite occurring in the state (Figure 3).

Stratigraphy of the Big Brown Mine includes the Wilcox Group, the Claiborne Group and Quaternary alluvium. Formations of the Wilcox Group include the Hooper, Simsboro, and Calvert Bluff Formations, with the Calvert Bluff Formation being the dominant formation occurring in the mine permit area. The Hooper Formation consists of deltaic and fluvial-deltaic deposits, while the Simsboro is dominated by fluvial sands. The Calvert Bluff Formation, which contains most of the commercially important lignite (Kaiser *et al.*, 1978), is interpreted as a fluvial-deltaic sequence with occurrences of thick sands and interbedded lignite, mudstones and thin sands. Lignite occurs primarily in the upper part of the Calvert Bluff Formation interbedded with interdistributary muds. Above the Wilcox Group is the Claiborne Group, which consists of the

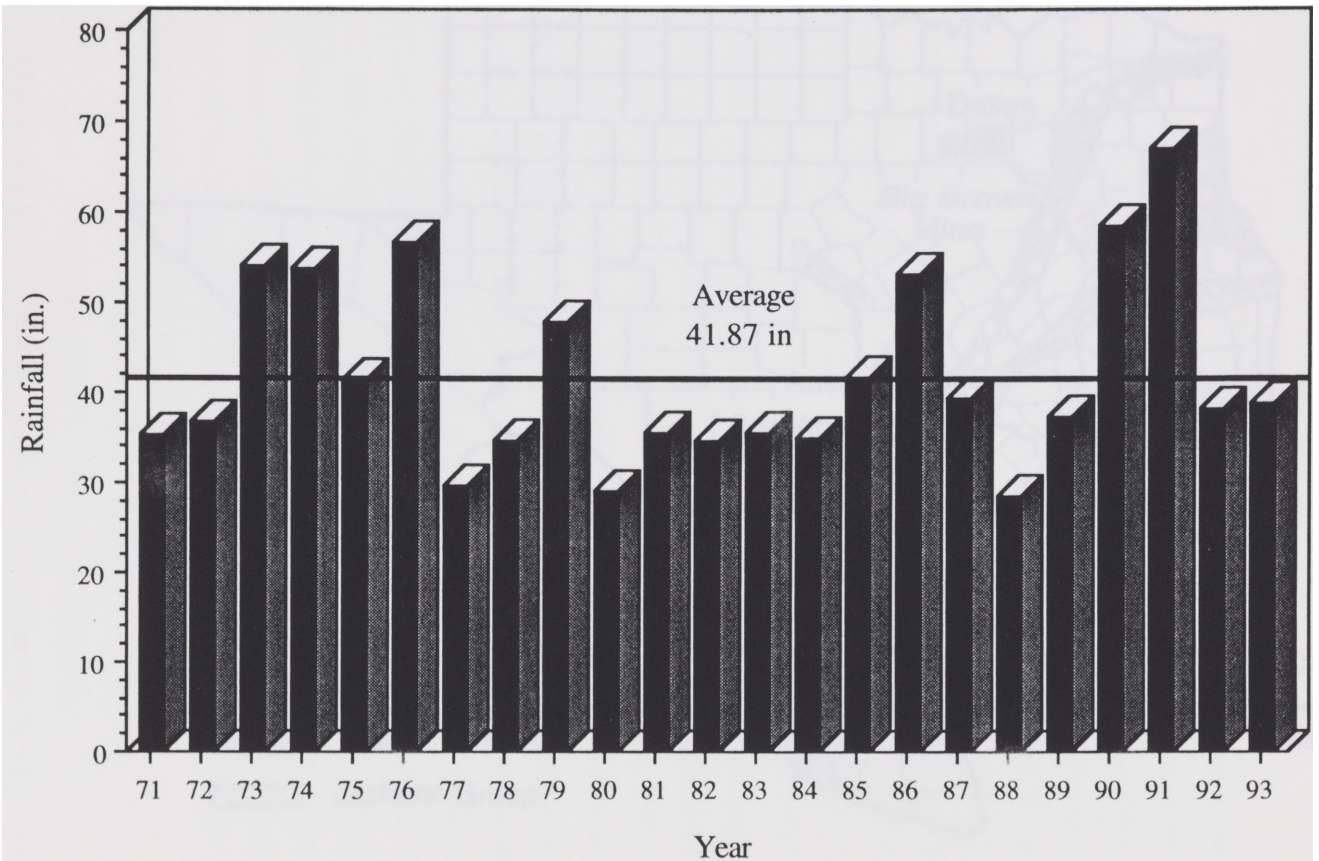

Figure 2. Annual Rainfall at Big Brown Mine, 1971-1993.

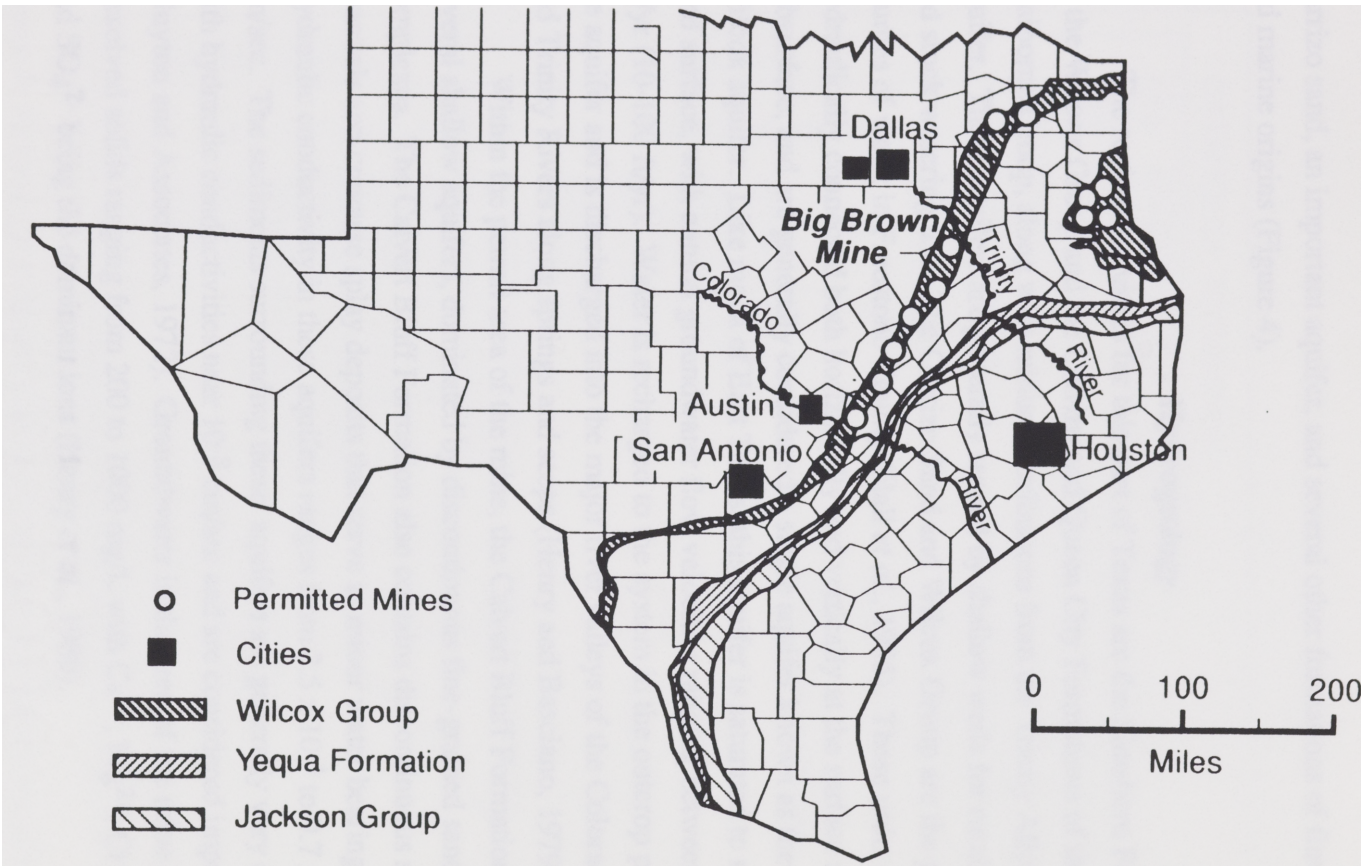

Figure 3. Lignite mines in the Wilcox Group, including the Big Brown Mine (Holzmer, 1992).

Carrizo sand, an important aquifer, and several other formations of fluvial-deltaic and marine origins (Figure 4).

Hydrogeology

The regional aquifers for this part of Texas are the Simsboro Formation of the Wilcox Group and the Carrizo and Queen City Formations of the Claiborne Group, along with minor contributions from the Trinity Alluvial aquifer. These aquifers are generally tapped by shallow wells for rural domestic and stock watering use. The Carrizo Sand and Wilcox Group are the primary sources of water in Freestone County (Hall *et al.*, 1985). These units are hydraulically connected both horizontally and vertically at the surface and subsurface, and are generally considered a single aquifer known as the Carrizo-Wilcox aquifer. Like much of East Texas, this aquifer is saturated to near the land surface, with natural groundwater flow velocities ranging between 3 to 30 m/yr (10-100 ft/yr). Water is recharged to the system in the outcrop portions of the aquifer and is discharged into the major river valleys of the Colorado, Brazos and Trinity Rivers along springs and seeps (Henry and Basciano, 1979).

Within the permit area of the mine, the Calvert Bluff Formation contains several shallow aquifers, dominated by discontinuous fine-grained sand channel complexes. The Calvert Bluff Formation also contains discontinuous silty-sand channels and crevasse splay deposits that serve as minor water bearing units. Hydraulic conductivity in these aquifers ranges from 2.5×10^{-4} to 9.7×10^{-4} cm/sec. The sediments surrounding these aquifers are generally very clay rich with hydraulic conductivities near 10^{-8} cm/sec and are considered impermeable (Guyton and Associates, 1972). Groundwater in the area of the mine has total dissolved solids ranging from 200 to 1000 mg/L with Ca^{2+}, Mg^{2+}, Cl^{-}, HCO_3^{-} and SO_4^{2-} being the dominant ions (Henry *et al.*, 1980).

Mining and Reclamation Methods

The setting at the Big Brown Mine is ideal for strip mining due to several factors including gently rolling topography, low dip of the strata, areal

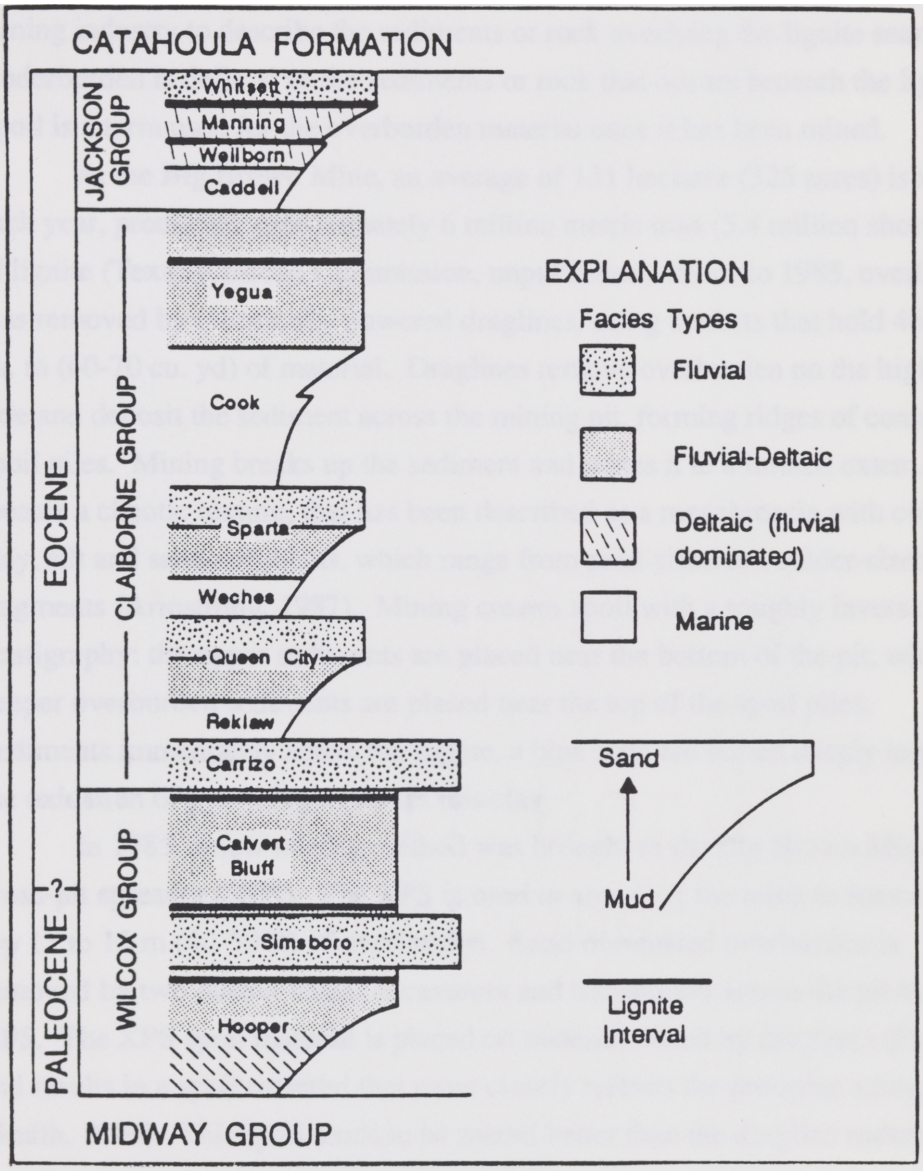

Figure 4. Stratigraphic column showing lithology and facies type of the Lower Tertiary Wilcox, Claiborne, and Jackson Groups (Kaiser *et al.*, 1978). The Big Brown Mine is stratigraphically located in the upper half of the Calvert Bluff Formation.

extent of the lignite, shallow depths at which the lignite occurs, unconsolidated overburden, and depths to major aquifers. Overburden is a term used by the mining industry to describe the sediments or rock overlying the lignite seams. Underburden is defined as the sediments or rock that occurs beneath the lignite. Spoil is a term used for the overburden material once it has been mined.

At the Big Brown Mine, an average of 131 hectares (325 acres) is mined each year, producing approximately 6 million metric tons (5.4 million short tons) of lignite (Texas Railroad Commission, unpublished). Prior to 1985, overburden was removed by electrically powered draglines, using buckets that hold 46 to 54 cu. m (60-70 cu. yd) of material. Draglines remove overburden on the highwall side and deposit the sediment across the mining pit, forming ridges of conical spoil piles. Mining breaks up the sediment and mixes it to a limited extent. This creates a chaotic texture, that has been described as a megabreccia with cohesive clay, silt and sand sediments, which range from sand-sized to boulder-sized fragments (Armstrong, 1987). Mining creates spoil with a roughly inverse stratigraphy: the upper sediments are placed near the bottom of the pit, while the deeper overburden sediments are placed near the top of the spoil piles. Sediments immediately above the lignite, a blue clay, are buried deeply to prevent the oxidation of pyrite found within this clay.

In 1985, a new mining method was brought to the Big Brown Mine: a cross-pit spreader (XPS). The XPS is used in area C of the mine to remove the top 12 to 15 m (40-50 ft) of overburden. Sand dominated overburden is removed by two bucket wheel excavators and transported across the pit by the XPS. The XPS spoil material is placed on material mined by draglines (Figure 5) and results in a spoil material that more closely reflects the pre-mine stratigraphy (Smith, 1986). This spoil tends to be mixed better than the dragline material forming a more homogeneous spoil material.

After mining, reclamation begins to restore the land to its previous productivity. Spoil piles are leveled and shaped to reflect pre-mine topography. Drainage patterns and sediment ponds are established to control surface runoff. The ponds serve as wetland habitats for the many species of birds found in the

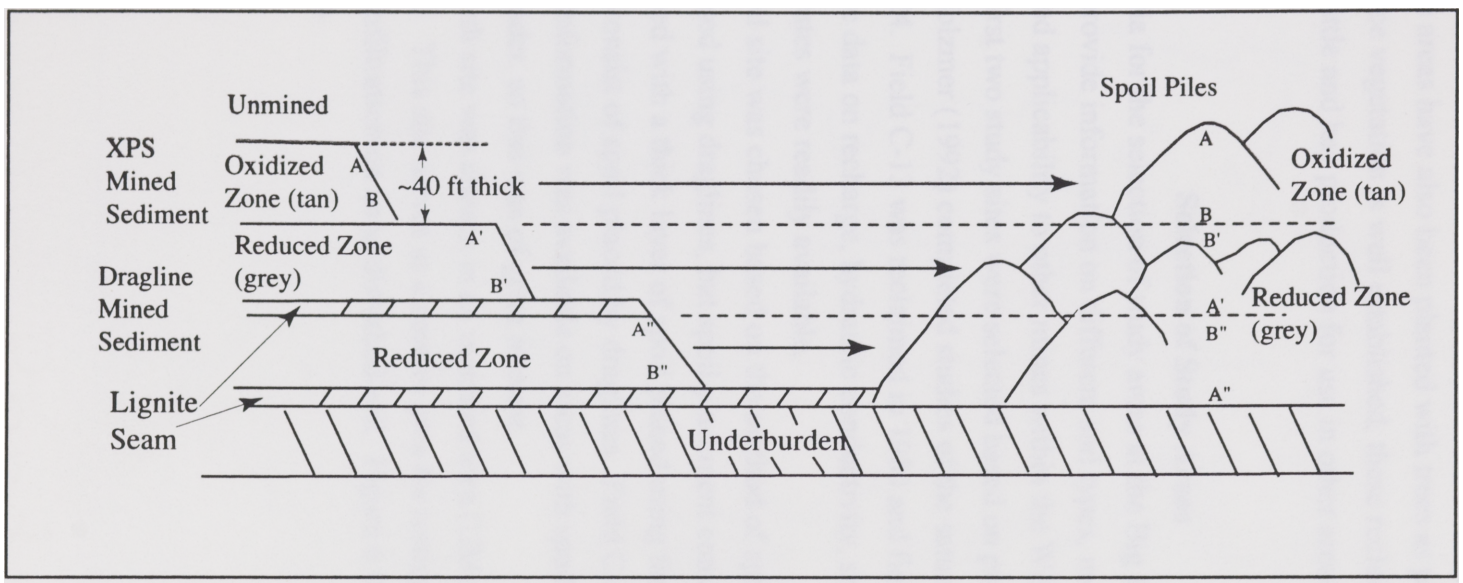

Figure 5. Placement of spoil using the cross-pit spreader (XPS) for the upper overburden and draglines for the deeper overburden. Modified from Holzmer (1992).

area. Reclaimed lands are seeded with coastal bermuda grass and crimson clover. Some areas have also been planted with trees as part of a reforestation program. Once vegetation is well established, these reclaimed lands are used for grazing cattle and hay production for use in other areas of the mine (White, 1978).

Selection of Study Areas

Criteria for the selection of study areas at the Big Brown Mine were designed to provide information on different soil types, methods of spoil placement, and applicability to other mines within the Wilcox Group.

The first two study sites were selected based on previous studies. Hewitt (1990) and Holzmer (1992) completed studies of the saturated zone in fields C-13 and C-24. Field C-13 was reclaimed in 1980 and field C-24 was reclaimed in 1985. Here data on recharge, hydraulic conductivity, soil type, and resaturation rates were readily available.

A third site was chosen based on the method of spoil placement. Field C-32 was mined using draglines, but spoil placement consists of dragline material topped with a thick layer of spoil placed using the XPS. Both fields C-13 and C-24 consist of spoil placed by draglines. Field C-32 was reclaimed in 1986. Little information was available on areas with spoil placed using the cross pit spreader, so this was of great interest.

A fourth site was chosen in an unmined area (UM) that occurs between areas B and C. This site serves as a control area for testing methods to characterize infiltration on an undisturbed soil. Figure 6 shows the location of the study sites.

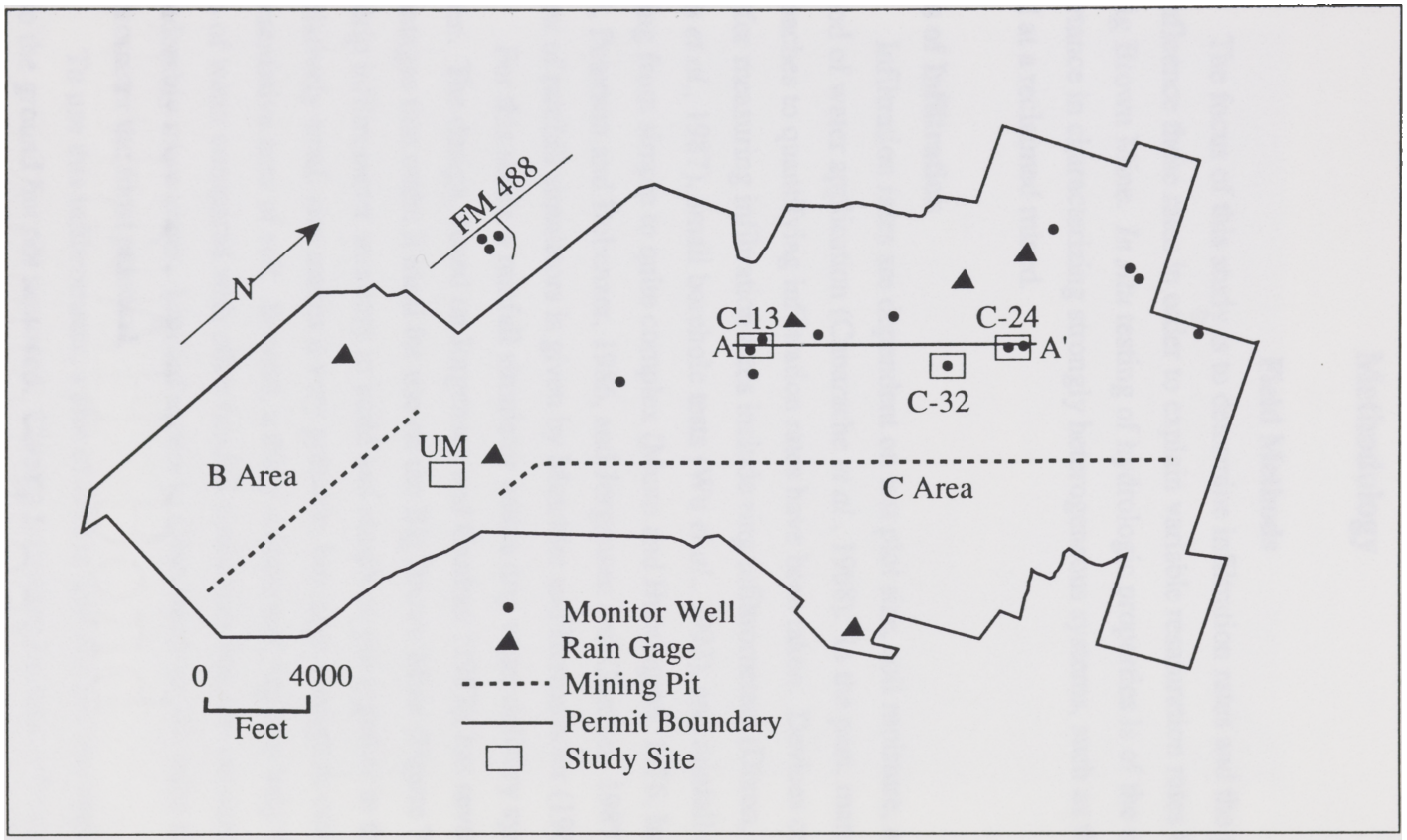

Figure 6. Study area at the Big Brown Mine. Modified from Holzmer(1992).

Methodology

Field Methods

The focus of this study is to determine infiltration rates and the properties that influence these rates in order to explain variable resaturation rates found at the Big Brown Mine. *In situ* testing of hydrologic properties is of the utmost importance in characterizing strongly heterogeneous systems, such as those found at a reclaimed mined.

Rates of Infiltration

Infiltration rates are dependent on test plot size, soil moisture, and method of water application (Canarache *et al.*, 1968). In the past, many approaches to quantifying infiltration rates have been taken. Devices commonly used for measuring infiltration rates include ring infiltrometers (Dixon, 1975 and Jarvis *et al.*, 1987), small borehole tests (Wu *et al.*, 1993), and rainfall simulators ranging from simple to quite complex (Munn and Huntington, 1976, Imeson, 1977, Peterson and Bubenzer, 1986, and Jorgensen and Gardner, 1987). A review of rainfall simulators is given by Mutchler and Hermsmeier (1965).

For this study, a rainfall simulator with a drip water delivery system was chosen. The design, based on Jorgensen and Gardner (1987), has several advantages that make it ideal for use on the Big Brown Mine (Figure 7). First, this drip infiltrometer was easy to build and simple to put together in the field. Its relatively small size makes it very portable, but large enough to cover a representative area of soil. Second, a thirty-minute test requires only 60 to 62 liters of water compared with other rainfall simulators that can consume considerably more water. Limited access to clean water on the mine made this infiltrometer the most practical.

To use this infiltrometer, a plot of land is selected and the vegetation is cut to the ground but not removed. Cutting is desired because tall vegetation intercepts a great deal of water and gives erroneously high infiltration rates.

Figure 7. Drip infiltrometer showing (A) adjustable legs, (B) water reservoirs, (C) water entry grid, (D) drop spreading screen, (E) collecting trough, and (F) calibrated collecting bucket. Modified from Jorgensen and Gardner (1987).

Total removal of vegetation is not acceptable because it alters the soil structure and changes the infiltration rates. Once the vegetation is cut, the infiltrometer is placed over the selected site and leveled by adjusting the legs. Small pieces of sheet metal are hammered into the ground along the back and sides of the infiltrometer to prevent water from leaking out in any low spots. To run an infiltration test, water is applied at a constant rate using shut-off valves to control the flow. The water runs through a series of copper tubes, and drips onto several layers of screening. The screening serves to spread the drops into an even distribution of water across the test plot and to create random drop sizes as would be expected in nature. Once the water hits the test plot it will either infiltrate or run-off the surface. For each time period of the test, two measurements are taken, the amount of water applied and the amount of runoff collected. The difference between the two measurements is the infiltration rate for that time period. Each test lasts 30 minutes with measurements taken at 2 minute intervals. The last 10 minutes of the test is assumed to be the final infiltration rate (Ritter and Gardner, 1993). In all cases, the amount of water applied exceeded the amount infiltrated. Twelve tests were run at each of the reclaimed study sites while six tests were run at the unmined study site. Tests were spread out over the fields to find an average rate for each study site. Tests occurred in fall and winter to examine seasonal variations in infiltration.

Saturated Hydraulic Conductivity

A Model 2800 KI Guelph Permeameter was used to quantify saturated hydraulic conductivity and matrix potential of the soil. These tests were done by standard methods described in the manual accompanying the instrument (Soil Moisture Equipment Company, 1986) and again were spread across the study fields to find an average value. These tests took place in the summer, winter, and spring to examine seasonal variations with a total of eight tests in each field of study.

Seasonal Soil Moisture Content

Soil moisture content is difficult to measure directly without disturbing the soil. Suction tensiometers, commonly used in agriculture, were setup to measure relative changes in soil moisture content. Tensiometers detect changes in pressure that correlate with soil moisture content (Wendt *et al.*, 1978, Stephens *et al.*, 1991, and Thomas and Phillips, 1991). The tensiometers are placed in the ground at the desired depths, filled with water, and evacuated of all air bubbles with a hand held pump; the tensiometers are then sealed with a cap. In a dry soil, water is pulled through the porous cup at the bottom of the tensiometer and out into the soil creating a suction in the tensiometer. This suction is read as centibars on a dial gauge attached to the tensiometer. When soils are saturated, water does not flow out into the surrounding soil and results in a reading of zero centibars on the dial gauge.

For fields C-13, C-24, and UM, tensiometers were installed at 30 cm (1 ft) intervals to a depth of 120 cm (4 ft). The tensiometers were arranged into 4 nests; each nest consists of 4 tensiometers with one installed at each depth, for a total of 16 tensiometers per field. In field C32, tensiometers were installed at 30 cm (1 ft) intervals to a depth of 150 cm (5 ft). These were also grouped into nest, but with five tensiometers per nest for a total of 20 for the field. Tensiometers were installed in July 1993, and were monitored regularly through July 1994. Figure 8 shows the arrangement of the nests with the relative positions of drip infiltrometer tests, Guelph Permeameter tests, and tracer tests.

Unsaturated Zone Tracer Tests

An understanding of water movement from the surface into the unsaturated zone and beyond is essential in the study of infiltration and resaturation. In the classic study by Horton (1940), factors affecting infiltration were divided into three categories: soil type, vegetative cover, and macrostructures within the soil. Numerous studies on infiltration involve the use of dyes and conservative tracers to mark macrostructures where water flows. A brief review of the literature shows extensive use of dye tracing tests over the

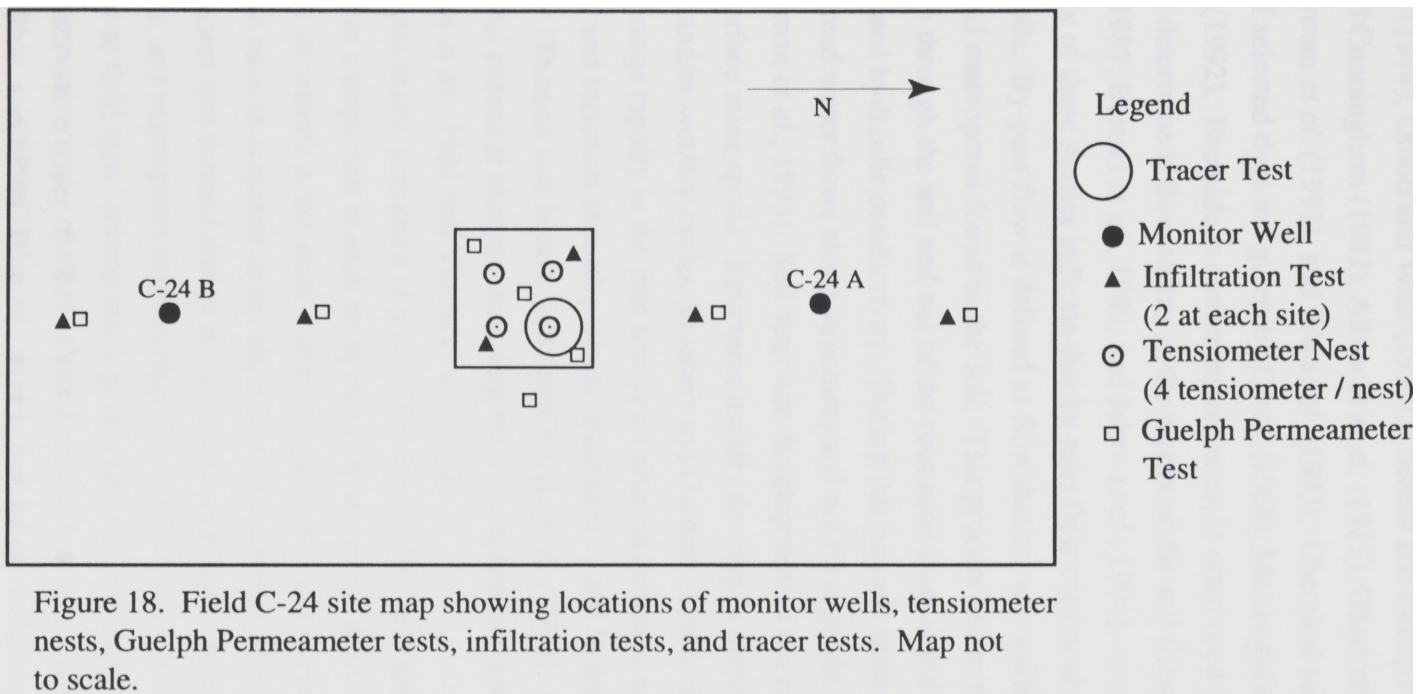

Figure 18. Field C-24 site map showing locations of monitor wells, tensiometer nests, Guelph Permeameter tests, infiltration tests, and tracer tests. Map not to scale.

last two decades to monitor water flow through soils including articles by Clarke and Vincent (1974), Omoti and Wild (1979), Thomas and Phillips (1979), Simpson and Cunningham (1982), Albrecht *et al.* (1989), Ghodrati and Jury (1990), Bowman *et al.* (1991), and Wu *et al.* (1993). Chemical and physical properties of selected dyes are given by Corey (1968), McLaughlin (1982), and Shiau *et al.* (1992). Bromide, a conservative tracer, is often used in conjunction with dyes to determine if flow occurs in the matrix of the soil (Levy and Chambers, 1987, Butters *et al.*, 1989, and Jabro *et al.*, 1991).

Many of these studies indicate that by-pass flow commonly occurs in structured soils. By-pass flow is defined as flow that occurs rapidly along structures and macropores found in the soil. This process can move water much more rapidly through the soil and out of the root zone than would be predicted by the saturated hydraulic conductivity. During this process saturation is not reached, instead water flows along structures and not through the matrix of the soil (Heuvelman *et al.*, 1993). Soil structure development is not uncommon in reclaimed surface mine spoils. Structures usually develop in response to freeze/thaw and/or wet/dry cycles (Guebert and Gardner, 1992). Physical properties change rapidly in the first few years after reclamation with decreases in bulk density and increases in total porosity, macropores, and hydraulic conductivity (Thomas and Jansen, 1985 and Varela *et al.*, 1993). Mineralogical alterations and chemical changes including metal complexation and oxidation also occur (Grube *et al.*, 1982 and Varela *et al.*, 1993).

For this study, a mixture of water, Rhodamine WT and sodium bromide was ponded in a large ring at each study site to determine if infiltration is enhanced by structures in the soils. Structures thought to be present include fractures that form in response to the shrink/swell properties of clays found in the soil, macropores that formed during reclamation as the spoil settled and consolidated, and macropores that develop due to biological activity.

Prior to field tests, several lab experiments were performed to determine dye and conservative tracer choices. Four dyes, Fluorescein, Rhodamine WT, Methylene Blue, and FD&C Blue #1, were tested on soil columns for sorption

properties and ease of visual identification. Rhodamine WT was found to sorb the least of the dyes tested and was visually distinctive on all soil type used in the tests. Sodium bromide was also tested in the soil columns for possible reactions with the clays in the soil. A solution of sodium bromide was poured through the soil column and collected in a beaker for analysis. Measurements for ppm bromide were made using an ion selective electrode both before pouring the solution through the column and after. Results showed no change in concentration for the solution poured through the soil column indicating that bromide was conservative in this soil and would be a suitable tracer for these experiments.

For field tests, a 2.9 m (9.6 ft) diameter galvanized metal ring was constructed by removing the bottom from a stock watering tank. The tank was split in half to make it easier to transport to the study sites and was bolted and sealed with silicon caulk when ready to set up. A single tracer test was performed at each study site, following the same procedure for all tests.

To prepare the site, a relatively level area that included at least one nest of tensiometers was chosen. The grass in the area was cut to the ground so it would not interfere with water application. The ring was placed over the site and the edge marked. A narrow trench was dug to a depth of 0.2 m (0.8 ft) and the ring was placed down into the trench. The trench was then back filled with a thick layer of bentonite and topped with soil to deter leaking around the edge.

A 1,136 liter (300 gallon) water tank, on loan from the mine, was used to transport water to the site. The water was supplied at a wash station located at the mine. Rhodamine WT and sodium bromide were mixed in before transporting to the test site. Dye was mixed to a concentration of 0.25 ml/liter. Sodium bromide was mixed to a concentration of 0.2 moles/liter. The water mixture was applied to the site through a pump, with all 1,136 liters (300 gallons) being applied at once. No effort was made to maintain a constant head in the test plot. A second mixture of water was applied later that day. Ponding depths did not exceed 30 cm (1 ft) in any test. A third mixture of water was applied 24 hours later if all water previously applied had infiltrated. Tensiometers inside the

plot were monitored to determine saturation depth; tensiometers outside the plot were also monitored for changes in saturation to determine if lateral flow occurred.

Forty-eight hours after the initial application of the dye, the ring was removed and the area was trenched. A back-hoe was used to dig a trench 0.9 to 1.2 m (3-4 ft) deep by 0.8 m (2.5 ft) wide. The trench wall was then sampled at regular intervals with a small soil core sampler to collect approximately 20 ml of soil to determine concentration of bromide in the pore water of the soil. Soil samples were taken at 30 cm (1 ft) intervals across the trench and at 3 depths resulting in 33 samples. Additional samples were collected at other points of interest in the cross-section. Each sample was placed in a clean specimen cup and sealed for evaluation in the lab. Drawings and photographs were made to show the location of dyed flow paths in the trench.

Analysis for bromide concentration was conducted using a Cole-Parmer Model 27502-04 Combination Bromide Electrode. The collected soil samples were mixed with 50 ml of deionized water and 1 ml of 5M $NaNO_3$, an ionic strength adjuster. The prepared samples were shaken to mix then placed on a magnetic stirrer. The combination bromide electrode was placed in the slurry along with a pH electrode; bromide concentration was measured in parts per million (ppm), and recorded along with a pH reading.

Water Levels

The elevation of the water table was measured in wells C-13 A and C-13 B located in field C-13, C-24 A and C-24 B located in field C-24, and C-46-R-92 located in field C-32. Measurements were taken every few months with an electric water level indicator (e-line) to monitor changes in the water table from July 1993 to July 1994.

Laboratory Methods

Grain-Size Analysis

Soil samples were collected from each study site using a hydraulic soil probe on loan the mine. Samples were taken at 30 cm (1 ft) intervals to a depth of 120 cm (4 ft) with an auger or soil core sampler depending on soil type. The auger was used in the sandy soils to obtain a complete sample, while the soil core sampler was used in finer-grained soils. Grain-size analyses were performed to determine percentages of sand, silt, and clay. For these tests, sand, silt, and clay describes a specific size class and not mineralogy. Grain-size classification is based on the particle diameter of:

sand: 2.00 - 0.063 mm
silt: 0.063 - 0.0020 mm
clay: < 0.0020 mm (Tucker, 1982).

Hydrometer tests were performed by standard methods (Day *et al.*, 1956), using sodium hexametaphosphate as a dispersing agent. A high speed blender was used to mix the samples to ensure that fine particles were well separated. Following hydrometer tests, dry sieve analyses were performed on soil samples from field UM and C-32. Wet sieve analyses were performed on samples from fields C-13 and C-24.

Soil Mineralogy

Soil mineralogy was determined using X-ray diffraction by methods described in Lynch (1994). One representative sample from each field of study was analyzed for percent weight of quartz, potassium feldspar, plagioclase, and total clay. The clay content, defined as grains smaller than 0.0020 mm, was separated and analyzed for percent weight of smectite, a shrink/swell clay, illite, kaolinite, and chlorite.

Groundwater Resaturation Model

To better understand the possible effects of variable infiltration on the resaturating ground water system, a numerical model was developed. A vertical

cross-section from field C-13 to field C-24 was programmed in FORTRAN using a 2-dimensional, transient-state, finite difference model. Previous efforts for modeling resaturation at the Big Brown Mine have been limited to characterizing a small area around well C-13 A (Holzmer, 1992). This model determined a distribution of hydraulic conductivity along with a value for storativity. To carry this modeling effort a few steps further, a new version of the program calculates hydraulic head along a cross-section line from field C-13 to field C-24 with wells C-13 A, C-13 B, C-24 A and C-24 B as known points. The objective of this model was to determine how variable amounts of recharge might control the variable resaturation rates seen across this area. Sensitivity analyses were conducted by varying recharge and hydraulic conductivity. Results were compared with field measurements for three separate dates.

Results

Field Methods

Rates of Infiltration

Infiltration rates are found to be highly variable over the area of each field, but show much less variation over the area of the mine as a whole (Appendix A). Values of infiltration rates from reclaimed areas show a significant reduction when compared with values from the unmined area. Infiltration rates also change significantly in response to the soil moisture content at the time of the test. Table 1 gives high and low values for each field along with mean values for data collected in the summer and winter. An overall mean infiltration rate is calculated for each field from all data points collected.

Field #	# of Samples	High (cm/hr)	Low (cm/hr)	Summer Mean (cm/hr)	Winter Mean (cm/hr)	Overall Mean (cm/hr)	Standard Deviation
UM	6	30.0	12.6	24.7	14.3	21.1	6.4
C-13	12	22.1	3.2	13.2	5.4	8.0	5.5
C-24	12	20.4	4.7	18.5	6.8	10.7	6.0
C-32	12	19.4	2.6	15.3	5.7	8.9	5.9

Table 1: High, low and mean infiltration rates.

Saturated Hydraulic Conductivity

Saturated hydraulic conductivity, a measure of water flow under saturated conditions, is primarily dependent on the texture of the soil. This holds true for both reclaimed and unmined fields at the Big Brown Mine where coarser soils, such as those found in fields UM and C-32, show higher saturated hydraulic conductivity rates than those measured in the finer grained soils of fields C-13 and C-24 (Table 2). Mining and reclamation alter values for saturated hydraulic conductivity slightly as shown by the order of magnitude difference between fields UM and C-32 which have similar soil types. Fields UM, C-24, and C-32

show little seasonal variation in saturated hydraulic conductivity in response to changes in soil moisture content. Conversely, field C-13 does show several orders of magnitude change between data collected in the summer and data collected in the spring (Appendix B).

Matrix flux potential, a measure of a soils ability to pull water by capillary force, shows little seasonal variation for all fields tested. Again, soil texture is the dominant factor in determining the matrix flux potential while mining and reclamation have a lesser effect. Mean values for saturated hydraulic conductivity and matrix flux potential are given in Table 2.

		Saturated Hydraulic Conductivity		Matrix Flux Potential	
Field #	# of Samples	mean (cm/sec)	standard deviation	mean (cm^2/sec)	standard deviation
UM	8	1.09×10^{-3}	8.09×10^{-4}	3.49×10^{-2}	2.30×10^{-2}
C-13	8	5.01×10^{-5}	6.74×10^{-5}	1.74×10^{-4}	2.00×10^{-4}
C-24	8	1.16×10^{-5}	1.20×10^{-5}	4.27×10^{-4}	6.34×10^{-4}
C-32	8	7.01×10^{-4}	1.26×10^{-4}	7.49×10^{-3}	6.51×10^{-3}

Table 2: Mean saturated hydraulic conductivity and matrix flux potential.

Seasonal Soil Moisture Content

Tensiometers monitored throughout the year show similar patterns of moisture fluctuations in each field. Generally, water is held near the surface in the top 60 cm (2 ft) of soil during the winter; tensiometer readings ranged from 0 to 10 centibars of soil suction. Low temperatures and low evapotranspiration rates leave moisture in the near surface. Below 60 cm (2 ft), tensiometer readings were higher, ranging up to 25 centibars. In the hot months of summer, surface soils are typically very dry. Tensiometer readings from 60 to over 100 centibars of soil suction are common in all fields and soil types. Below 60 cm (2 ft), soils are usually wetter with tensiometer reading ranging from 30 to 70

centibars in fields UM, C-13, and C-24. At a depth of 60 cm (2 ft) in field C-32, tensiometer readings are lower ranging from 0 to 30 centibars for the summer months. These readings are attributed to a shallower root system and the coarser texture of the soil here. Spring and fall months tend to be intermediate between summer and winter. Typical relative soil moisture curves showing seasonal variations are shown in Figures 9, 10, 11, and 12.

Unsaturated Zone Tracer Tests

Unsaturated zone tracer tests were performed in each study site to determine if by-pass flow exists in reclaimed soils of the Big Brown Mine. The Rhodamine WT, used to mark water flow paths through the soil, sorbed strongly at the land surface and showed little movement into the soil in reclaimed areas of the mine. This reaction is attributed to the acidic nature of the reclaimed soils. Although an earlier study shows that reclaimed soils at the Big Brown Mine are generally neutral (Yao, 1994), pH values collected during analysis of bromide range from 3.2 to 6.3 for fields C-13, C-24 and C-32. In contrast dye sorbed only slightly to the land surface in field UM and did move into the soil column. Here pH values range from 7.2 to 8.5. Though the dye did not work as expected, bromide, used as a conservative tracer, did show preferential movement through the soils in all fields.

In field UM, dye was applied in three 1,136-liter batches. Dyed water infiltrated rapidly into the soil as indicated by extensive bubbling observed during application of the water and the short period of time required for all water to infiltrate (approximately 6 hours). Excavation of the trench took place 24 hours after the initial application of water. In all other fields, trenching did not occur for at least 48 hours. The trench dug through the dyed area of field UM showed a soil cross-section that consists of a sand layer approximately 70 to 80 cm (2.3-2.5 ft) thick with a clay rich color mottled layer below (Figure 13). The sand layer was uniform in texture and color. The root zone extended approximately 30 to 40 cm (1.0-1.5 ft) below the surface, with a few very fine roots extending deeper. The clay layer below the sand was much denser, but close inspection

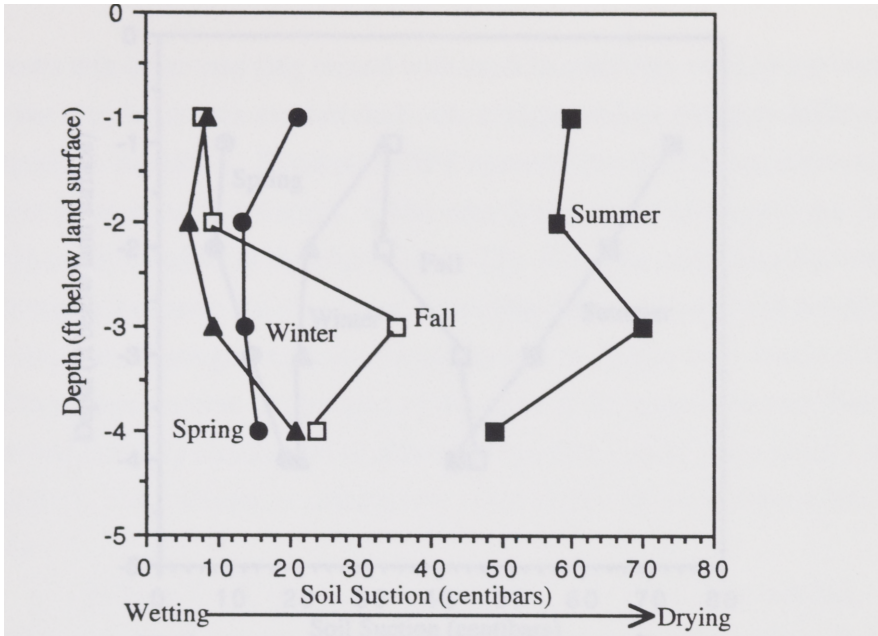

Figure 9. Representative seasonal soil moisture content of field UM.

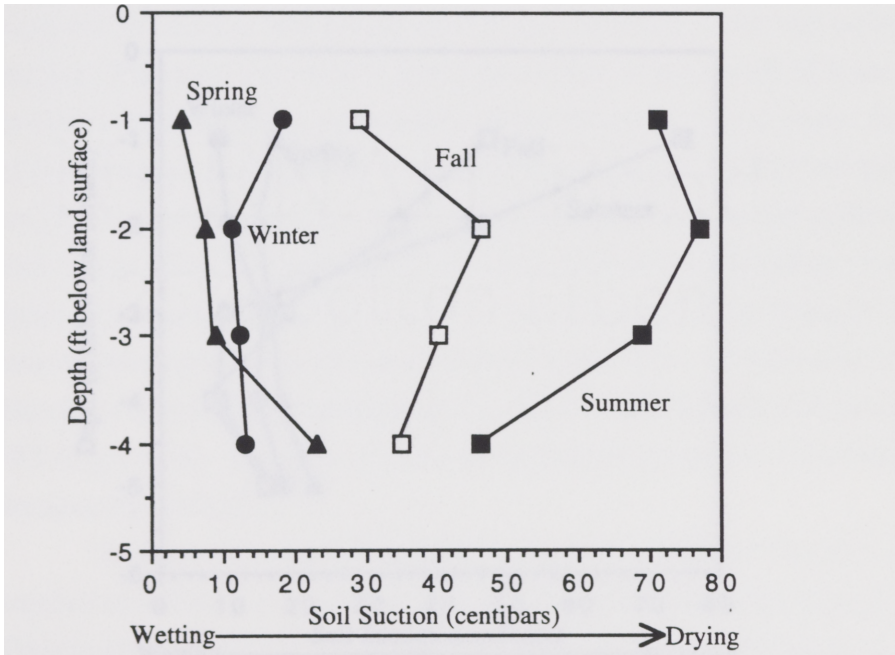

Figure 10. Representative seasonal soil moisture content of field C-13.

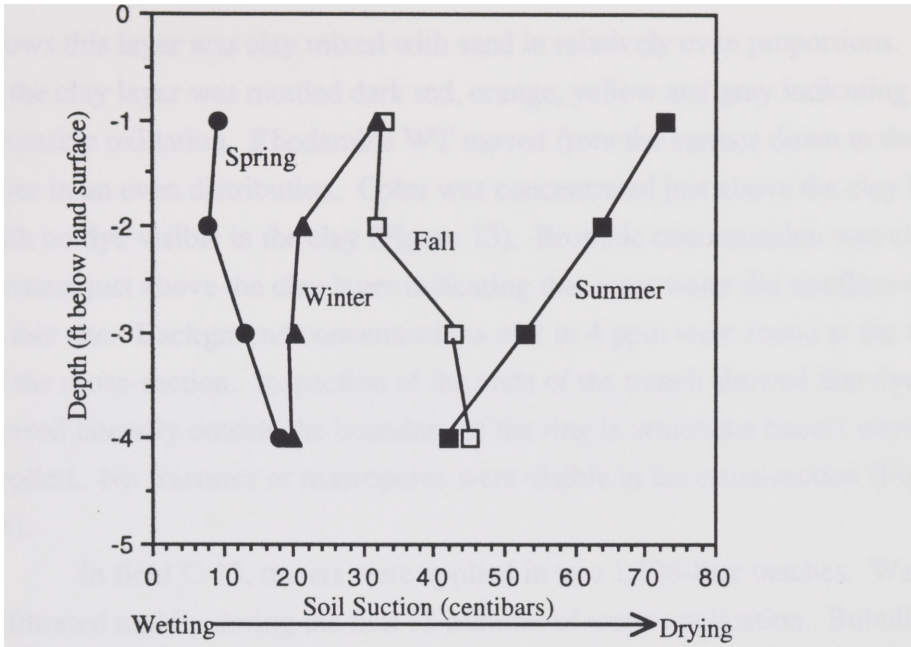

Figure 11. Representative seasonal soil moisture content of field C-24.

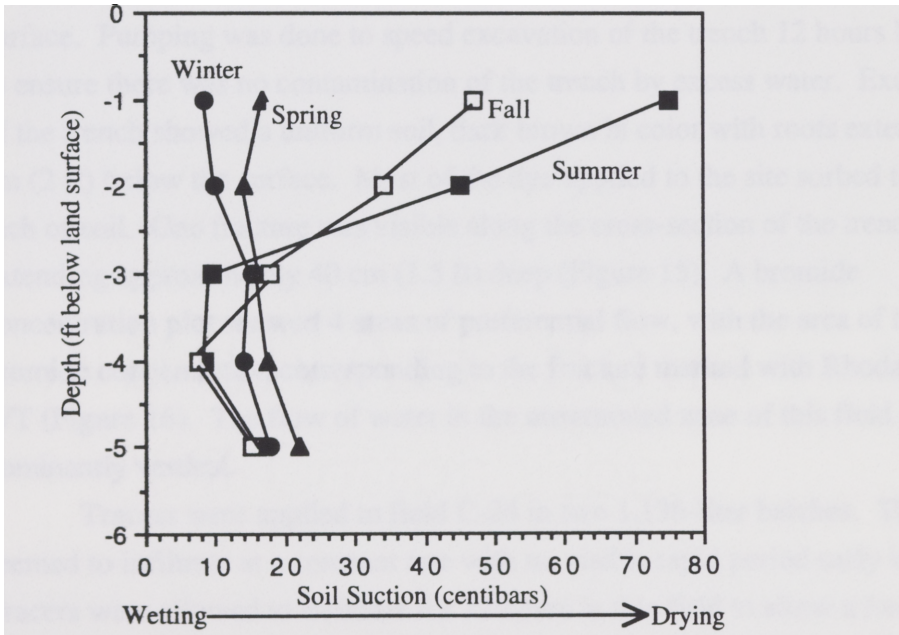

Figure 12. Representative seasonal soil moisture content of field C-32.

shows this layer was clay mixed with sand in relatively even proportions. Color in the clay layer was mottled dark red, orange, yellow and gray indicating extensive oxidation. Rhodamine WT moved from the surface down to the clay layer in an even distribution. Color was concentrated just above the clay layer with no dye visible in the clay (Figure 13). Bromide concentration was also greatest just above the clay layer indicating that most water did not flow deeper at this site. Background concentrations of 2 to 4 ppm were found at the bottom of the cross-section. Inspection of the ends of the trench showed that dyed water moved laterally outside the boundary of the ring in which the tracers were applied. No fractures or macropores were visible in the cross-section (Figure 14).

In field C-13, tracers were applied in two 1,136-liter batches. Water infiltrated rapidly during the first 15 minutes of water application. Bubbling was observed in several areas of the test site and the water level dropped rapidly, but after the first few minutes, infiltration slowed greatly. The test site was allowed to sit for 36 hours at which time most of the remaining water was pumped off the surface. Pumping was done to speed excavation of the trench 12 hours later and to ensure there was no contamination of the trench by excess water. Excavation of the trench showed a uniform soil, dark brown in color with roots extending 60 cm (2 ft) below the surface. Most of the dye applied to the site sorbed to the top inch of soil. One fracture was visible along the cross-section of the trench, extending approximately 40 cm (1.5 ft) deep (Figure 15). A bromide concentration plot showed 4 areas of preferential flow, with the area of highest bromide concentration corresponding to the fracture marked with Rhodamine WT (Figure 16). The flow of water in the unsaturated zone of this field is dominantly vertical.

Tracers were applied to field C-24 in two 1,136-liter batches. The water seemed to infiltrate at a constant rate with no visible rapid period early in the test. Tracers were allowed to infiltrate for 72 hours in this field to allow a longer period of time for the dye to penetrate. No pumping was necessary because all water had infiltrated prior to trenching. The soil cross-section

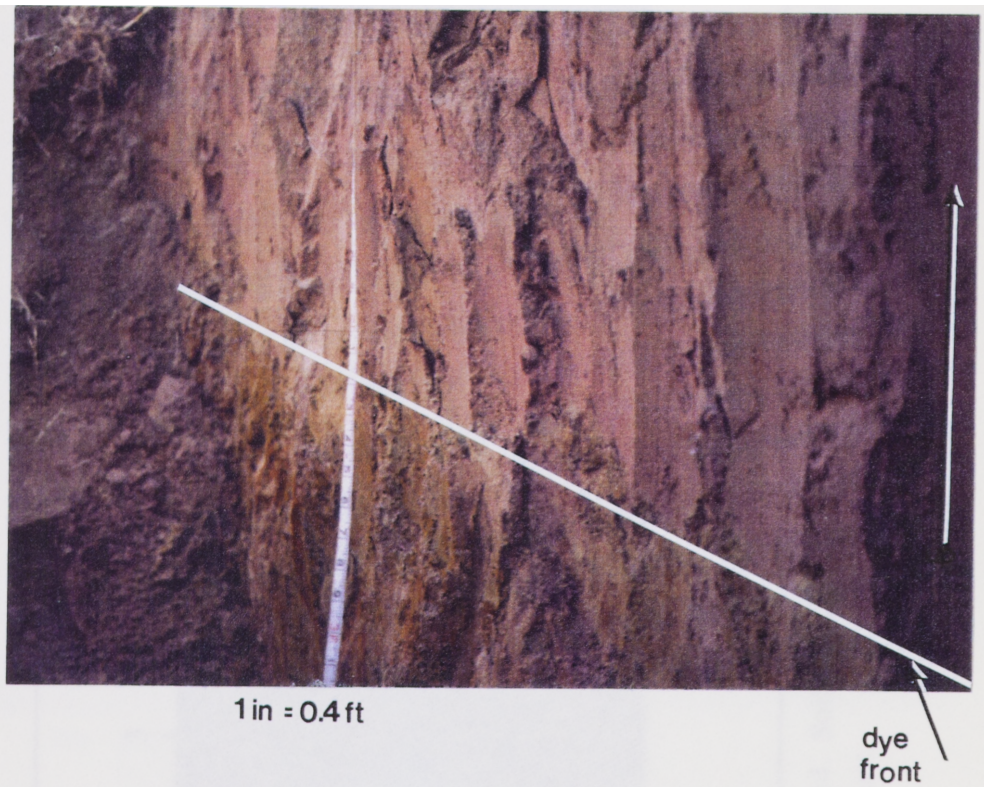

Figure 13. Photograph showing movement of Rhodamine WT through the soil in field UM. Photograph shows a vertical cross section cut by a back-hoe through the soil.

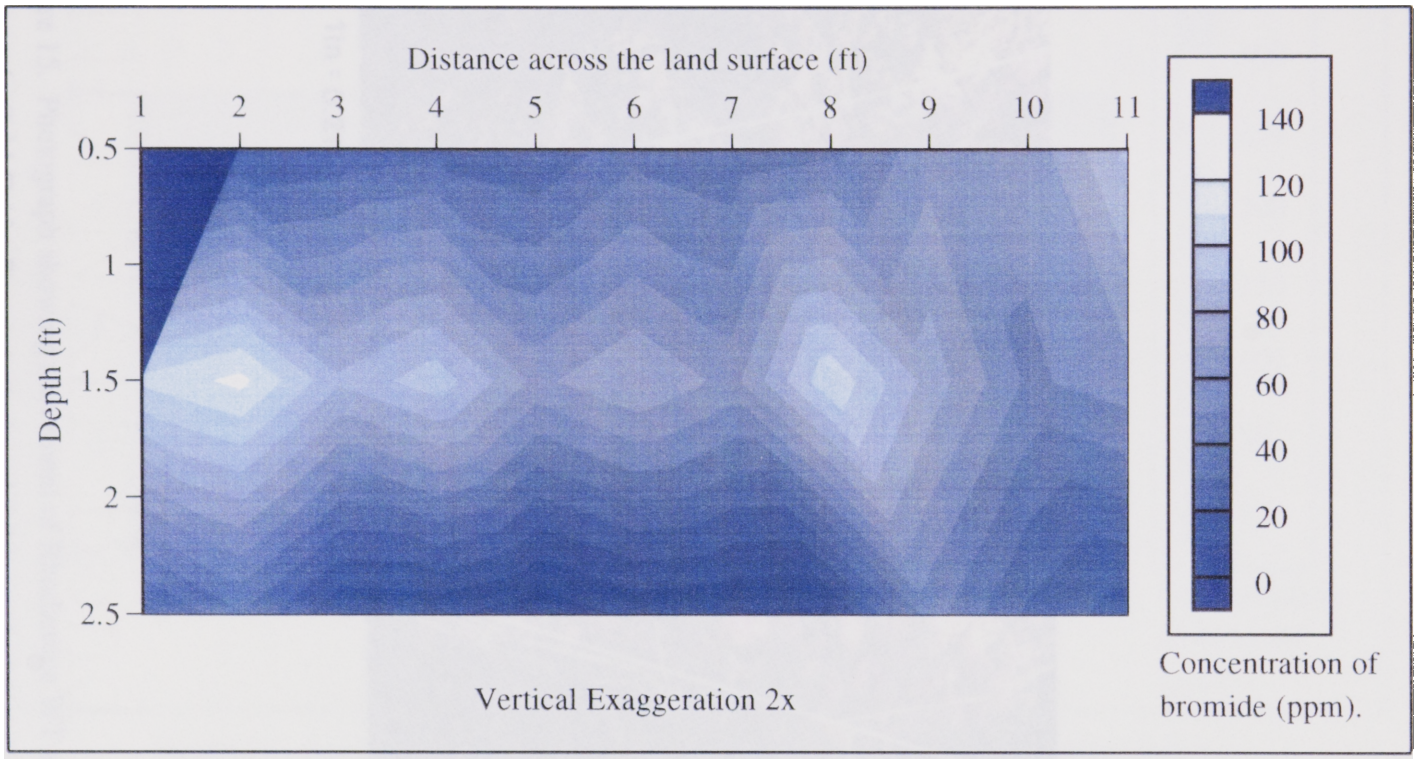

Figure 14. Soil cross section for field UM showing bromide concentration during tracer tests.

Figure 15. Photograph showing movement of Rhodamine WT along a soil structure in field C-13. Photograph shows a dye marked macropore.

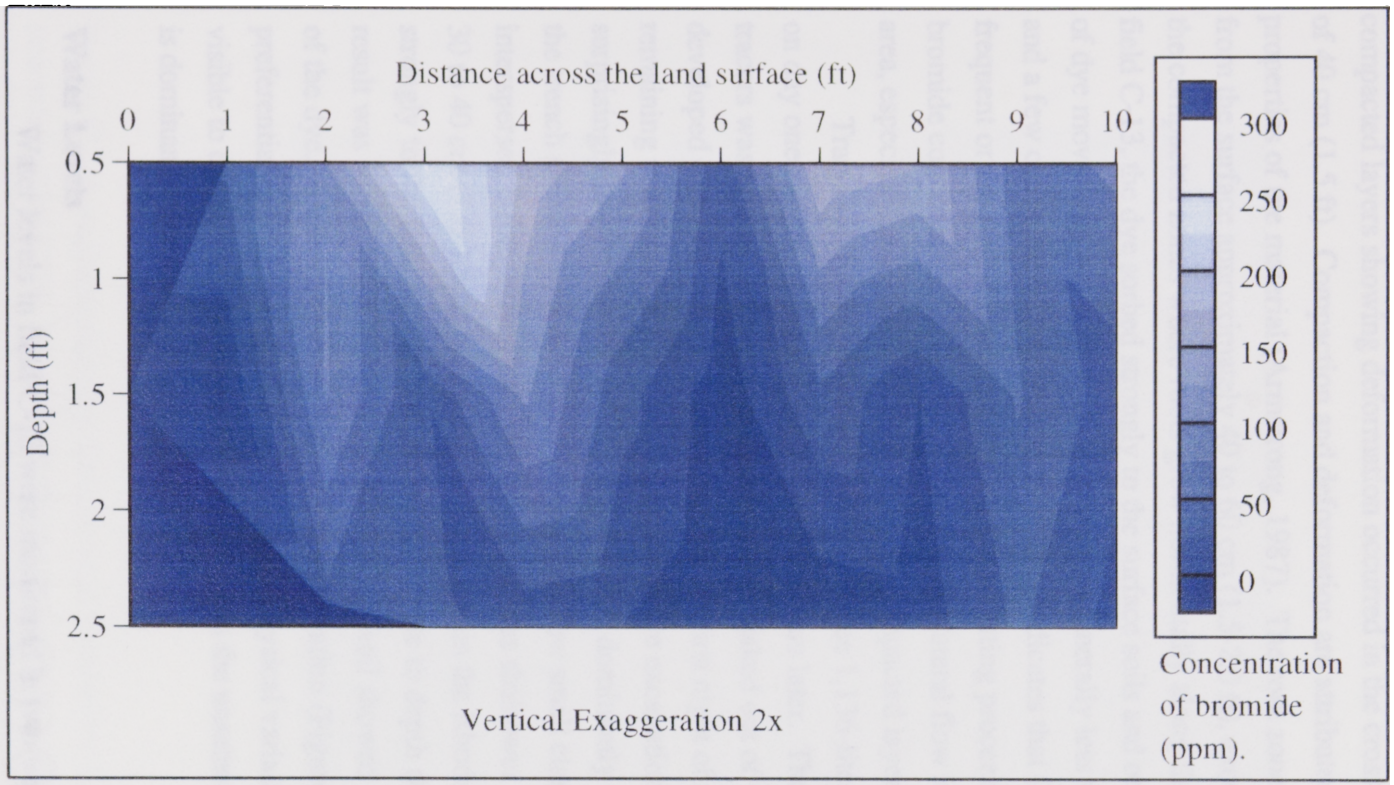

Figure 16. Soil cross section for field C-13 showing bromide concentration during tracer tests.

showed a uniform dark brown soil similar to that found in field C-13. Two dense compacted layers showing deformation occurred in the cross-section at a depth of 40 cm (1.5 ft). Compaction and deformation are attributed to the shrink/swell properties of the material (Armstrong, 1987). The root zone extended down from the surface approximately 40 to 60 cm (1.5-2.0 ft), except in the areas of the compacted zones where roots grew horizontally along the top edge. As in field C-13, the dye sorbed strongly to the surface soils and only a small amount of dye movement was visible along structures generally less than 1 cm in width and a few centimeters long (Figure 17). This indicates that fractures are less frequent or are sealed by expanding clays as wetting proceeds. A contour plot of bromide concentration (Figure 18) showed that lateral flow is dominant in this area, especially in response to more densely compacted layers.

Tracers in field C-32 were applied in three 1,136-liter batches; 2,272 liters on day one and an additional 1,136 liters 24 hours later. The third batch of tracers was applied after a great deal of water leaked out of the ring at a hole that developed (likely dug by an animal) during the first night of the test. All remaining water was pumped off 12 hours before excavation. This site showed a surprisingly low infiltration rate for a soil that is dominantly sand. Excavation of the trench showed a uniform sand layer with a few small clasts of clay interspersed through the area. The root zone was shallower here extending only 30 to 40 cm (1.0-1.5 ft) below the surface. Again the Rhodamine WT sorbed strongly to the land surface and did not penetrate to depth (Figure 19). This result was surprising because lab tests with this soil showed virtually no sorption of the dye. A contour plot of bromide concentration (Figure 20) showed good preferential movement of water, although no physical variations in the soil were visible to explain this movement. Water flow in the unsaturated zone of this field is dominantly vertical.

Water Levels

Water levels in field C-13 were monitored in two wells, C-13 A and C-13 B. Here the water table has apparently reached steady state with only

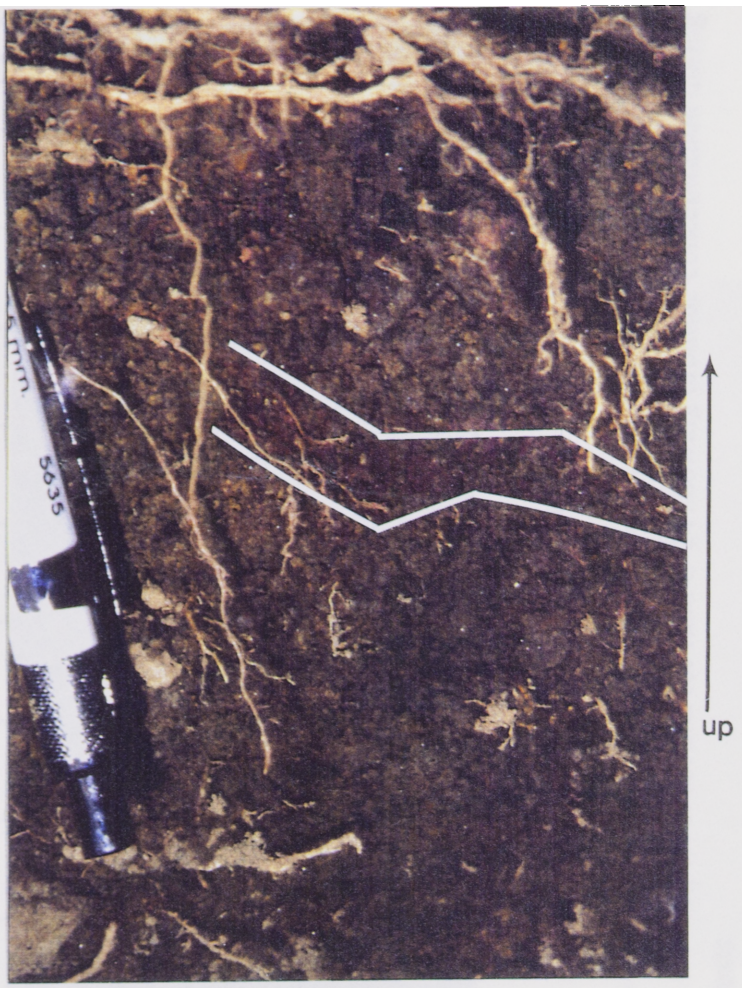

Figure 17. Photograph showing movement of Rhodamine WT along a soil structure in field C-24. Photograph shows dye movement along small macropores.

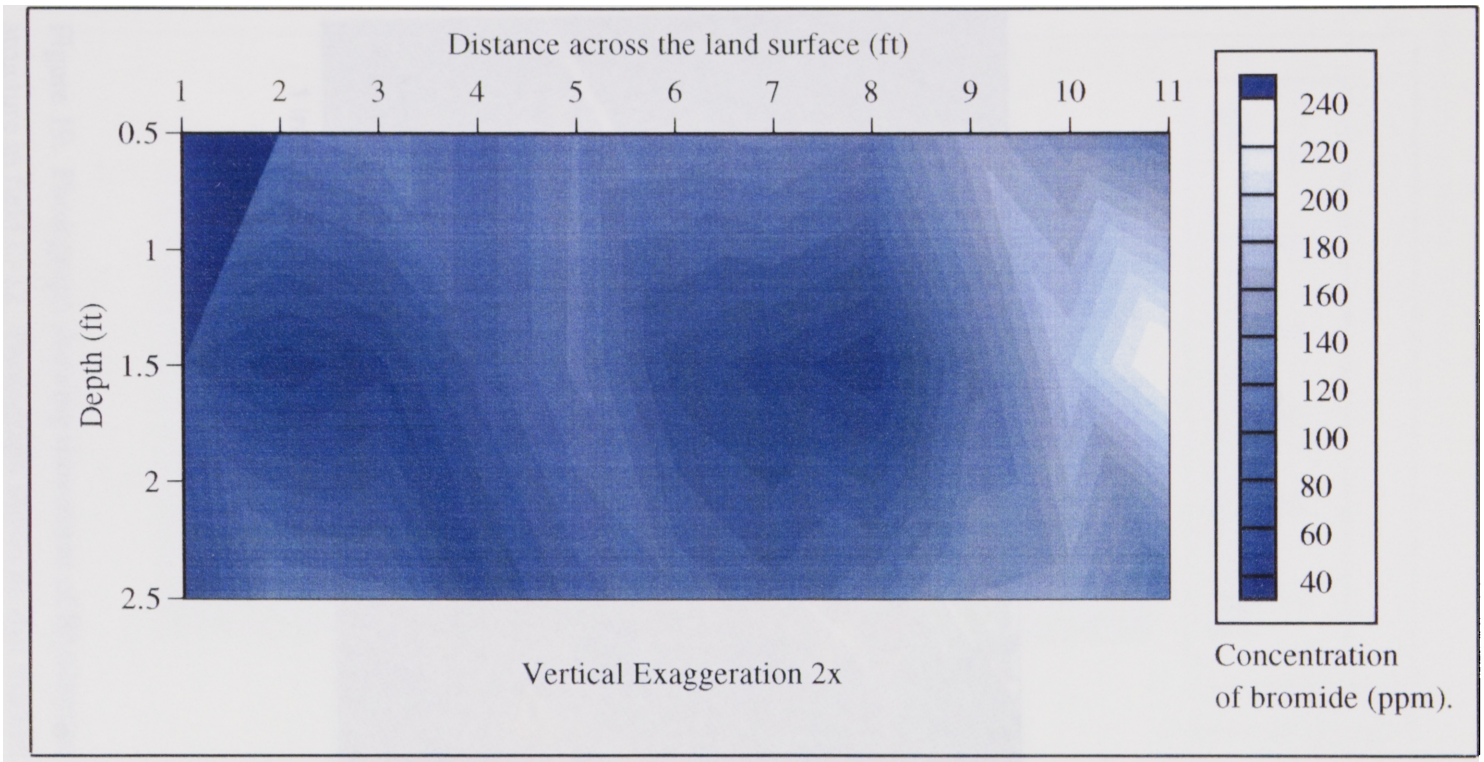

Figure 18. Soil cross section for field C-24 showing bromide concentration during tracer tests.

Figure 19. Photograph showing movement of Rhodamine WT along a soil structure in field C-32. Photograph shows no dye marked flow paths.

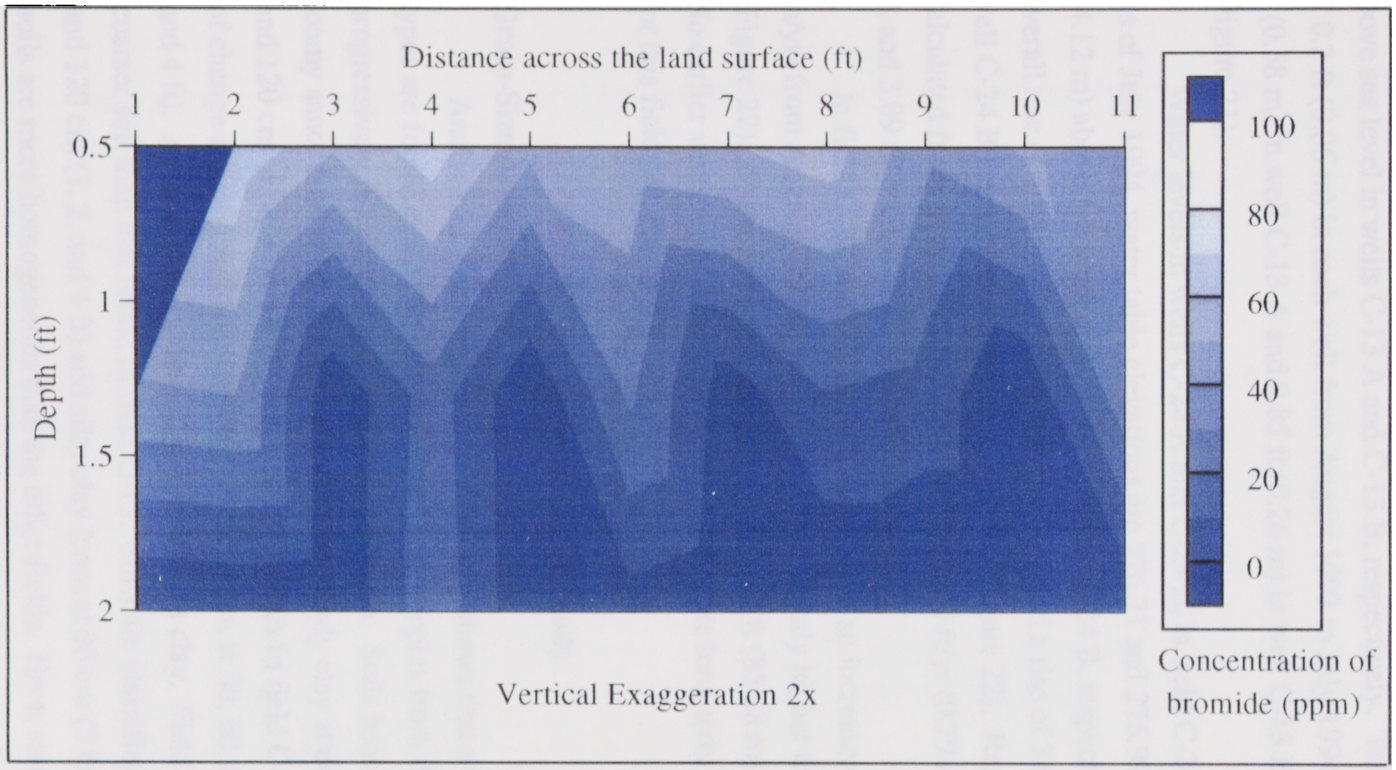

Figure 20. Soil cross section for field C-32 showing bromide concentration during tracer tests.

minor fluctuations. Elevations are 346.60 and 345.55 ft (105.64 and 105.32 m) above sea level in wells C-13 A and C-13 B, respectively. This is an overall drop of 0.2 ft (0.06 m) in each well from August 1993 to July 1994 and a drop of 1.93 ft (0.58 m) in well C-13 A and 0.85 ft (0.26 m) in well C-13 B since April 1992 (Figure 21).

Water levels in wells C-24 A and C-24 B, in field C-24, continue to rise. As of July 1994, water table elevations are 276.71 and 275.99 ft (84.34 and 84.12 m) above sea level in wells C-24 A and C-24 B, respectively. This gives an overall rise of 1.88 ft (0.57 m) in well C-24 A and a rise of 3.99 ft (1.22 m) in well C-24 B from August 1993 to July 1994 (Figure 22). Resaturation rates, calculated from April 1992 to July 1994, are 2.60 ft/yr (0.79 m/yr) for well C-24 A and 3.09 ft/yr (0.94 m/yr) for wells C-24 B.

In field C-32, well C-46-R-92 has shown an increase of 4.38 ft/yr (1.34 m/yr) from August 1993 to July 1994, a rate slightly higher than field C-24 (Figure 22). The water table elevation is 279.80 ft (85.28 m) above sea level. No earlier water level data is available to calculate long term resaturation rates for this field (Appendix C).

Laboratory Methods

Grain-Size Analysis

Analysis of soil samples from each field shows that a wide variety of soil types are found at the Big Brown Mine. Soil samples from the field UM get progressively finer moving down the soil column. Soils here are classified as loamy sand, sandy clay loam, sandy clay and sandy clay at depths of 30, 60, 90, and 120 cm (1, 2, 3, and 4 ft), respectively. Soils in field C-13 show no pattern of change at depth and are classified as clay loam at 30, 60, and 120 cm (1, 2, and 4 ft). At 90 cm (3 ft), the soil is classified as clay. Field C-24 has a slightly coarser soil than that found in field C-13. Soils are classified as loam at 30, 60, and 120 cm (1, 2, and 4 ft) and silty clay loam at 90 cm (3 ft) deep. Field C-32 soils are more homogeneous than the other fields. Here, sand dominates the soil giving a soil type of sandy loam at 30, 90, and 120 cm (1, 3, and 4 ft). At 60 cm

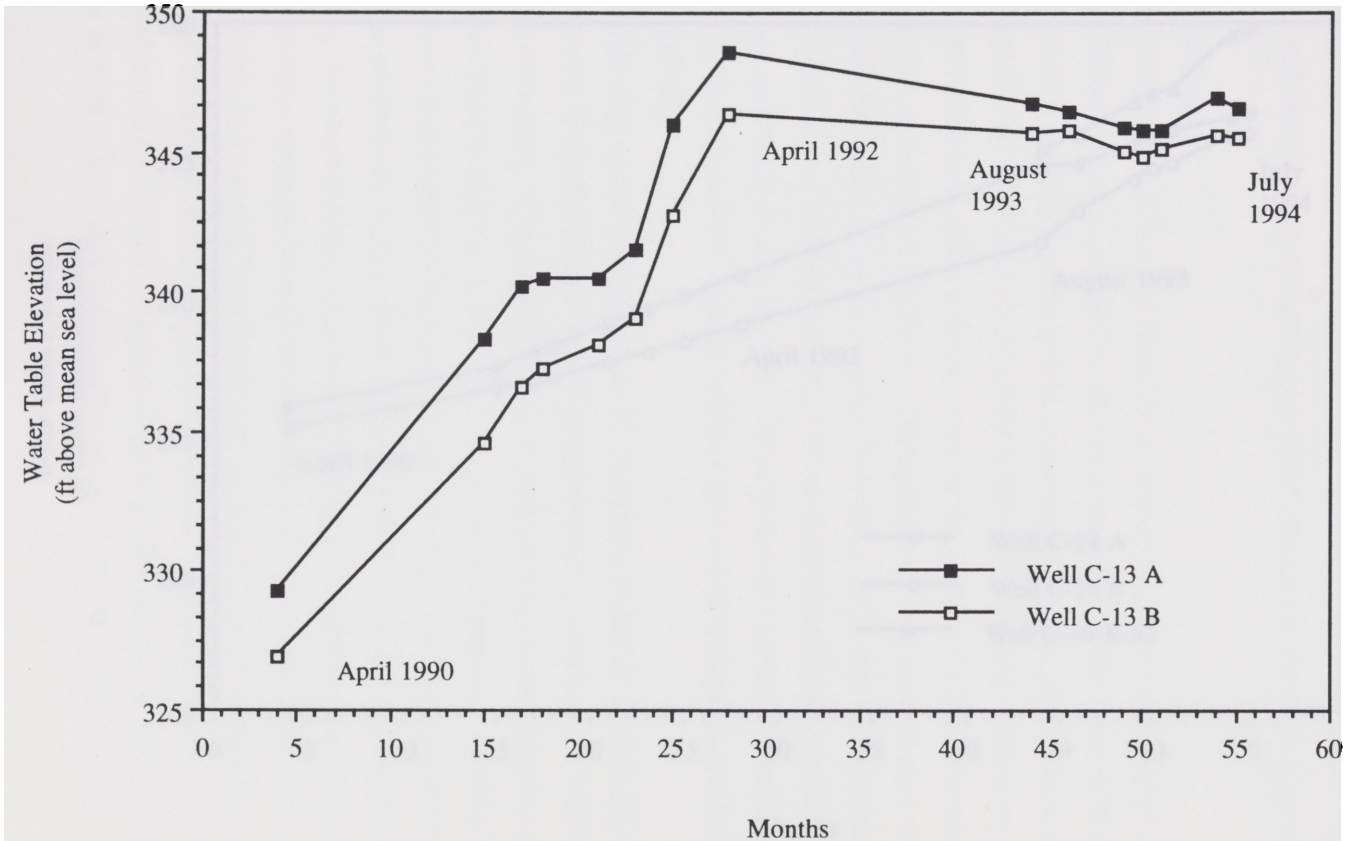

Figure 21. Well C-13 A and C-13 B hydrographs.

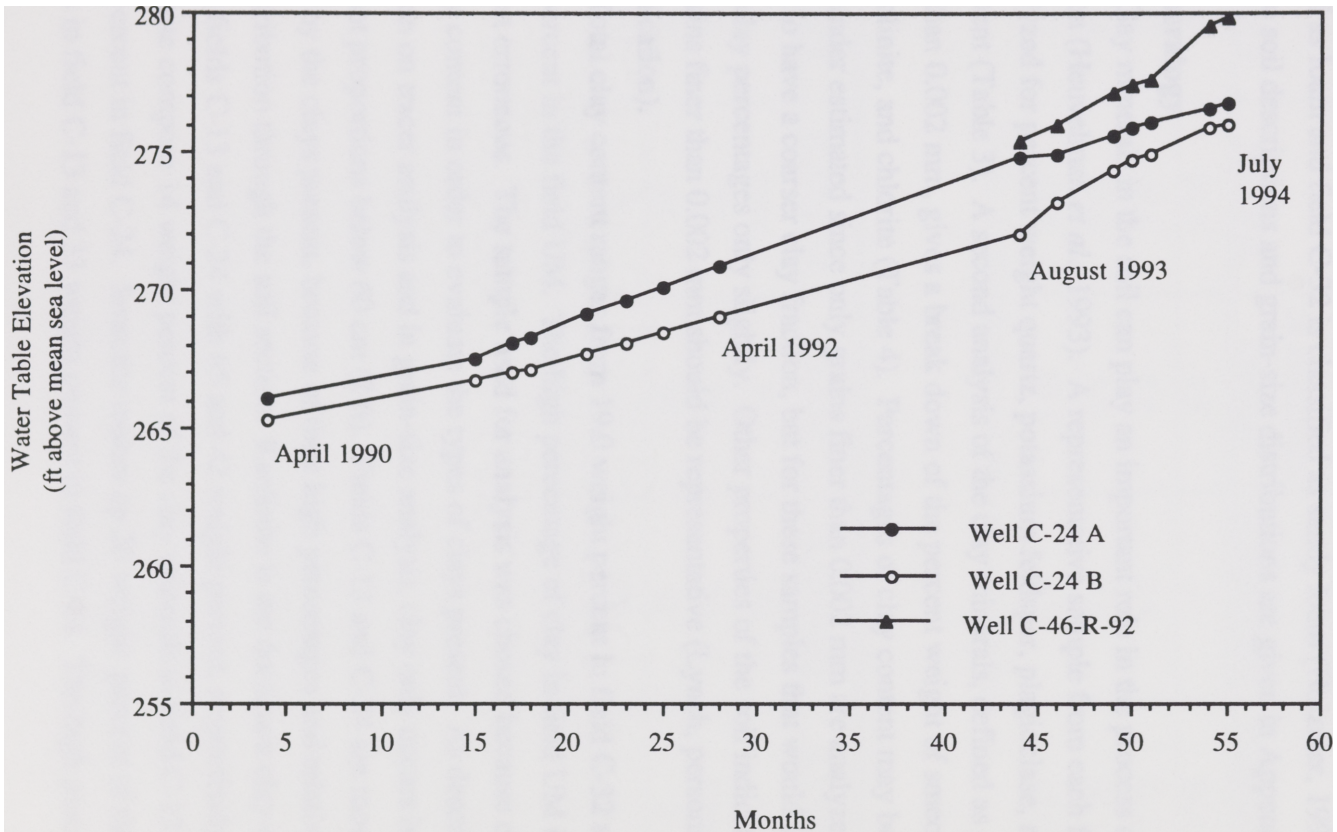

Figure 22. Well C-24 A, C-24 B, and C-46-R-92 hydrographs.

(2 ft), a slightly higher percentage of sand gives a soil type of loamy sand (Figure 23). These results are congruent with a post-mine soil survey done at the mine in 1989. From that survey, field C-13 is classified as clay loam, field C-24 is classified as loam and field C-32 is classified as sandy loam (Holzmer, 1992). Complete soil descriptions and grain-size distributions are given in Appendix D.

Soil Mineralogy

Clay minerals in the soil can play an important role in the process of infiltration (Heuvelman *et al.*, 1993). A representative sample from each field was analyzed for percent weight quartz, potassium feldspar, plagioclase, and total clay content (Table 3). A second analysis of the clay minerals, defined as grains smaller than 0.002 mm, gives a break down of the percent weight of smectite, illite, kaolinite, and chlorite (Table 4). Percentages of clay content may be slightly under estimated since only grains finer than 0.002 mm are analyzed. It is possible to have a coarser clay fraction, but for these samples that would likely bias the clay percentages only slightly. Other properties of the soil indicate that using grains finer than 0.002 mm should be representative (Lynch, personal communication).

Total clay content ranges from 19.0 weight percent in field C-32 to 59.1 weight percent in the field UM. The high percentage of clay in field UM is somewhat erroneous. The sample used for analysis was chosen because of its high clay content in order to evaluate the types of clays present. As described in the section on tracer analysis and in grain-size analysis, clay only occurs in significant proportions below 60 cm (2 ft). Fields C-13 and C-24 are most affected by the clays present, because of their high percentages and relatively even distribution through the soil section. Kaolinite is the dominant clay mineral found in fields C-13 and C-24 with 65 and 42 weight percent, respectively. Illite and chlorite compose 14 weight percent of the clay minerals in field C-13 and 26 weight percent in field C-24. Smectite makes up 20 weight percent of the clay minerals in field C-13 and 33 weight percent in field C-24. The high percentage

of smectite in field C-24 may account for the compacted and deformed zones seen in the soil cross-section during the tracer test.

Sample #	% Quartz	% Potassium Feldspar	% Plagioclase	% Total Clay
UM	34.5	7.5	--	58.1
C-13	49.4	5.4	3.7	41.6
C-24	35.6	5.0	3.3	56.1
C-32	53.4	20.8	6.9	19.0

Table 3: Weight percent mineral composition.

Sample #	% Smectite	% Illite	% Kaolinite	% Chlorite
UM	trace	30	70	--
C-13	20	14	65	trace
C-24	33	23	41	3
C-32	7	22	70	--

Table 4: Weight percent clay mineral composition.

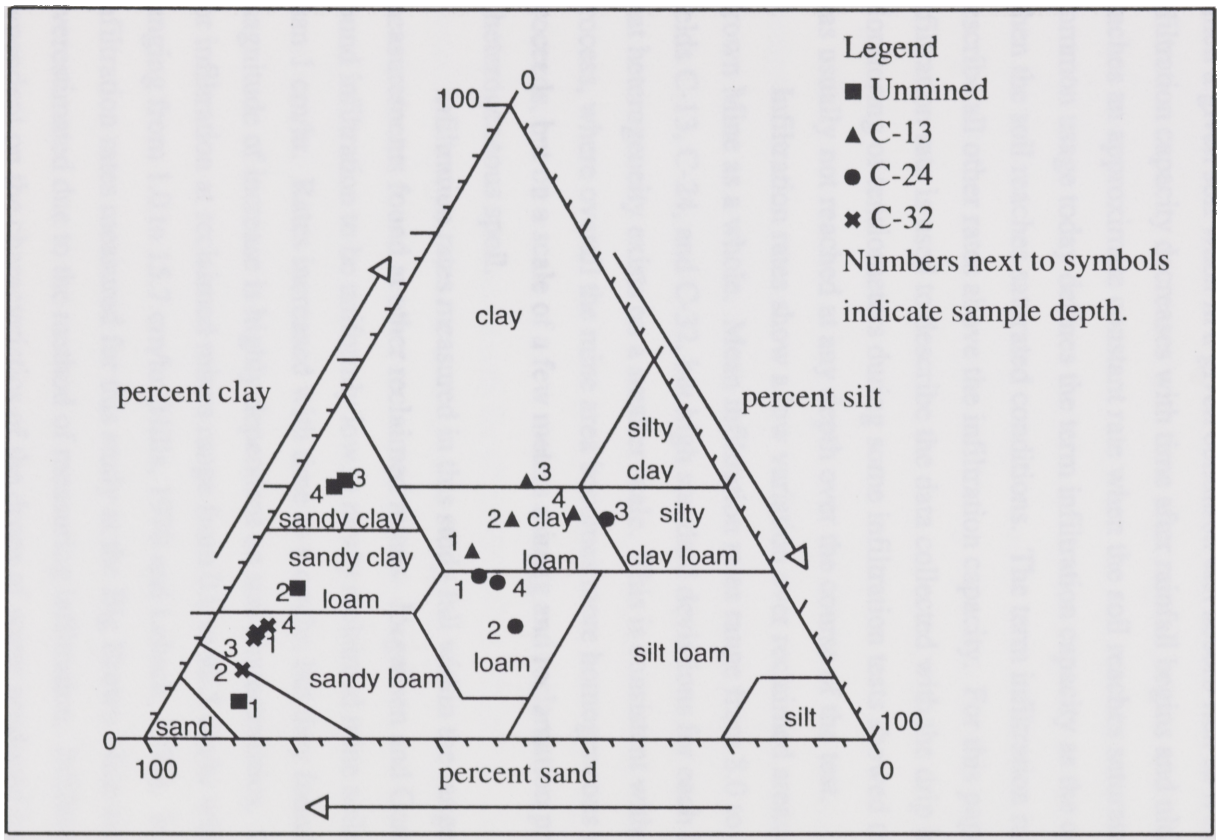

Figure 23. Distribution of soil types in study areas.
(Unified Soil Classification System, 1953)

Infiltration Rates and Influencing Factors

Horton (1940) defined infiltration capacity as "the maximum rate at which a given soil when in a given condition can absorb rain as it falls". The infiltration capacity decreases with time after rainfall begins and ultimately reaches an approximate constant rate when the soil reaches saturated conditions. Common usage today defines the term infiltration capacity as the constant rate when the soil reaches saturated conditions. The term infiltration rate is used to describe all other rates above the infiltration capacity. For this paper, the term infiltration rate is used to describe the data collected with the drip infiltrometer. Monitoring of tensiometers during some infiltration tests showed that saturation was usually not reached at any depth over the course of the test.

Infiltration rates show a low variation over reclaimed areas of the Big Brown Mine as a whole. Mean infiltration rates range from 8.0 to 10.5 cm/hr for fields C-13, C-24, and C-32, but high standard deviations for each field indicate that heterogeneity exists on a smaller scale. This is consistent with the mining process, where overall the mine area becomes more homogeneous as mining proceeds, but on a scale of a few meters mining and reclamation processes create a heterogeneous spoil.

Infiltration rates measured in this study fall within the range of measurements found at other reclaimed mines. Jorgensen and Gardner (1993) found infiltration to be uniformly low in newly reclaimed mine soils, generally less than 1 cm/hr. Rates increased with time to 6 cm/hr, but they found that the magnitude of increase is highly dependent on soil characteristics. Other estimates for infiltration at reclaimed mines range from 0.0 to 92.5 cm/hr with mean values ranging from 1.0 to 15.7 cm/hr (Hills, 1970 and Lehsch, 1979). It is possible that infiltration rates measured for this study at the Big Brown Mine are overestimated due to the method of measuring infiltration. Infiltration is dependent on the characteristics of the drops of water produced by the infiltrometer. Of particular importance is the drop energy at impact and rainfall intensity. Since most rainfall events at the Big Brown Mine are high intensity

events, drops would impact the soil at terminal velocity. The drip infiltrometer used for this study has a maximum drop height of 1 m (3.25 ft) and delivers drops at approximately 50 percent of terminal velocity. This lower energy may cause infiltration rates to be over estimated (Hosner, personal communication). On bare soil this is a critical factor causing a significant over estimation of the rates, but on well vegetated soils, such as those found in this study, the effect would be less extreme. The rainfall intensity used for these tests was very high at 31 cm/hr (12.2 in/hr). Using a high intensity rainfall event guaranteed that runoff would occur early in the test making it possible to determine an infiltration rate at each time step to determine an infiltration curve for each field (Figures 24, 25, 26, and 27).

Factors that influence the infiltration rates at the Big Brown Mine are dominated by the effects of mining and reclamation and seasonal soil moisture content with lesser effects from soil heterogeneity, and saturated hydraulic conductivity. Infiltration rates for field UM are 53 percent higher than rates in mined and reclaimed areas indicating that these processes significantly lower infiltration rates. Seasonal soil moisture content is also very important in determining infiltration rates. A good correlation of higher infiltration rates and low soil moisture content exists for all fields tested. Figure 28 shows two clusters of data points with data collected in the early fall clustering at the dry end of the scale, with soil suction ranging from 44 to 78 centibars. Data for winter tests cluster around the wet end of the scale with soil suction values in the range of 0 to 15 centibars. Data for the summer show a wider scatter than those points measured in the winter. This indicates that infiltration and soil moisture content is more heterogeneous in the dryer summer months than in the winter, where soil moisture is relatively constant.

The effects of soil texture, soil mineralogy, and saturated hydraulic conductivity on infiltration rates is less well understood. Coarser soils like those found in field C-32 would be expected to show a higher infiltration rate than the finer soils of C-13 and C-24. Instead, C-32 has an intermediate value of

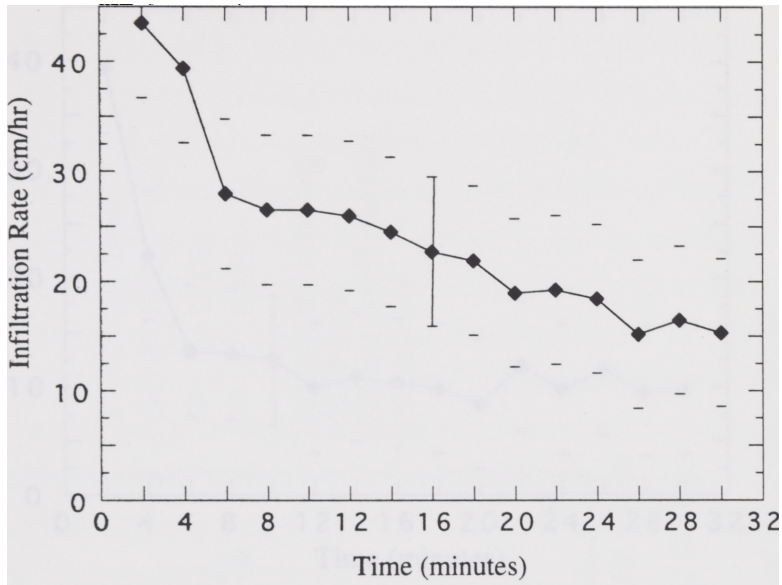

Figure 24. Average infiltration curve measured in field UM. A standard deviation of 6.8 is shown by the dashed lines above and below the curve.

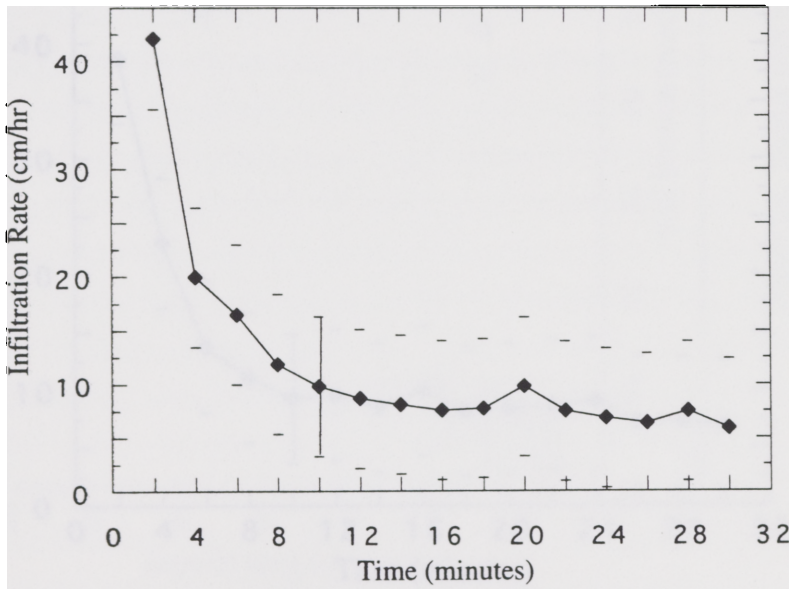

Figure 25. Average infiltration curve measured in field C-13. Standard Deviation=6.5

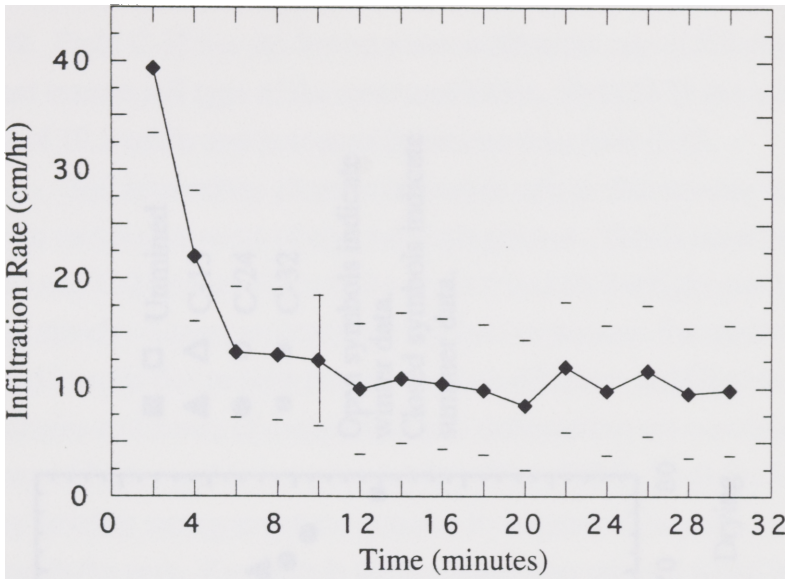

Figure 26. Average infiltraton curve measured in field C-24. Standard Deviation=6.0

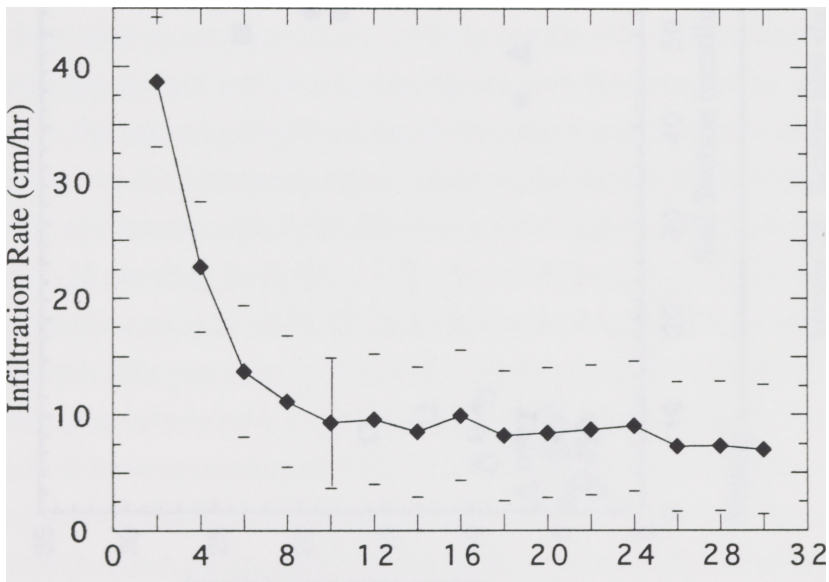

Figure 27. Average infiltration curve measured in field C-32. Standard Deviation=5.6

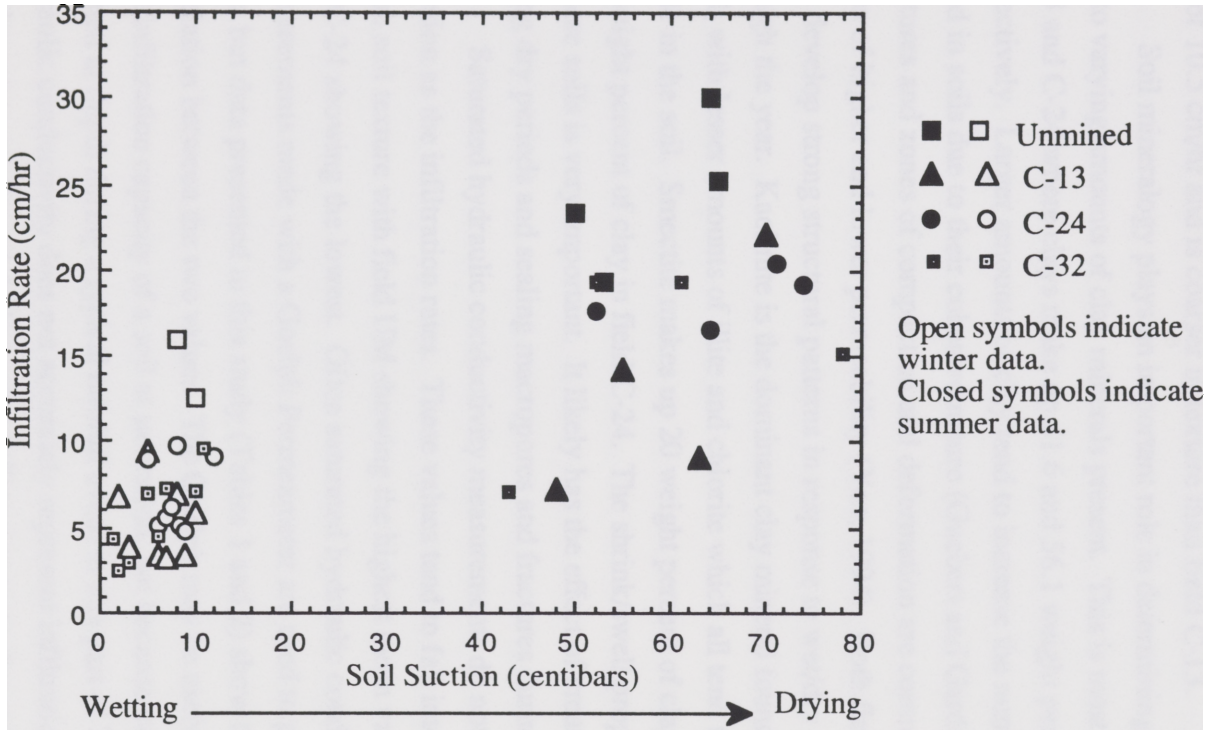

Figure 28. Scatter plot showing range of infiltration rates in responce to soil moisture content.

8.9 cm/hr; the lowest infiltration rate of 2.6 cm/hr was also measured in field C-32. Field C-13 has the lowest mean infiltration rate of 8.0 cm/hr with the finest texture soil type of the measured fields. Field C-24 has a higher infiltration rate of 10.5 cm/hr and is coarser in texture than field C-13.

Soil mineralogy plays an important role in determining infiltration rates due to varying amounts of clay minerals present. This is most important in fields C-13 and C-24 where clays make up 41.6 and 56.1 weight percent of the soil, respectively. Larger amounts of clay tend to increase the number of structures found in soils due to their cohesive nature (Guebert and Gardner, 1992). Fractures and zones of compaction and deformation are common and create zones of higher and lower permeability (Yao, 1994). Both fields C-13 and C-24 may develop strong structural patterns in response to wet/dry cycles seen through the year. Kaolinite is the dominant clay mineral found in fields C-13 and C-24, with lesser amounts of illite and chlorite which all tend to be physically stable in the soil. Smectite makes up 20 weight percent of clay in field C-13 and 33 weight percent of clay in field C-24. The shrink/swell properties of smectite in these soils is very important. It likely has the effect of creating more fractures during dry periods and sealing macropores and fractures during wetting cycles.

Saturated hydraulic conductivity measurements do not show as much variation as the infiltration rates. These values tend to fall into ranges predicted by the soil texture with field UM showing the highest mean value and fields C-13 and C-24 showing the lowest. Often saturated hydraulic conductivity measurements made with a Guelph Permeameter are used to predict infiltration rates, but data presented in this study (Tables 1 and 2) show that there is no correlation between the two values. The Guelph may be useful in calculating the final infiltration capacity of a soil at saturation, but because saturation is not reached at depth during a typical rainfall event in this part of Texas the saturated hydraulic conductivity does not accurately represent infiltration rates. Tensiometers monitored during some infiltration tests showed that saturation below the surface is not reached during a 30 minute test. Usually two hours were required for the tensiometer installed at 30 cm (1 ft) to indicate saturation.

Surface runoff usually began 2 to 4 minutes into a test indicating that the infiltration capacity of the soil had been exceeded and that the surface soil was saturated. This rapid surface saturation is attributed to the very high intensity rain fall event created over the plot. In a natural rainfall event, intensity is usually not this high, so surface saturation takes longer to reach.

The spoil of field C-32 was placed with the XPS. This may help explain its lower infiltration rates. Because the XPS system breaks up the sediments more than the draglines, a more homogeneous spoil is formed. The trench dug for the tracer tests showed a very uniform spoil material with little structure development. It is difficult to compare hydrogeologic properties of areas with dragline placed spoil and areas of XPS placed spoil directly because they are used on two different soil types. The XPS is used to mine sand rich sediments while draglines are used to mine the silt and clay sediments of the area. Therefore, two distinctly different spoils are created.

Unsaturated zone tracer tests showed that bypass flow does exist in some of the reclaimed mine soils. Rhodamine WT sorbed strongly to the surface soil and did not show much movement at depth in the reclaimed areas. Dye in fields C-13 and C-24 did show some movement along structures in areas of the cross-section. Bromide tracing proved very useful in showing preferential flow paths in all four fields of study. High concentrations of bromide did occur in discrete regions in all cross-sections. Bromide was also detected out of those regions at lower concentrations indicating that flow also occurs through the matrix of the soil and not just along channels. Concentration plots of bromide show two distinct patterns in the fields tested. In fields UM and C-24, lateral flow dominates water movement in the unsaturated zone. In field UM, this flow is along a contact between two soil types; in field C-24 the lateral flow is along zones of compaction. Fields C-13 and C-32 are dominated by vertical flow.

Overall, no one factor can explain all the variations in infiltration rates seen across the area of the mine. Mining and reclamation reduce infiltration rates from pre-mine values, but variations in reclaimed areas are difficult to attribute to any one variable. All properties including, soil texture, ambient soil moisture

content, spoil mineralogy, and method of spoil placement effect infiltration to varying degrees.

The point of this study was to determine if variations in infiltration control variations in resaturation. Simply put, it is unlikely that the small variations in infiltration rates seen in fields C-13 and C-24 could account for their large differences in resaturation. Data from this study combined with resaturation rates from Holzmer (1992) show that an inverse relationship exists between resaturation and infiltration rates. A possible explanation for this inverse relationship could lie in the type of groundwater flow dominant in each field. By examining data from the tracer tests, we see that water flow was dominantly vertical in field C-13, whereas in field C-24 much of the flow was lateral around zones of compaction. An earlier study by Dutton (1982) found lateral flow to occur in areas of the mine, while no saturated zone was forming. For field C-24, lateral flow through the area could slow resaturation rates, because infiltrated water may flow out of the area as interflow instead of recharging the groundwater system.

However, can the small areas used in the tracer tests represent properties over an entire field? This question is particularly difficult to answer. On a small scale, reclaimed mine soils are very heterogeneous, so the compacted zone in field C-24 could occur in an isolated area, but it is also possible that it represents the general trends seen throughout the field. An argument can be made that the small areas used for tracer tests represent properties over the whole field. For this study, a single soil core was collected in each field to determine a grain-size distribution. The post-mine soil survey collected samples every 61 m (200 ft) across the fields for the same purpose (Holzmer, 1992). Both samplings gave the same soil classification for every field, one based on a single sample and the other based on multiple sampling points. It is possible that the small areas used for the tracer tests are representative of the field as a whole, making the characteristics determined there valid for a larger area.

Groundwater Resaturation Model

A numerical model was used to simulate groundwater flow along a cross-sectional line extending from field C-13 to field C-24 by solving for a distribution of hydraulic head in a two-dimensional region. The observed variations in resaturation rates imply that variations in hydraulic properties exist in these two fields. Properties that may be different between the two fields include hydraulic conductivity, storativity, and recharge. This model mathematically tests the effects of variations in hydraulic conductivity and recharge on the groundwater flow system and attempts to match hydraulic head values in wells C-13 A, C-13 B, C-24 A, and C-24 B for three dates, April 1992, August 1993 and July 1994.

This model is based on the cross-sectional system developed by Toth (1962), which was used to determine an analytical solution for hydraulic head distribution. The original system consisted of no-flow boundaries along the sides and bottom usually at groundwater divides and points of discharge, while the top of the cross-section represented the water table. The solution by Toth required a homogeneous, isotropic, steady-state flow system, but the model used for this study simulates resaturation through time requiring a transient-state flow system, which can also be programmed as heterogeneous and anisotropic.

Conceptual Model

The hypothesis to be tested with this model is:

> Are variations in hydraulic conductivity and/or recharge responsible for variations measured in the resaturation rates of fields C-13 and C-24?

This model tests hydraulic conductivity and variable recharge individually to determine a distribution of hydraulic head along a cross-section line between these fields. A node-centered finite difference grid is laid along the cross-section line A-A' (Figure 6) extending from field C-13 to field C-24. The grid for this problem consists of 5 rows and 480 columns with a node spacing of 25 ft (7.6 m) along both the X and Z axes, for a total length of 12,000 ft (3,658 m) and a depth

of 125 ft (38 m). Initial hydraulic head values and calibration points are based on field data from 1991 to 1994. Table 5 shows the initial head values for wells C-13 A, C-13 B, C-24 A and C-24 B, along with the calibration points for 1992 to 1994.

Well #	March 1991 (0 days)	April 1992 (400 days)	August 1993 (950 days)	July 1994 (1300 days)
C-13 A	338.28 ft	348.53 ft	346.80 ft	346.95 ft
C-13 B	334.60 ft	346.40 ft	345.73 ft	345.60 ft
C-24 A	267.48 ft	270.86 ft	274.83 ft	276.56 ft
C-24 B	266.75 ft	269.04 ft	273.19 ft	275.88 ft

Table 5. Initial and calibration points for groundwater resaturation models.

Four conceptual models were tested for this system. Hydraulic properties were varied as follows:

1. Homogeneous and isotropic: hydraulic conductivity and recharge are constant across the grid.
2. Heterogeneous and isotropic: horizontal and vertical hydraulic conductivity are equal at a point, but decrease with depth. Recharge is constant.
3. Heterogeneous and anisotropic: horizontal and vertical hydraulic conductivities have different values depending on their field location and depth. Recharge is constant.
4. Heterogeneous and isotropic: horizontal and vertical hydraulic conductivity are equal at a point, but decrease with depth. Recharge varies along the cross-section.

Boundary Conditions, Initial Conditions, and Assumptions

A transient-state, 2-dimensional, finite difference flow model was programmed in FORTRAN 77 along a cross-section line (A-A') extending from

the west end of field C-13 to the east end of field C-24. Boundaries are defined as no-flow along the west edge at a groundwater divide, no-flow along the east at the contact between the spoil material and unmined material, and no-flow along the bottom of the cross-section at an impermeable clay layer found at the base of the mine (Figure 29). The no flow boundary along the east edge of the model at the contact between the spoil and unmined material, is likely a seepage face with some flow occurring out of the spoil and into the unmined sediment. Because of changes in hydraulic conductivity, flow conditions at this boundary are not known with any certainty. For simplification of the model, this boundary is treated as no flow. This simplification is acceptable because of the relatively long distance between the wells in field C-24 and the boundary.

Initial conditions are set at wells C-13 A, C-13 B, C-24 A, and C-24 B for March 1991. These water table elevations occur at time zero in the model. Time steps of 1 day are used to move forward in time to points of interest at April 1992 (400 days), August 1993 (950 days), and July 1994 (1300 days).

Mathematically, the system is treated as a quasi-confined aquifer with uniform thickness. This assumption allows the use of a rectangular finite difference grid that would be used in a confined aquifer model, but also allows for the use of a storativity coefficient of an unconfined aquifer. This simplifies the program by eliminating the need to add new nodes to the grid over time due to resaturation.

Mathematical Basis

The mathematical basis for this model is a transient form of Poisson's equation:

$$Kx\frac{\partial^2 h}{\partial x^2} + Kz\frac{\partial^2 h}{\partial z^2} = S\frac{\partial h}{\partial t} - R.$$

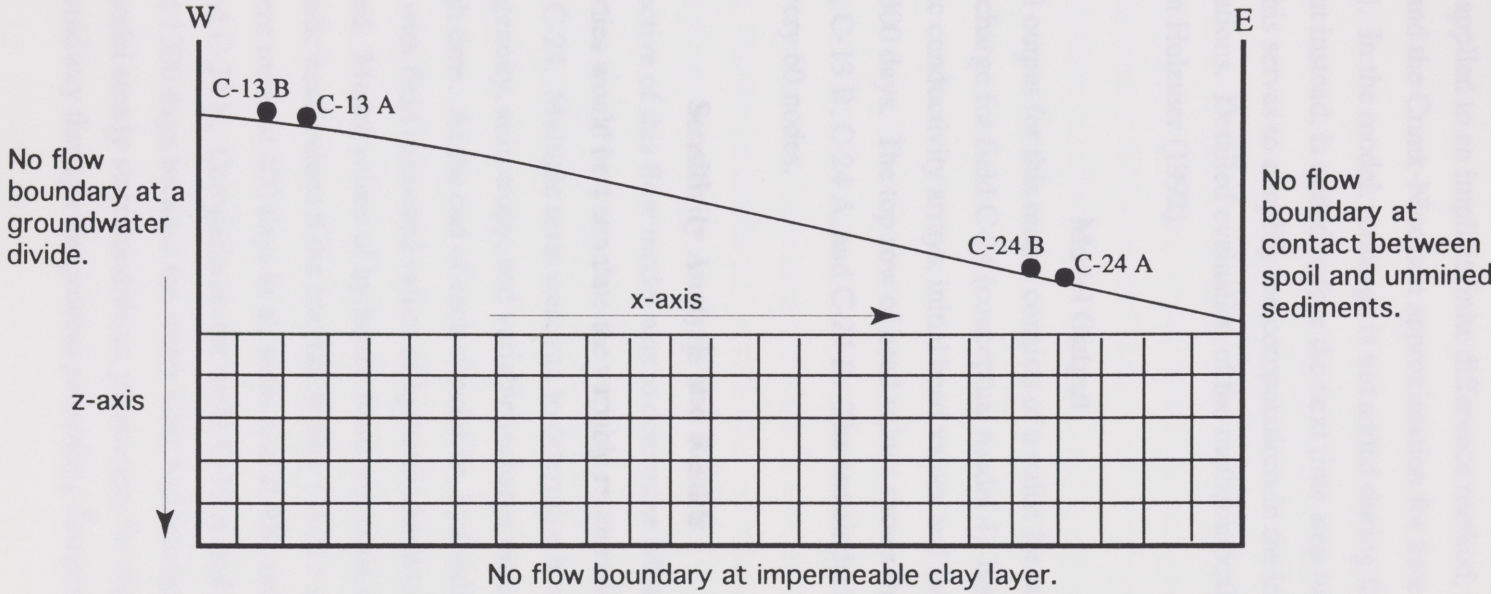

Figure 29. Conceptual model of the groundwater flow system, showing boundary conditions, approximate location of the water table, and finite difference grid. Map not to scale.

This equation is applied to an implicit finite difference method, with a Gauss-Seidel iteration and the Crank-Nicolson approximation for time steps (Wang and Anderson, 1982). In the model, recharge is not added during the calculation of the new head, but instead, is added before the next time step to the top row of image nodes. This serves to simplify the computations in the innermost loop and speed the calculations. Detailed evaluation of the mathematical basis for this model is given in Holzmer (1992).

Model Output

The final output for this model consists of a value for storativity, percentage of recharge for field C-24 (conceptual model 4), horizontal and vertical hydraulic conductivity arrays, initial head values and final head values at 400, 950, and 1300 days. The top row of head values shows the hydraulic head at wells C-13 A, C-13 B, C-24 A, and C-24 B. The remainder of the head values are printed at every 60 nodes.

Sensitivity Analysis and Results

The objective of this flow model was to determine what combination of hydraulic properties would best simulate the variable resaturation rates seen if fields C-13 and C-24. Multiple tests were run to determine how homogeneity, isotropy, heterogeneity, anisotropy, and variable recharge rates effect the water table rise through time. At the end of each simulation, hydraulic head values were compared with field measured values of hydraulic head to determine if an agreement existed. Model values of hydraulic head were said to agree with measured hydraulic head values if the two fall within 1 ft (0.3 m) of each other. Comparisons were made at 400 days in all wells and at 950 and 1300 days for wells C-24 A and C-24 B. Comparisons for wells C-13 A and C-13 B were not made at 950 and 1300 days because the water table had reached steady-state by that time. To model steady state conditions, parameters for the model would need to change midway through the process presenting complications that were

not incorporated in this model. Instead, resaturation is the only condition possible in this model.

Values of storativity, hydraulic conductivity, and recharge were based on earlier studies (Hewitt, 1990 and Holzmer, 1992). Storage coefficients (S) determined during previous modeling efforts range from 0.04 to 0.06. Initial evaluations with this model showed that the narrow range of storage coefficients did not create a significant difference in the outcome of the hydraulic head values, so an intermediate value of 0.05 was used in all 4 conceptual models. A range of hydraulic conductivities was determined by packer and slug tests for fields C-13 and C-24 (Hewitt, 1990). Values range from 2.57×10^{-4} cm/sec to 4.41×10^{-4} cm/sec for field C-13, with a mean value of 3.9×10^{-4} cm/sec (0.284 ft/day). Values range from 6.95×10^{-5} cm/sec to 6.24×10^{-6} cm/sec for field C-24 with a mean value of 4.4×10^{-5} cm/sec (0.113 ft/day). The mean hydraulic conductivity across both fields is 7.0×10^{-5} cm/sec (0.198 ft/day). Recharge by direct infiltration of precipitation was estimated from March 1991 to January 1992 (Holzmer, 1992). For the 10 month period recharge was estimated at 21.95 cm (0.72 ft). Recharge was added at a constant rate of 7.32 cm/day (2.4×10^{-3} ft/day) to the top row of nodes before the next time step of the model began. For conceptual model 4, varying amounts of recharge were applied to the nodes based on their location in the grid.

Conceptual Model 1: Homogeneous and Isotropic

Model 1 (Appendix E) simulated resaturation of the shallow spoil aquifers using the simplest conditions of homogeneous and isotropic values for hydraulic conductivity and a single value of recharge across the grid. Results showed that using a hydraulic conductivity value of 7.0×10^{-5} cm/sec (0.198 ft/day) underestimated hydraulic head values in wells C-13 A and C-13 B for 400 days and overestimated values for hydraulic head in wells C-24 A and C-24 B for 400, 950, and 1,300 days (Figure 30).

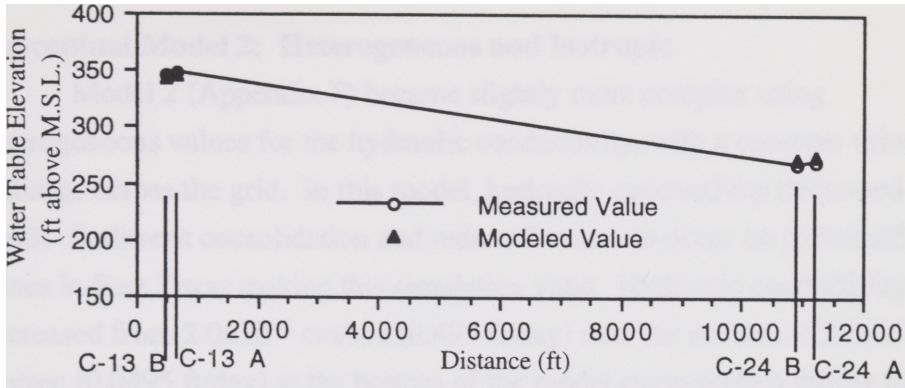

Measured and modeled hydraulic head values at 400 days.

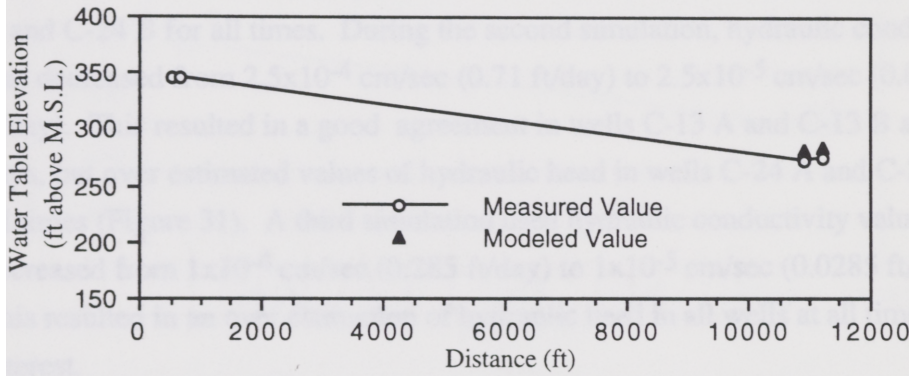

Measured and modeled hydraulic head values at 950 days.

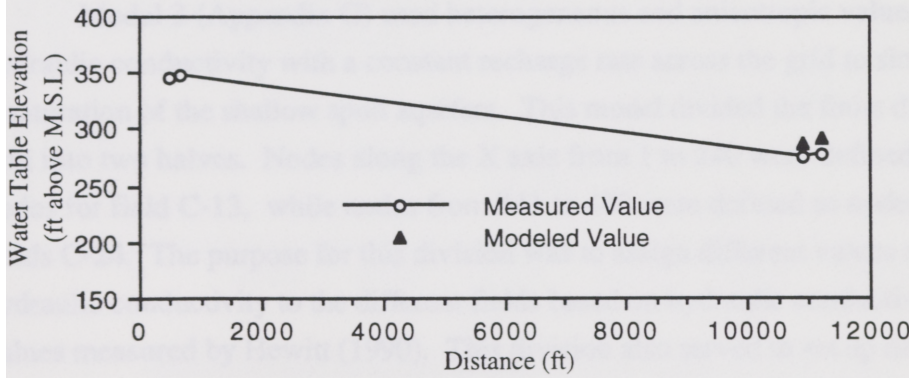

Measured and modeled hydraulic head values at 1300 days.

Figure 30. Conceptual model 1 hydraulic head values.

Conceptual Model 2: Heterogeneous and Isotropic

Model 2 (Appendix F) became slightly more complex using heterogeneous values for the hydraulic conductivity, with a constant value of recharge across the grid. In this model, hydraulic conductivity decreased with depth. Sediment consolidation and redensification do occur on reclaimed lignite mines in East Texas making this simulation valid. Hydraulic conductivity was decreased from $2.0x10^{-4}$ cm/sec (0.495 ft/day) near the surface to $2.0x10^{-5}$ cm/sec (0.0495 ft/day) at the bottom of the model cross-section during the first simulation. This resulted in a good agreement of hydraulic head values for wells C-13 A and C-13 B at 400 days, but an over estimation of values for wells C-24 A and C-24 B for all times. During the second simulation, hydraulic conductivity was decreased from $2.5x10^{-4}$ cm/sec (0.71 ft/day) to $2.5x10^{-5}$ cm/sec (0.071 ft/day). This resulted in a good agreement in wells C-13 A and C-13 B at 400 days, but over estimated values of hydraulic head in wells C-24 A and C-24 B for all times (Figure 31). A third simulation used hydraulic conductivity values that decreased from $1x10^{-4}$ cm/sec (0.285 ft/day) to $1x10^{-5}$ cm/sec (0.0285 ft/day). This resulted in an over estimation of hydraulic head in all wells at all times of interest.

Conceptual Model 3: Heterogeneous and Anisotropic

Model 3 (Appendix G) used heterogeneous and anisotropic values of hydraulic conductivity with a constant recharge rate across the grid to simulate resaturation of the shallow spoil aquifers. This model divided the finite difference grid into two halves. Nodes along the X axis from 1 to 240 were defined as nodes for field C-13, while nodes from 241 to 480 were defined as nodes for fields C-24. The purpose for this division was to assign different values of hydraulic conductivity to the different fields based on hydraulic conductivity values measured by Hewitt (1990). This division also served to set up different horizontal and vertical hydraulic conductivity arrays for each field. Tracer tests showed that in the unsaturated zone of field C-13 vertical flow was dominant, whereas in field C-24 lateral flow was dominant. By dividing the

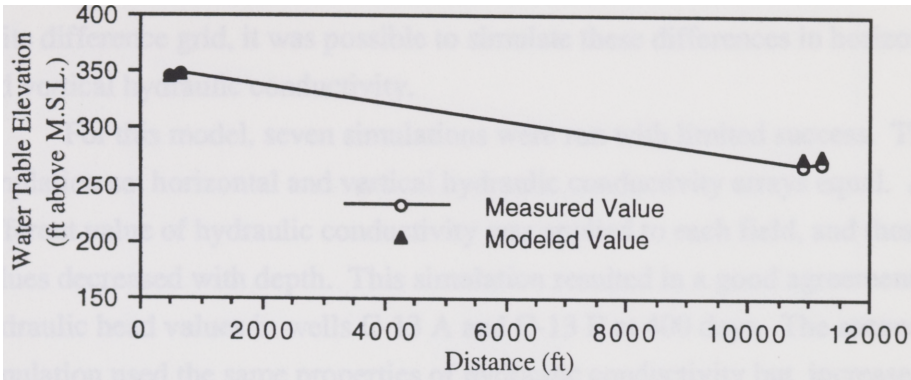

Measured and modeled hydraulic head values at 400 days.

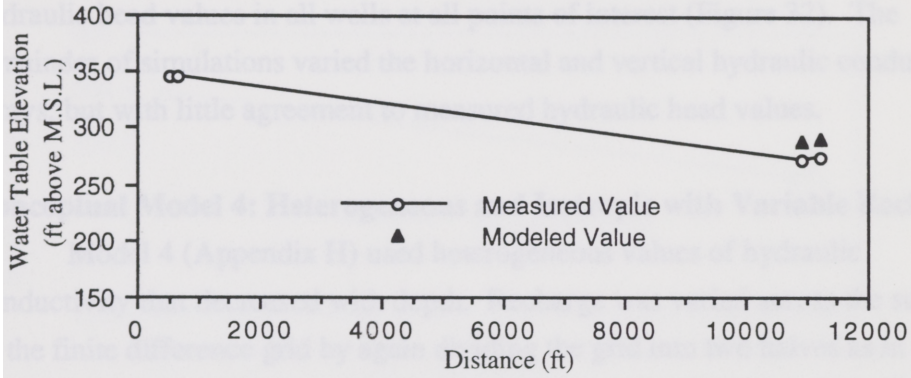

Measured and modeled hydraulic head values at 950 days.

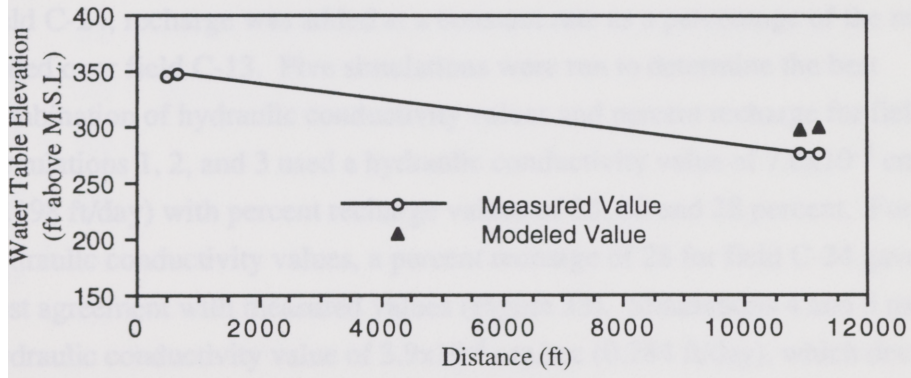

Measured and modeled hydraulic head values at 1300 days.

Figure 31. Conceptual model 2, simulation 2 hydraulic head values.

finite difference grid, it was possible to simulate these differences in horizontal and vertical hydraulic conductivity.

For this model, seven simulations were run with limited success. The first simulation set horizontal and vertical hydraulic conductivity arrays equal. A different value of hydraulic conductivity was applied to each field, and these values decreased with depth. This simulation resulted in a good agreement of hydraulic head values in wells C-13 A and C-13 B at 400 days. The second simulation used the same properties of hydraulic conductivity but increased hydraulic conductivity in field C-24. This resulted in a good agreement of hydraulic head values in all wells at all points of interest (Figure 32). The remainder of simulations varied the horizontal and vertical hydraulic conductivity arrays, but with little agreement to measured hydraulic head values.

Conceptual Model 4: Heterogeneous and Isotropic with Variable Recharge

Model 4 (Appendix H) used heterogeneous values of hydraulic conductivity that decreased with depth. Recharge was varied across the surface of the finite difference grid by again dividing the grid into two halves as in model 3. In this case, recharge was added at the constant rate of 7.32 cm/day (2.4×10^{-3} ft/day) for nodes 1 to 240 along the X axis for field C-13. For nodes 241 to 480, field C-24, recharge was added at a constant rate as a percentage of the recharge added over field C-13. Five simulations were run to determine the best combination of hydraulic conductivity values and percent recharge for field C-24. Simulations 1, 2, and 3 used a hydraulic conductivity value of 7.0×10^{-5} cm/sec (0.198 ft/day) with percent recharge values of 25, 50 and 28 percent. For these hydraulic conductivity values, a percent recharge of 28 for field C-24 gave the best agreement with measured values (Figure 33). Simulations 4 and 5 used a hydraulic conductivity value of 3.9×10^{-4} cm/sec (0.284 ft/day), which decreased with depth in the cross section. Percent recharge was tested at 30 and 32 percent of the recharge value in field C-13, with 32 percent giving the best agreement with measured values (Figure 34).

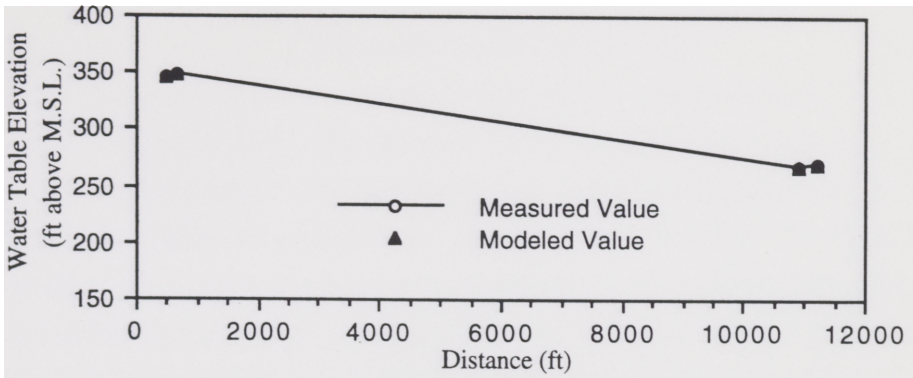

Measured and modeled hydraulic head values at 400 days.

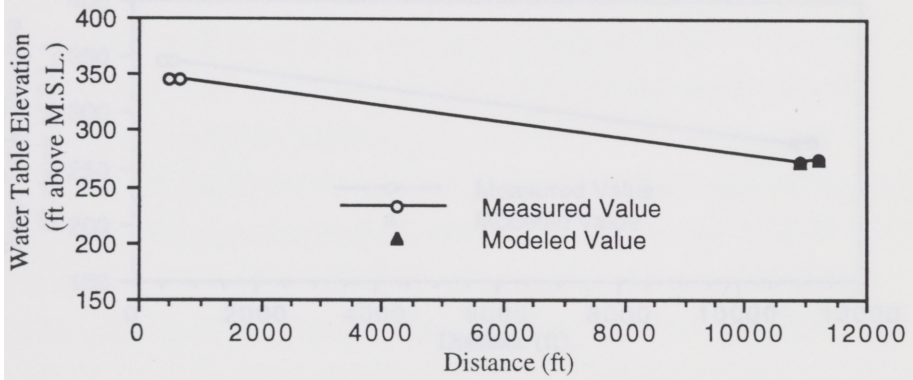

Measured and modeled hydraulic head values at 950 days.

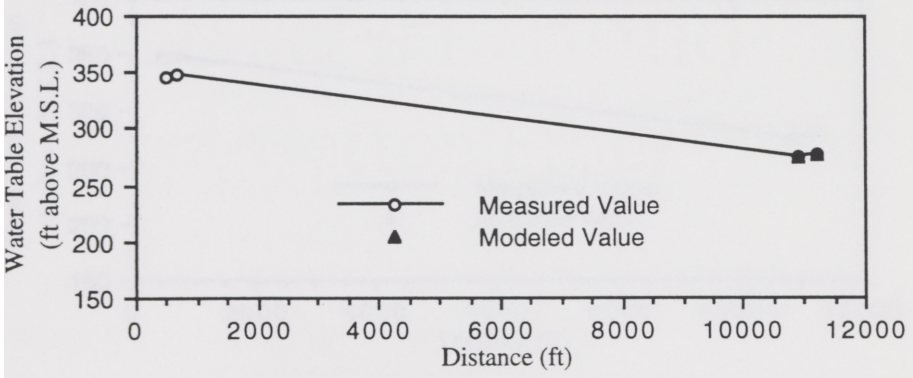

Measured and modeled hydraulic head values at 1300 days.

Figure 32. Conceptual model 3, simulation 2 hydraulic head values.

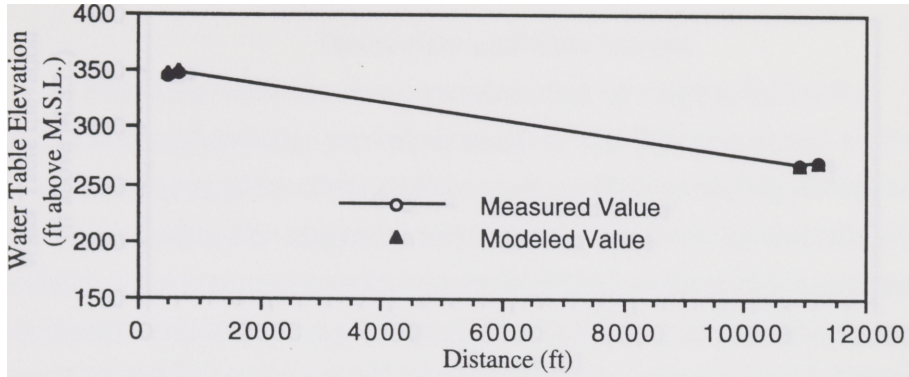

Measured and Modeled Hydraulic Head Values at 400 days.

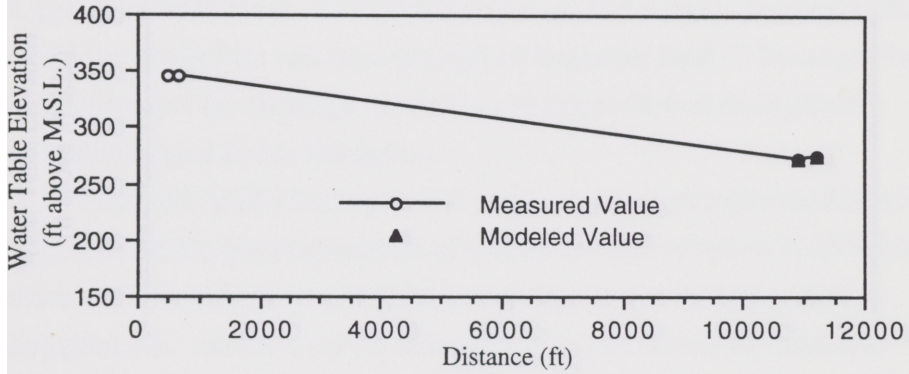

Measured and modeled hydraulic head values at 950 days.

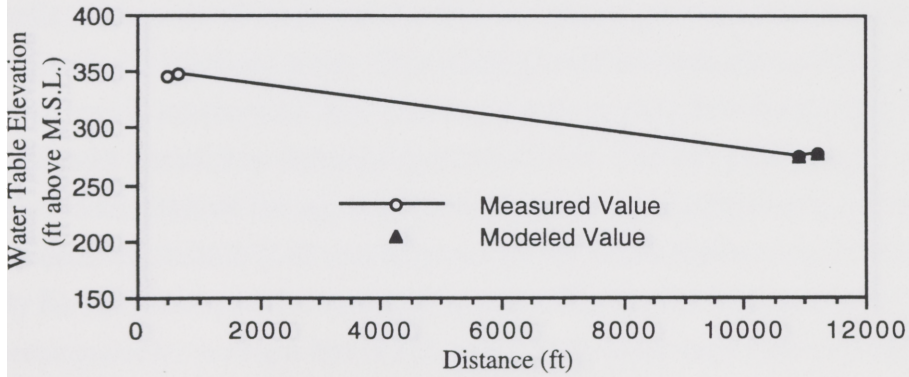

Measured and modeled hydraulic head values at 1300 days.

Figure 33. Conceptual model 4, simulation 3 hydraulic head values.

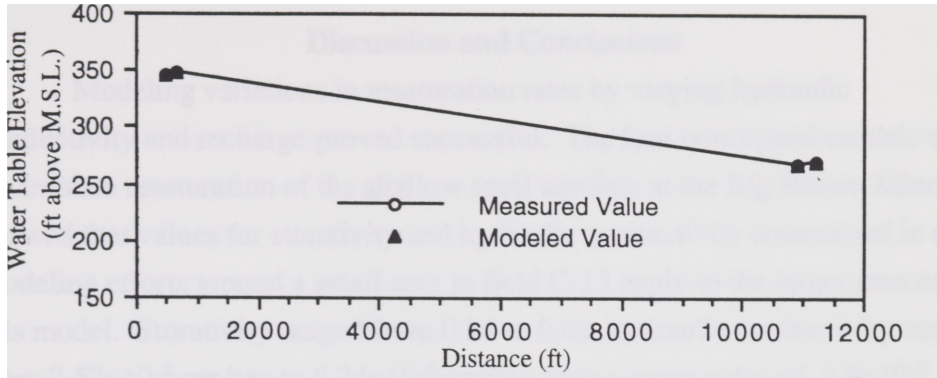

Measured and Modeled Hydraulic Head Values at 400 days.

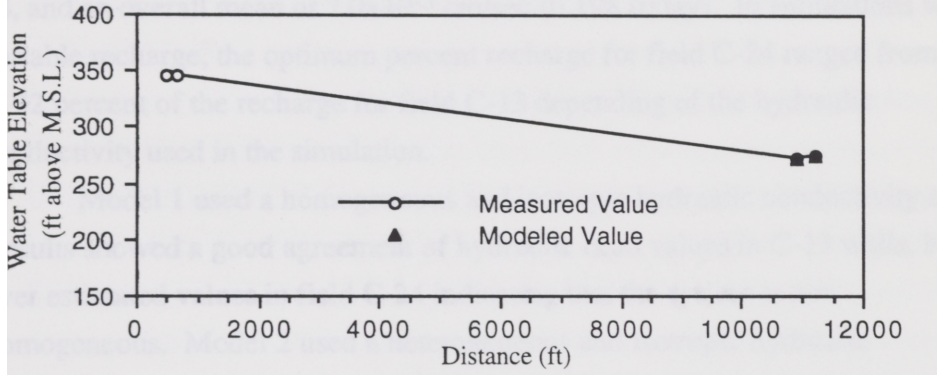

Measured and modeled hydraulic head values at 950 days.

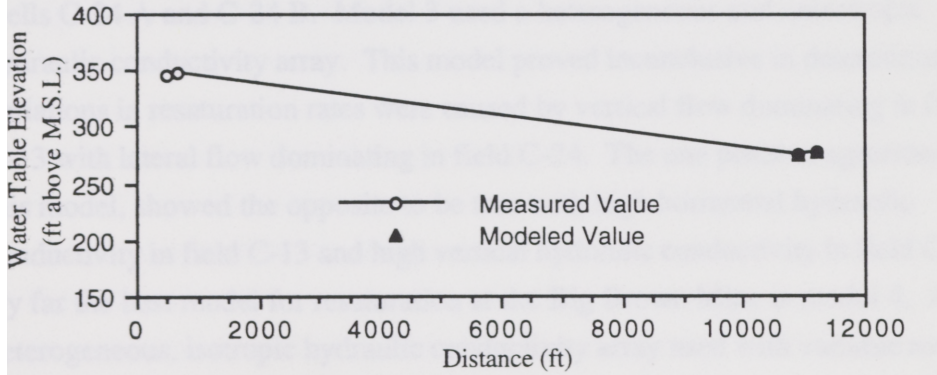

Measured and modeled hydraulic head values at 1300 days.

Figure 34. Conceptual model 4, simulation 5 hydraulic head values.

Discussion and Conclusions

Modeling variations in resaturation rates by varying hydraulic conductivity and recharge proved successful. The four conceptual models used to simulate resaturation of the shallow spoil aquifers at the Big Brown Mine showed that values for storativity and hydraulic conductivity determined in earlier modeling efforts around a small area in field C-13 apply to the larger area used in this model. Storativity ranged from 0.04 to 0.06; hydraulic conductivity ranged from 2.57×10^{-4} cm/sec to 6.24×10^{-6} cm/sec with a mean value of 3.9×10^{-4} cm/sec (0.284 ft/day) for field C-13, 4.4×10^{-5} cm/sec (0.113 ft/day) for field C-24, and an overall mean of 7.0×10^{-5} cm/sec (0.198 ft/day). In simulations with variable recharge, the optimum percent recharge for field C-24 ranged from 28 to 32 percent of the recharge for field C-13 depending of the hydraulic conductivity used in the simulation.

Model 1 used a homogeneous and isotropic hydraulic conductivity array. Results showed a good agreement of hydraulic head values in C-13 wells, but over estimated values in field C-24 indicating that the system is not homogeneous. Model 2 used a heterogeneous and isotropic hydraulic conductivity array. Again results for this model showed a good agreement of hydraulic head in wells C-13 A and C-13 B but strongly overestimated values in wells C-24 A and C-24 B. Model 3 used a heterogeneous and anisotropic hydraulic conductivity array. This model proved inconclusive in determining if variations in resaturation rates were caused by vertical flow dominating in field C-13 with lateral flow dominating in field C-24. The one positive agreement for this model, showed the opposite to be true with high horizontal hydraulic conductivity in field C-13 and high vertical hydraulic conductivity in field C-24. By far the best model for resaturation at the Big Brown Mine is model 4. A heterogeneous, isotropic hydraulic conductivity array used with variable recharge gives the best agreement of hydraulic head values. Possible explanations for the lowering of recharge to field C-24 include variations in soil mineralogy, flow in the unsaturated zone being dominantly lateral, more water being stored in the unsaturated zone in field C-24, and variations in ambient soil moisture content.

Conclusions

1. Infiltration rates of reclaimed mine soils are significantly lower than unmined soils. An overall decrease of 53 percent is seen in reclaimed fields C-13, C-24, and C-32 when compared to field UM.
2. Mean infiltration rates in fields C-13, C-24 and C-32 show low variability despite difference in soil classification. Fields C-13 is classified as a clay loam and has a mean infiltration rate of 8.0 cm/hr (3.1 in/hr). Field C-24 is classified as a loam and has a mean infiltration rate of 10.5 cm/hr (4.1 in/hr). Field C-32 is classified as a sandy loam and has a mean infiltration rate of 8.9 cm/hr (3.5 in/hr).
3. Infiltration varies in response to seasonal changes in soil moisture content. Mean winter values are 58 percent lower than mean summer values in field UM. In fields C-13, C-24, and C-32, mean winter values are 38 percent lower than mean summer values.
4. Saturated hydraulic conductivity is controlled by the texture of the soil and does not correlate with infiltration rates measured with the drip infiltrometer.
5. Tracer tests, using Rhodamine WT to mark water flow paths, proved inconclusive in delineating by-pass flow in reclaimed soils. Higher than expected soil acidity inferred with the movement of Rhodamine WT through the soil causing most of the dye to sorb to the surface soils and mark only a few flow paths.
6. Tracer tests, using bromide as a conservative tracer, did show preferential flow through the reclaimed soils. Vertical preferential flow occurred along one fracture marked with Rhodamine WT and three other structures in field C-13. Field C-24 showed lateral preferential flow along compacted layers present in the soil section. Vertical preferential flow in field C-32 was shown by a concentration plot of bromide, but no physical variability was observed in the trenched cross-section.

7. Water levels in field C-13 have reached steady state, but resaturation of shallow spoil aquifers continues in field C-24 at a rate of 0.6-0.9 m/hr (2 to 3 ft/yr). Water levels in field C-32 are rising slightly faster at 1.2 m/yr (4 ft/yr).
8. On the basis of resaturation rates calculated by Holzmer (1992), there is an inverse relationship between infiltration rates and resaturation rates. Field C-13 had a higher resaturation rate of 2.7-3.0 m/yr (9 to 10 ft/yr) but an infiltration rate lower than field C-24. Field C-24 had a lower resaturation rate of 0.6-0.9 m/yr (2 to 3 ft/yr) but a higher infiltration rate than field C-13.
9. Variations in infiltration rates measured with the drip infiltrometer are not significant and do not control the variations in resaturation rates seen in fields C-13 and C-24.
10. Characteristics measured in a small area of a field of study can be considered representative of the field as a whole.
11. Modeling of a cross-sectional line from field C-13 to field C-24 showed that variations in the amount of recharge applied to the system can account for the variations seen in the resaturation rates of fields C-13 and C-24.

Implications

Variable resaturation of shallow spoil aquifers still continues today at the Big Brown Mine. Variability in infiltration rates was found to be quite low across reclaimed areas of the mine indicating that other sources of recharge to the system may exist. Possible sources of recharge include flow from surrounding aquifers in unmined areas, leaking ponds, and influent streams.

From an operational standpoint, lower infiltration rates are advantageous because slope stability of the spoil piles is controlled by the amount of water present. When the spoil becomes too wet, piles fail and re-handling of the material is required taking up time and resources at the mine. Despite the coarse texture of the spoil material placed with the XPS, infiltration rates are still quite low which decreases water flow into the spoil material. Because this material is placed on top of dragline material which may have a slightly higher infiltration

rate, the overall effect is a lowering of water flow into the spoil piles. This is particularly important close to the active mining pit.

For reclamation purposes, lower infiltration rates in the XPS material may lower resaturation rates for the area. Because the XPS material has a higher saturated hydraulic conductivity than dragline spoil a perched water table could form at the boundary between the two spoil types. This could increase near surface soil moisture content and help speed re-vegetation.

Appendix A

Infiltration Rates of Fields Unmined and C-13

Sample #	Date	Infiltration Rate (cm/hr)
UM IT 1	10/2/93	30.0
UM IT 2	10/2/93	25.3
UM IT 3	10/3/93	19.4
UM IT 4	10/3/93	23.4
UM IT 5	2/12/94	12.6
UM IT 6	2/13/94	15.9
C-13 IT 1	10/2/93	22.1
C-13 IT 2	10/2/93	9.1
C-13 IT 3	10/3/93	7.3
C-13 IT 4	10/3/93	14.3
C-13 IT 5	2/12/94	9.5
C-13 IT 6	2/12/94	6.8
C-13 IT 7	2/12/94	5.9
C-13 IT 8	2/13/94	7.0
C-13 IT 9	2/13/94	3.9
C-13 IT 10	2/13/94	3.4
C-13 IT 11	2/24/94	3.2
C-13 IT 12	2/25/94	3.3

Appendix A
Infiltration Rates of Fields C-24 and C-32

Sample #	Date	Infiltration Rate (cm/hr)
C-24 IT 1	10/23/93	19.3
C-24 IT 2	10/23/93	20.4
C-24 IT 3	10/24/93	17.7
C-24 IT 4	10/24/93	16.6
C-24 IT 5	2/24/94	5.6
C-24 IT 6	2/24/94	9.2
C-24 IT 7	2/24/94	5.2
C-24 IT 8	2/24/94	4.7
C-24 IT 9	2/25/94	9.0
C-24 IT 10	2/25/94	9.8
C-24 IT 11	2/25/94	5.1
C-24 IT 12	2/25/94	6.1
C-32 IT 1	10/23/93	19.3
C-32 IT 2	10/23/93	15.2
C-32 IT 3	10/24/93	19.4
C-32 IT 4	10/24/93	7.2
C-32 IT 5	2/26/94	9.5
C-32 IT 6	2/26/94	7.1
C-32 IT 7	2/26/94	4.6
C-32 IT 8	2/26/94	2.6
C-32 IT 9	2/27/94	6.9
C-32 IT 10	2/27/94	7.3
C-32 IT 11	2/27/94	3.0
C-32 IT 12	2/27/94	4.3

Appendix B

Saturated Hydraulic Conductivity and Matrix Flux Potential of Fields Unmined and C-13

Sample #	Date	Saturated Hydraulic Conductivity (cm/sec)	Matrix Flux Potential (cm^2/sec)
UM GP 1	7/13/93	4.06×10^{-4}	3.45×10^{-2}
UM GP 2	7/13/93	1.63×10^{-3}	5.96×10^{-2}
UM GP 3	7/14/93	7.55×10^{-4}	4.09×10^{-2}
UM GP 4	1/11/94	1.22×10^{-4}	4.27×10^{-4}
UM GP 5	1/11/94	3.55×10^{-4}	4.39×10^{-2}
UM GP 6	1/11/94	1.41×10^{-3}	6.55×10^{-2}
UM GP 7	3/14/94	1.54×10^{-3}	2.79×10^{-2}
UM GP 8	3/14/94	2.48×10^{-3}	6.38×10^{-3}
C-13 GP 1	7/14/93	1.75×10^{-4}	2.08×10^{-4}
C-13 GP 2	7/14/93	9.49×10^{-5}	2.19×10^{-4}
C-13 GP 3	7/14/93	1.10×10^{-4}	1.65×10^{-4}
C-13 GP 4	3/15/94	5.84×10^{-7}	1.53×10^{-5}
C-13 GP 5	3/15/94	9.21×10^{-6}	6.25×10^{-4}
C-13 GP 6	3/17/94	3.77×10^{-6}	9.71×10^{-5}
C-13 GP 7	3/17/94	1.15×10^{-7}	5.60×10^{-5}
C-13 GP 8	3/17/94	7.05×10^{-6}	2.95×10^{-6}

Appendix B
Saturated Hydraulic Conductivity and Matrix Flux Potential of Fields C-24 and C-32

Sample #	Date	Saturated Hydraulic Conductivity (cm/sec)	Matrix Flux Potential (cm^2/sec)
C-24 GP 1	7/15/93	4.07×10^{-6}	4.01×10^{-4}
C-24 GP 2	7/15/93	1.60×10^{-5}	3.32×10^{-4}
C-24 GP 3	7/15/93	3.71×10^{-5}	5.39×10^{-4}
C-24 GP 4	1/13/94	1.78×10^{-5}	9.06×10^{-4}
C-24 GP 5	1/13/94	1.01×10^{-5}	1.91×10^{-3}
C-24 GP 6	1/13/94	4.18×10^{-6}	8.37×10^{-6}
C-24 GP 7	2/15/94	2.49×10^{-6}	7.30×10^{-6}
C-24 GP 8	2/15/94	1.18×10^{-6}	3.05×10^{-5}
C-32 GP 1	7/22/93	1.06×10^{-6}	2.29×10^{-3}
C-32 GP 2	7/22/93	1.65×10^{-4}	5.82×10^{-4}
C-32 GP 3	7/22/93	7.09×10^{-5}	4.24×10^{-3}
C-32 GP 4	3/16/94	3.76×10^{-3}	1.21×10^{-2}
C-32 GP 5	3/16/94	4.66×10^{-4}	9.59×10^{-3}
C-32 GP 6	3/16/94	6.12×10^{-4}	1.58×10^{-2}
C-32 GP 7	3/16/94	5.31×10^{-4}	1.53×10^{-2}
C-32 GP 8	3/16/94	1.09×10^{-6}	3.15×10^{-5}

Appendix C

Water Table Elevations in Wells C-13 A, C-13 B, C-24 A and C-24 B

Well #	Date	Surface Elev. (ft)	Water Elev. (ft)	Δ Water Elev. (ft)
C-13 A	4/20/92	365	348.53	--
C-13 A	8/16/93	365	346.80	-1.73
C-13 A	10/3/93	365	346.45	-0.35
C-13 A	1/12/94	365	345.91	-0.54
C-13 A	3/15/94	365	345.80	-0.11
C-13 A	6/29/94	365	346.95	1.15
C-13 A	7/29/94	365	346.60	-0.35
C-13 B	4/20/92	364.05	346.40	--
C-13 B	8/16/93	364.05	345.73	-0.67
C-13 B	10/3/93	364.05	345.80	0.07
C-13 B	1/12/94	364.05	345.03	-0.77
C-13 B	3/15/94	364.05	345.15	0.12
C-13 B	6/29/94	364.05	345.60	0.45
C-13 B	7/29/94	364.05	345.55	-0.05
C-24 A	4/20/92	350.41	270.86	--
C-24 A	8/16/93	350.41	274.83	3.97
C-24 A	10/3/93	350.41	274.86	0.03
C-24 A	1/12/94	350.41	275.54	0.68
C-24 A	3/15/94	350.41	276.06	0.52
C-24 A	6/29/94	350.41	276.56	0.50
C-24 A	7/29/94	350.41	276.71	0.15

Appendix C
Water Table Elevations in Wells C-24 B and C-46-R-92

Well #	Date	Surface Elev. (ft)	Water Elev. (ft)	Δ Water Elev. (ft)
C-24 B	4/20/92	355.54	269.04	--
C-24 B	8/16/93	355.54	272.00	2.96
C-24 B	10/3/93	355.54	273.19	1.19
C-24 B	1/12/94	355.54	274.35	1.16
C-24 B	3/15/94	355.54	274.94	0.59
C-24 B	6/29/94	355.54	275.88	0.94
C-24 B	7/29/94	355.54	275.99	0.11
C-46-R-92	4/20/92	400.70	Dry	--
C-46-R-92	8/16/93	400.70	275.42	--
C-46-R-92	10/3/93	400.70	276.00	0.58
C-46-R-92	1/12/94	400.70	277.08	1.08
C-46-R-92	3/15/94	400.70	277.55	0.47
C-46-R-92	6/29/94	400.70	279.50	1.95
C-46-R-92	7/29/94	400.70	279.80	0.30

Appendix D

Soil Descriptions and Grain-size Distribution Curves

Unmined Field

Depth	Soil Description
0-1 ft	Pale brown gray, 10 YR 7/2 (Munsell Soil Color Charts, 1973), sandy loam, well sorted, plant fragments, plant roots, small ironstone nodules, dominated by quartz (80 %).
1-2 ft	Very pale brown, 10 YR 7/4 , sandy clay loam, moderately sorted, plant roots, small isolated clay clasts, dominated by quartz (70%).
2-3 ft	Red, 10 R 4/6, color mottled, sandy clay, poorly sorted, bi-modal, small amount of organic material present, quartz (39%), potassium feldspar (11%), clay minerals (51%).
3-4 ft	Red, 10 R 4/6, color mottled, sandy clay, poorly sorted, bi-modal, small amount of organic material, mineral distribution similar to 2-3 ft depth.

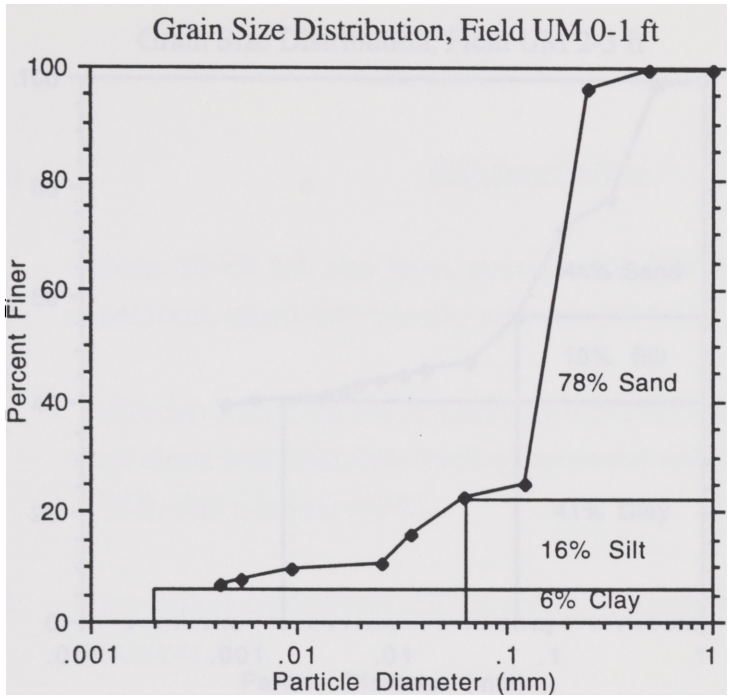
Grain Size Distribution, Field UM 0-1 ft
Percent Finer
100
80
60
40
20
0
.001
.01
.1
1
Particle Diameter (mm)
78% Sand
16% Silt
6% Clay

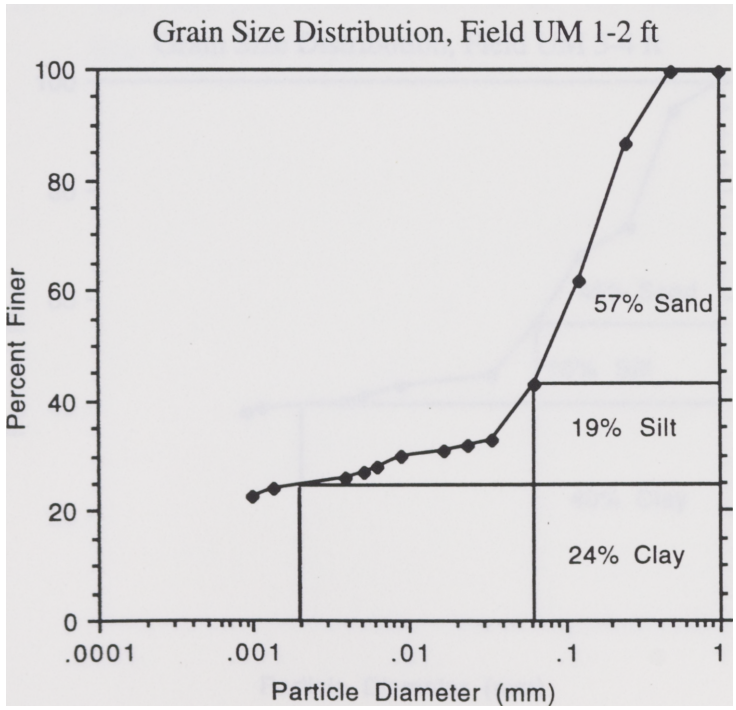
Grain Size Distribution, Field UM 1-2 ft
Percent Finer
100
80
60
40
20
0
.0001
.001
.01
.1
1
Particle Diameter (mm)
57% Sand
19% Silt
24% Clay

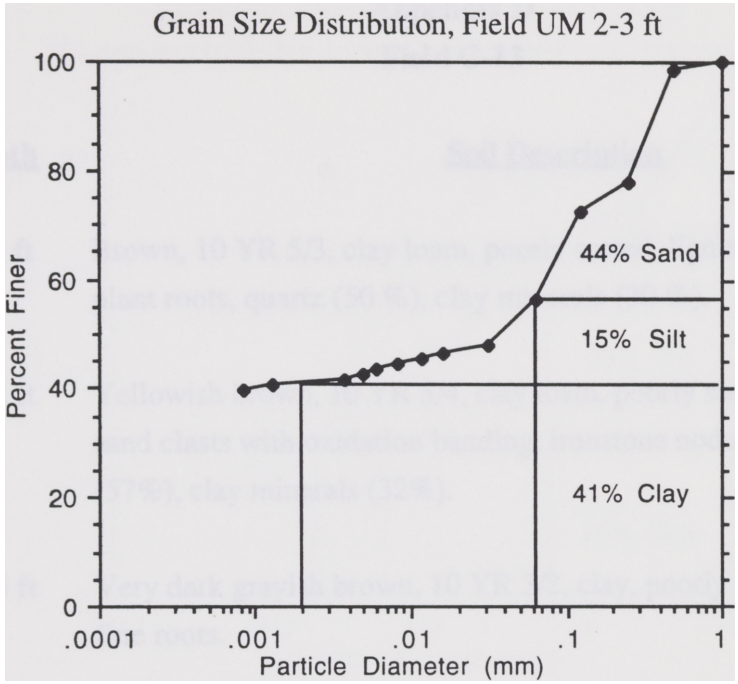
Grain Size Distribution, Field UM 2-3 ft
Percent Finer
100
80
60
40
20
0
.0001
.001
.01
.1
1
Particle Diameter (mm)
44% Sand
15% Silt
41% Clay

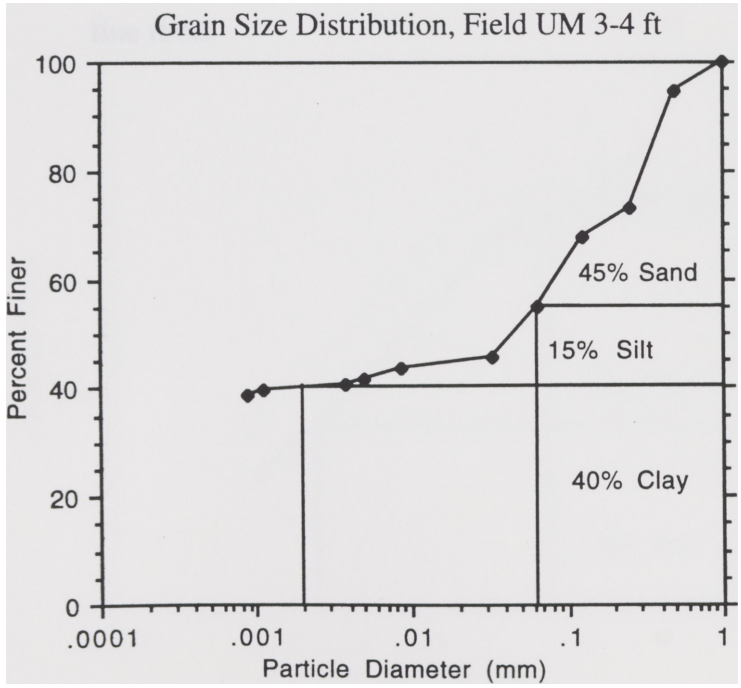
Grain Size Distribution, Field UM 3-4 ft
Percent Finer
100
80
60
40
20
0
.0001
.001
.01
.1
1
Particle Diameter (mm)
45% Sand
15% Silt
40% Clay

Appendix D
Field C-13

Depth	Soil Description
0-1 ft	Brown, 10 YR 5/3, clay loam, poorly sorted, lignite, ironstone nodules, plant roots, quartz (50 %), clay minerals (30 %).
1-2 ft	Yellowish brown, 10 YR 5/4, clay loam, poorly sorted, lignite, small sand clasts with oxidation banding, ironstone nodules, plant roots, quartz (57%), clay minerals (32%).
2-3 ft	Very dark grayish brown, 10 YR 3/2, clay, poorly sorted, lignite, very fine roots.
3-4 ft	Very dark grayish brown, 10 YR 3/2, clay, poorly sorted, lignite, very fine roots.

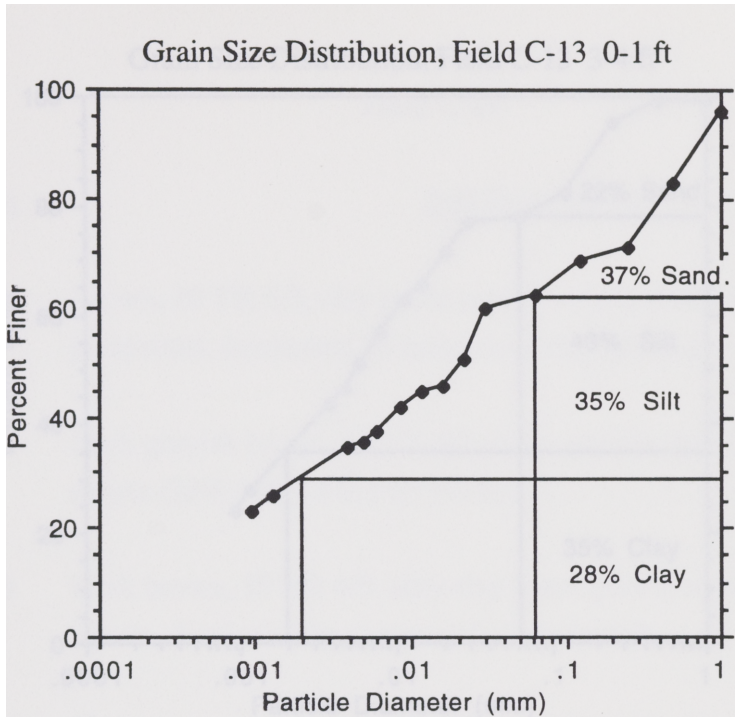
Grain Size Distribution, Field C-13 0-1 ft
100
80
60
40
20
0
Percent Finer
37% Sand
35% Silt
28% Clay
.0001
.001
.01
.1
1
Particle Diameter (mm)

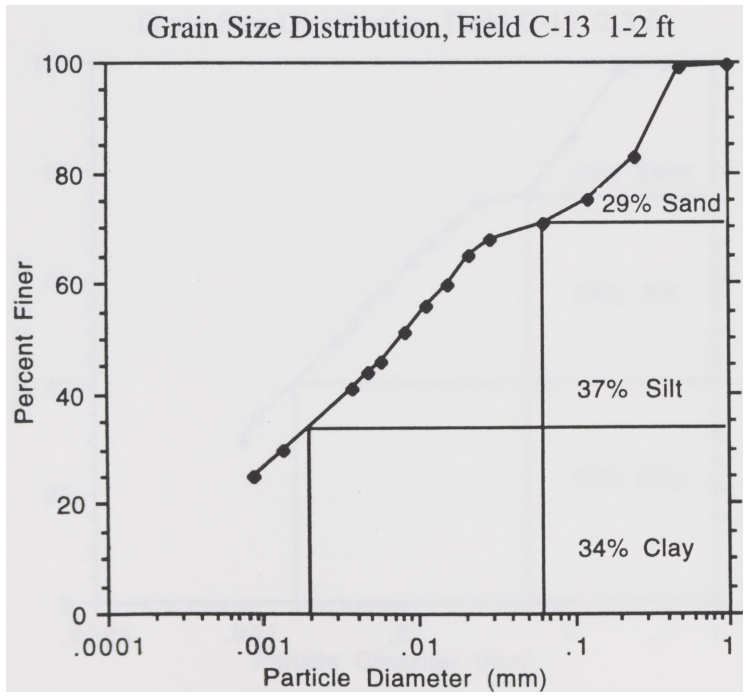
Grain Size Distribution, Field C-13 1-2 ft
100
80
60
40
20
0
Percent Finer
29% Sand
37% Silt
34% Clay
.0001
.001
.01
.1
1
Particle Diameter (mm)

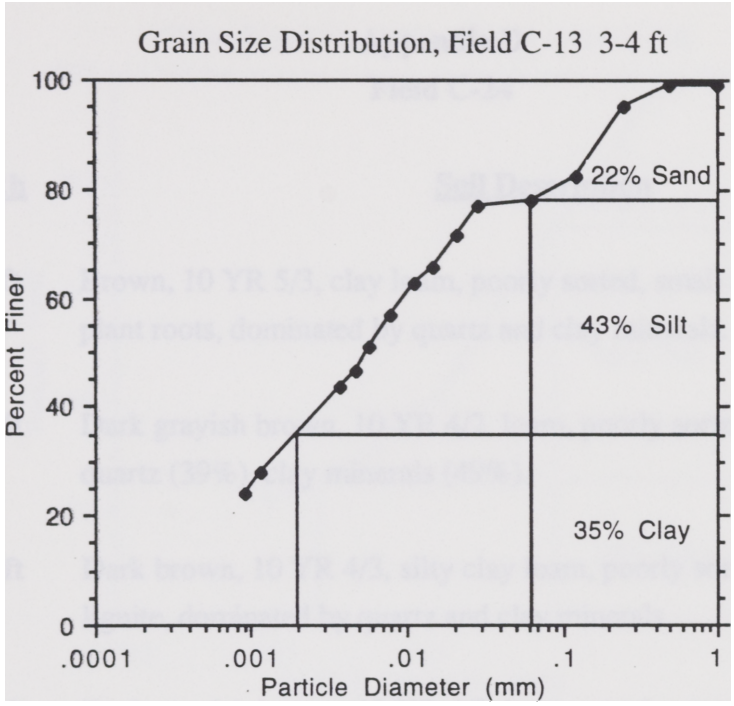
Grain Size Distribution, Field C-13 3-4 ft
Percent Finer
100
80
60
40
20
0
.0001
.001
.01
.1
1
Particle Diameter (mm)
22% Sand
43% Silt
35% Clay

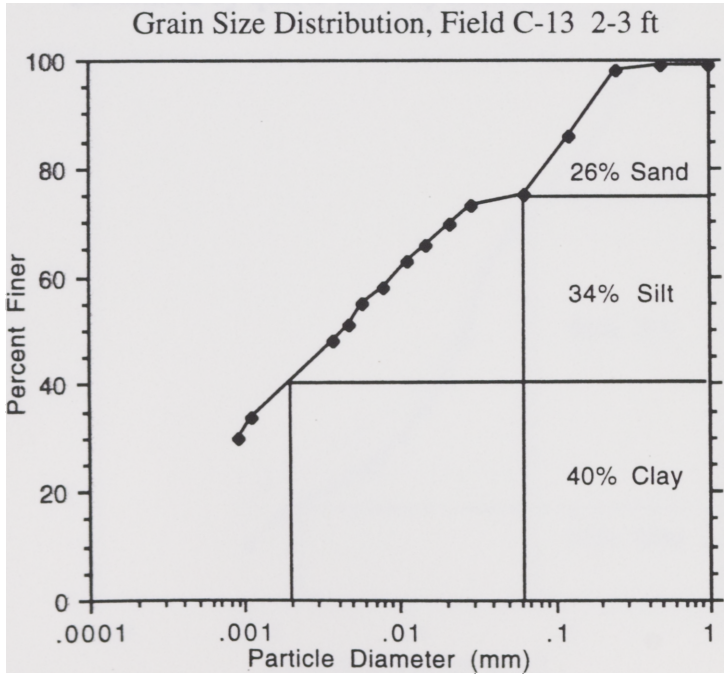
Grain Size Distribution, Field C-13 2-3 ft
Percent Finer
100
80
60
40
20
0
.0001
.001
.01
.1
1
Particle Diameter (mm)
26% Sand
34% Silt
40% Clay

Appendix D
Field C-24

Depth	Soil Description
0-1 ft	Brown, 10 YR 5/3, clay loam, poorly sorted, small amount of lignite, plant roots, dominated by quartz and clay minerals.
1-2 ft	Dark grayish brown, 10 YR 4/2, loam, poorly sorted, plant roots, lignite, quartz (39%), clay minerals (49%).
2-3 ft	Dark brown, 10 YR 4/3, silty clay loam, poorly sorted, very fine roots, lignite, dominated by quartz and clay minerals.
3-4 ft	Dark grayish brown, 10 YR 4/2, loam, poorly sorted, few plant roots, dominated by quartz and clay minerals.

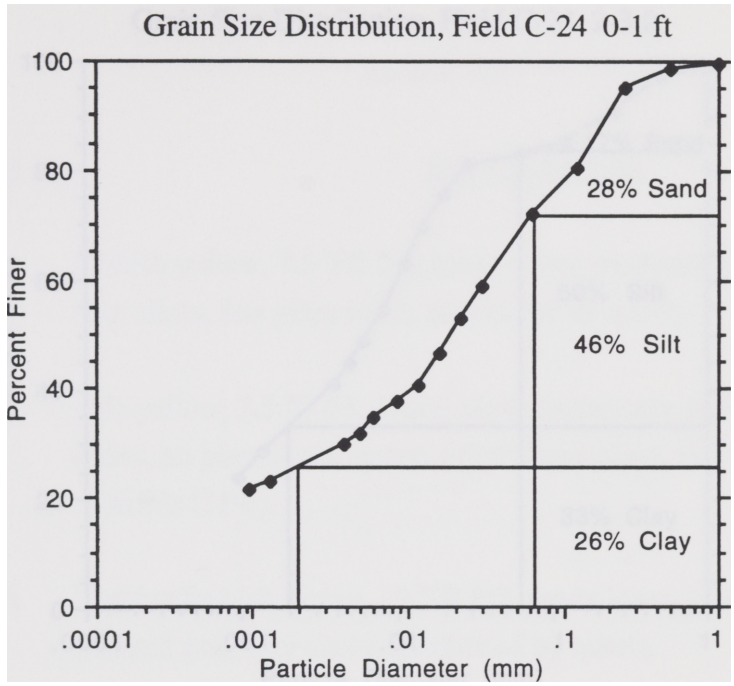
Grain Size Distribution, Field C-24 0-1 ft
100
80
60
40
20
0
Percent Finer
28% Sand
46% Silt
26% Clay
.0001
.001
.01
.1
1
Particle Diameter (mm)

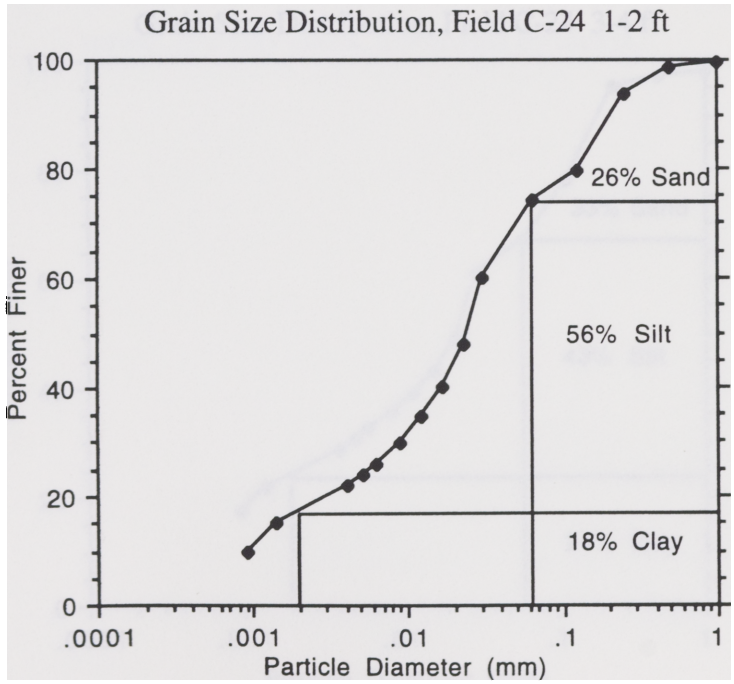
Grain Size Distribution, Field C-24 1-2 ft
100
80
60
40
20
0
Percent Finer
26% Sand
56% Silt
18% Clay
.0001
.001
.01
.1
1
Particle Diameter (mm)

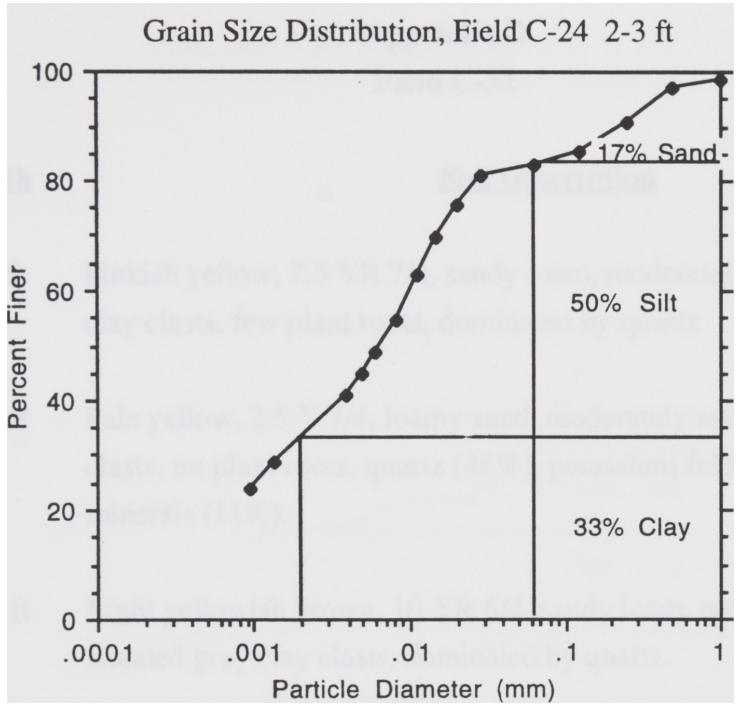
Grain Size Distribution, Field C-24 2-3 ft
Percent Finer
100
80
60
40
20
0
.0001
.001
.01
.1
1
Particle Diameter (mm)
17% Sand
50% Silt
33% Clay

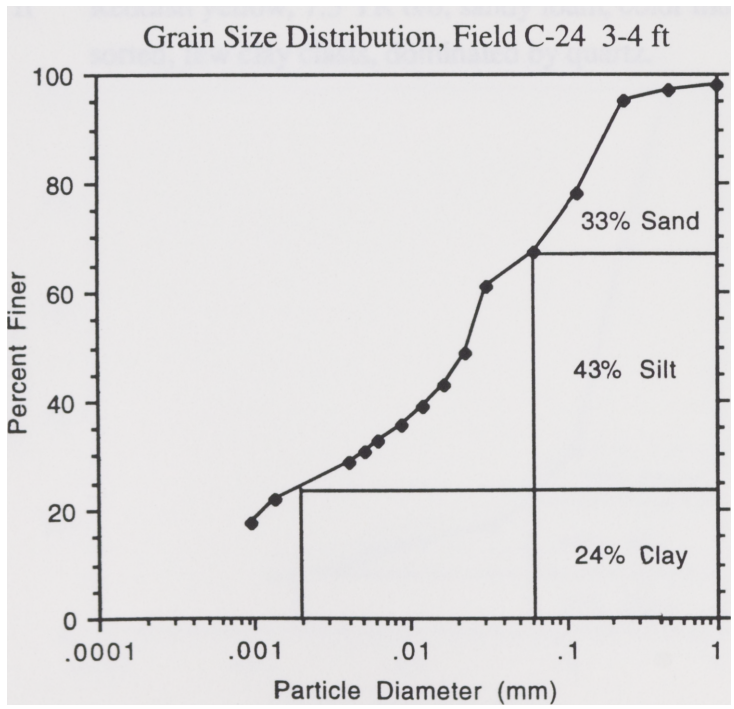
Grain Size Distribution, Field C-24 3-4 ft
Percent Finer
100
80
60
40
20
0
.0001
.001
.01
.1
1
Particle Diameter (mm)
33% Sand
43% Silt
24% Clay

Appendix D
Field C-32

Depth	Soil Description
0-1 ft	Pinkish yellow, 7.5 YR 7/4, sandy loam, moderately sorted, isolated gray clay clasts, few plant roots, dominated by quartz
1-2 ft	Pale yellow, 2.5 Y 7/4, loamy sand, moderately sorted, isolated gray clay clasts, no plant roots, quartz (48%), potassium feldspar (37%), clay minerals (11%).
2-3 ft	Light yellowish brown, 10 YR 6/4, sandy loam, moderately sorted, isolated gray clay clasts, dominated by quartz.
3-4 ft	Reddish yellow, 7.5 YR 6/6, sandy loam, color mottled, moderately sorted, few clay clasts, dominated by quartz.

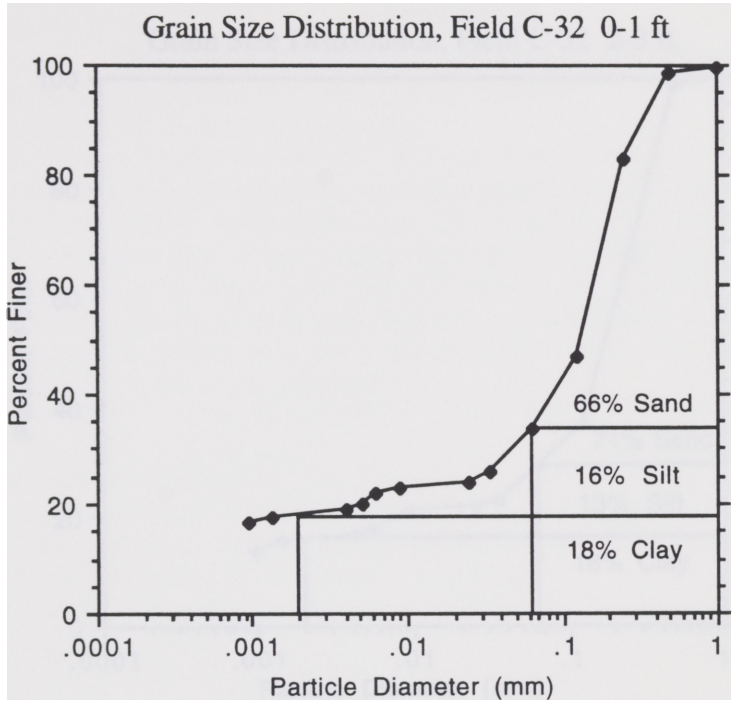
Grain Size Distribution, Field C-32 0-1 ft
Percent Finer
100
80
60
40
20
0
.0001
.001
.01
.1
1
Particle Diameter (mm)
66% Sand
16% Silt
18% Clay

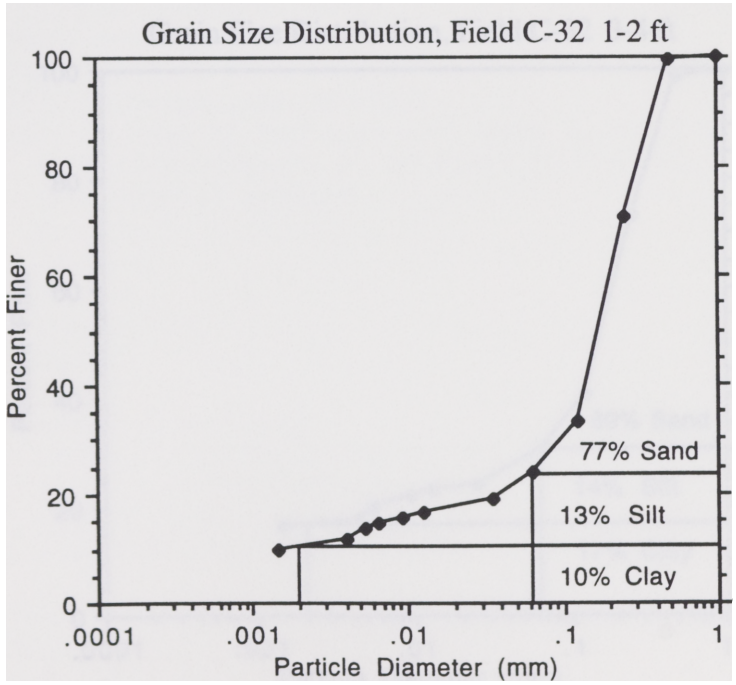
Grain Size Distribution, Field C-32 1-2 ft
Percent Finer
100
80
60
40
20
0
.0001
.001
.01
.1
1
Particle Diameter (mm)
77% Sand
13% Silt
10% Clay

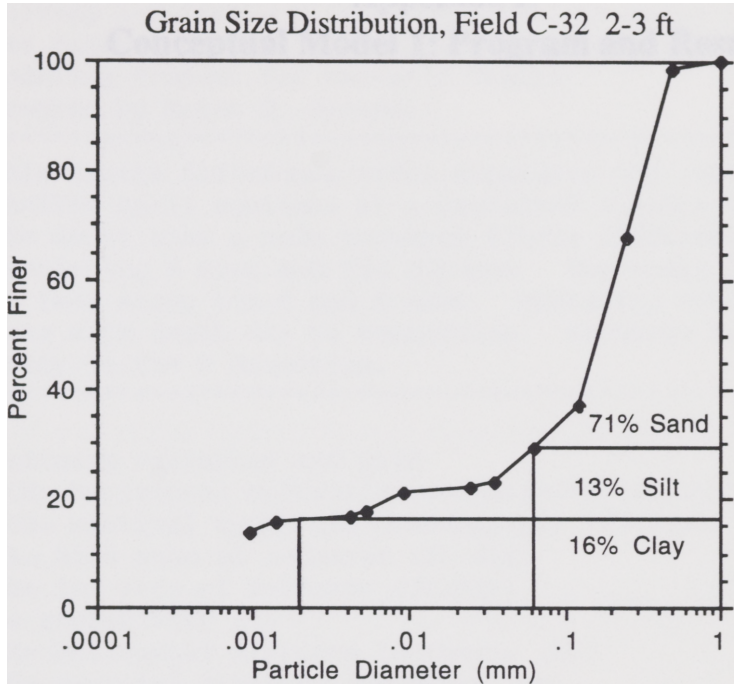
Grain Size Distribution, Field C-32 2-3 ft
100
80
60
40
20
0
Percent Finer
71% Sand
13% Silt
16% Clay
.0001
.001
.01
.1
1
Particle Diameter (mm)

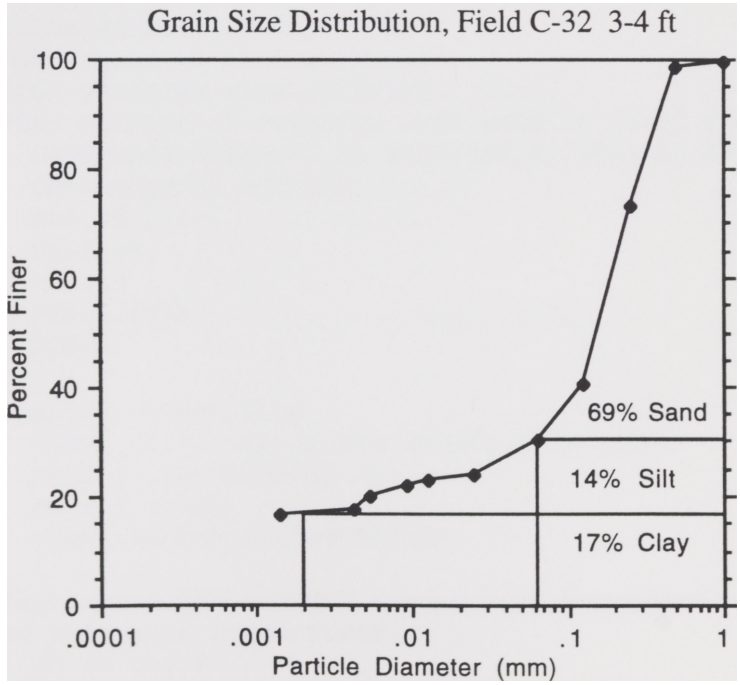
Grain Size Distribution, Field C-32 3-4 ft
100
80
60
40
20
0
Percent Finer
69% Sand
14% Silt
17% Clay
.0001
.001
.01
.1
1
Particle Diameter (mm)

Appendix E
Conceptual Model 1: Program and Results

```
C ***************************************************************
C * Solving 2-D finite difference transient state flow model of
C * the resaturation of a reclaimed lignite mine.
C * Modeling Project for Master's Thesis
C * Program by Karen E. Jarocki
C ***************************************************************
C * This finite difference model simulates the resaturation of
C * shallow spoil aquifers at a reclaimed lignite mine.
C * The model uses a node centered finite difference grid
C * consisting 6 rows and 240 columns.  The nodes are spaced at
C * 25 feet along the X and Z axes.  Hydraulic conductivity can
decrease with depth due to compaction.  Recharge can vary
spatially in the X direction.
C ***************************************************************

C * Defining variables and grid
C * HCX= horizontal hydraulic conductivity (ft/day)
C * HCZ= vertical hydraulic conductivity (ft/day)
C * R1= high rate of recharge (ft/day)
C * R2= low rate of recharge (ft/day)
C * S= storativity (-)
C * DX= horizontal distance increment (ft)
C * DZ= vertical distance increment (ft)
C * DX=DZ=25 ft
C * DT= time increment (day)
C * HOLD= head at time step n
C * HNEW= head at time step n+1
C * REC= recharge rate (ft/day)
C * PER= percent of recharge rate used in field C-24
      DIMENSION HNEW(480,5),HOLD(480,5),HCX(480,5),HCZ(480,5)
      CHARACTER*12 OUTFILE
      S=0.05
      DX=25.0
      DT=1.0
      REC=0.0024
      PER=1

C * Opening output file
      WRITE (*,*) 'Enter the output file name.'
      READ (*,10) OUTFILE
10    FORMAT (A12)
      OPEN (UNIT=6,FILE=OUTFILE)

C * Initialize HCX and HCZ arrays with homogeneous values
C * of hydraulic conductivity
      DO 20 J=1,5
        DO 20 I=1,480
```

```
         HCX(I,J)=0.198
         HCZ(I,J)=0.198
         IF (J.EQ.2)THEN
            HCX(I,J)=HCX(I,J)*1.0
            HCZ(I,J)=HCZ(I,J)*1.0
            ELSEIF (J.EQ.3) THEN
            HCX(I,J)=HCX(I,J)*1.0
            HCZ(I,J)=HCZ(I,J)*1.0
            ELSEIF (J.EQ.4) THEN
            HCX(I,J)=HCX(I,J)*1.0
            HCZ(I,J)=HCZ(I,J)*1.0
         ENDIF
20    CONTINUE

C * Begin writing output with storativity and hydraulic
C * conductivity
      WRITE (6,30) S
30    FORMAT (1X, 'Storativity = ', F4.3)
      WRITE (6,40)
40    FORMAT (/ 1X, 'Horizontal Hydraulic Conductivity Array')
      WRITE (6,50) ((HCX(I,J),I=1,480,80),J=1,5)
50    FORMAT (1X,6F10.6)
      WRITE (6,60)
60    FORMAT (/ 1X, 'Vertical Hydraulic Conductivity Array')
      WRITE (6,70) ((HCZ(I,J),I=1,480,80),J=1,5)
70    FORMAT (1X,6F10.6)

C * Initialize head values at all nodes.
      DO 80 J=1,5
         DO 80 I=1,480
            HOLD(I,J)=341.5-I*0.17
            HNEW(I,J)=341.5-I*0.17
80    CONTINUE

C * Initialize head values for known nodes
      HOLD(20,2)=338.28
      HOLD(32,2)=334.6
      HOLD(436,2)=267.48
      HOLD(448,2)=266.75
      HOLD(479,2)=260.0
      HNEW(20,2)=338.28
      HNEW(32,2)=334.60
      HNEW(436,2)=267.48
      HNEW(448,2)=266.75
      HNEW(479,2)=260.0

C * Initialize head values for top image nodes
```

```
      DO 90 I=1,480
         IF (I.LT.240) THEN
           HOLD(I,1)=HOLD(I,2)+REC*DX/HCZ(I,2)
           HNEW(I,1)=HNEW(I,2)+REC*DX/HCZ(I,2)
           ELSE
           HOLD(I,1)=HOLD(I,2)+REC*PER*DX/HCZ(I,2)
           HNEW(I,1)=HNEW(I,2)+REC*PER*DX/HCZ(I,2)
         ENDIF
90    CONTINUE

C * Write initial head values for the grid
      WRITE (6,120)
120   FORMAT (/ 1X, 'Initial head values')
      WRITE (6,130)
     +HOLD(20,2),HOLD(32,2),HOLD(436,2),HOLD(448,2)
130   FORMAT (1X, 4F9.2)
      WRITE (6,140) ((HOLD(I,J),I=1,480,60),J=1,5)
140   FORMAT (1X, 8F9.2)

C * Using the Crank-Nicolson approximation to iterate through
C * the nodes
      ALPHA=0.5
      TIME=0.0
      K=0
      NEND=1300
      DO 270 N=1,NEND
         NUMIT=0
         TIME=TIME+DT
180      AMAX=0.0
         NUMIT=NUMIT+1
         DO 200 J=2,4
            DO 190 I=2,479
               IF (I.EQ.479) GO TO 200
               OLDVAL=HNEW(I,J)
               H1=(HCX(I,J)*(HOLD(I-1,J)+HOLD(I+1,J))+HCZ(I,J)*
     +            (HOLD(I,J-1)+HOLD(I,J+1)))/2.0
               H2=(HCX(I,J)*(HNEW(I-1,J)+HNEW(I+1,J))+HCZ(I,J)*
     +            (HNEW(I,J-1)+HNEW(I,J+1)))/2.0
               F1=DX*S/(2.0*DT)
               F2=ALPHA*(HCX(I,J)+HCZ(I,J))
               F3=1/(F1+F2)
               HNEW(I,J)=F3*((F1*HOLD(I,J))+(1.0-ALPHA)*
     +          (H1(HCX(I,J)+HCZ(I,J))*HOLD(I,J))+ALPHA*H2)
               ERR=ABS(HNEW(I,J)-OLDVAL)
               IF (ERR.GT.AMAX) AMAX=ERR
190         CONTINUE
200      CONTINUE
```

```
C * Assigning new values for left, right, and bottom image
C * points
         DO 210 J=1,5
            HNEW(1,J)=HNEW(3,J)
            HNEW(480,J)=HNEW(478,J)
210      CONTINUE
         DO 220 I=1,480
            HNEW(I,5)=HNEW(I,3)
220      CONTINUE
         IF (AMAX.GT.0.01) GO TO 180

C * Prepare for next time step
225      DO 230 I=1,480
            DO 230 J=1,5
               IF (J.EQ.1.AND.I.LE.240) THEN
                 HOLD(I,1)=HNEW(I,1)
                 HNEW(I,1)=HNEW(I,2)+REC*DX/HCZ(I,J)
                 ELSEIF (J.EQ.1.AND.I.GT.240) THEN
                 HOLD(I,1)=HNEW(I,1)
                 HNEW(I,1)=HNEW(I,2)+REC*PER*DX/HCZ(I,J)
                 ELSE
                 HOLD(I,J)=HNEW(I,J)
               ENDIF
230      CONTINUE

C * Output of final results
         K=K+1
         IF (K.EQ.400.OR.K.EQ.950.OR.K.EQ.1300) THEN
           WRITE (6,240) TIME, NUMIT
240        FORMAT (/ 1X,'Number of days =',F7.2, 5X,
     +             'Number of iterations =',I4)
           WRITE (6,250)
250        FORMAT (1X, 'Final Head Values')
           WRITE (6,255)
     +     HOLD(20,2),HOLD(32,2),HOLD(436,2),HOLD(448,2)
255        FORMAT (1X,4F9.2)
           WRITE (6,260) ((HOLD(I,J),I=1,480,60),J=1,5)
260        FORMAT (1X,8F9.2)
         ELSE
           K=K
         ENDIF
270   CONTINUE
1000  STOP
      END
```

Model 1, Simulation 1
Storativity = .050

Horizontal Hydraulic Conductivity Array

.198000	.198000	.198000	.198000	.198000	.198000
.198000	.198000	.198000	.198000	.198000	.198000
.198000	.198000	.198000	.198000	.198000	.198000
.198000	.198000	.198000	.198000	.198000	.198000
.198000	.198000	.198000	.198000	.198000	.198000

Vertical Hydraulic Conductivity Array

.198000	.198000	.198000	.198000	.198000	.198000
.198000	.198000	.198000	.198000	.198000	.198000
.198000	.198000	.198000	.198000	.198000	.198000
.198000	.198000	.198000	.198000	.198000	.198000
.198000	.198000	.198000	.198000	.198000	.198000

Initial head values

338.28	334.60	267.48	266.75				
341.63	331.43	321.23	311.03	300.83	290.63	280.43	270.23
341.33	331.13	320.93	310.73	300.53	290.33	280.13	269.93
341.33	331.13	320.93	310.73	300.53	290.33	280.13	269.93
341.33	331.13	320.93	310.73	300.53	290.33	280.13	269.93
341.33	331.13	320.93	310.73	300.53	290.33	280.13	269.93

Number of days = 400.00 Number of iterations = 2
Final Head Values

345.22	343.24	274.60	272.56				
347.17	338.62	328.42	318.22	308.02	297.82	287.62	277.42
346.88	338.33	328.13	317.93	307.73	297.53	287.33	277.13
346.71	338.16	327.96	317.76	307.56	297.36	287.16	276.96
346.65	338.10	327.90	317.70	307.50	297.30	287.10	276.90
346.71	338.16	327.96	317.76	307.56	297.36	287.16	276.96

Number of days = 950.00 Number of iterations = 2
Final Head Values

354.64	352.92	284.31	282.02				
356.12	348.37	338.17	327.97	317.77	307.57	297.37	287.17
355.83	348.08	337.88	327.68	317.48	307.28	297.08	286.89
355.66	347.91	337.71	327.51	317.31	307.11	296.91	286.71
355.61	347.85	337.66	327.46	317.26	307.06	296.86	286.66
355.66	347.91	337.71	327.51	317.31	307.11	296.91	286.71

Number of days =1300.00 Number of iterations = 2
Final Head Values

360.61	359.03	290.41	287.68				
361.94	354.57	344.37	334.17	323.97	313.77	303.57	293.37
361.65	354.28	344.09	333.89	323.69	313.49	303.29	293.08
361.48	354.11	343.92	333.72	323.52	313.32	303.12	292.91
361.42	354.06	343.86	333.66	323.46	313.26	303.06	292.85
361.48	354.11	343.92	333.72	323.52	313.32	303.12	292.91

Model 1, Simulation 2

Storativity = .050

Horizontal Hydraulic Conductivity Array

.284000	.284000	.284000	.284000	.284000	.284000
.284000	.284000	.284000	.284000	.284000	.284000
.284000	.284000	.284000	.284000	.284000	.284000
.284000	.284000	.284000	.284000	.284000	.284000
.284000	.284000	.284000	.284000	.284000	.284000

Vertical Hydraulic Conductivity Array

.284000	.284000	.284000	.284000	.284000	.284000
.284000	.284000	.284000	.284000	.284000	.284000
.284000	.284000	.284000	.284000	.284000	.284000
.284000	.284000	.284000	.284000	.284000	.284000
.284000	.284000	.284000	.284000	.284000	.284000

Initial head values

338.28	334.60	267.48	266.75				
341.54	331.34	321.14	310.94	300.74	290.54	280.34	270.14
341.33	331.13	320.93	310.73	300.53	290.33	280.13	269.93
341.33	331.13	320.93	310.73	300.53	290.33	280.13	269.93
341.33	331.13	320.93	310.73	300.53	290.33	280.13	269.93
341.33	331.13	320.93	310.73	300.53	290.33	280.13	269.93

Number of days = 400.00 Number of iterations = 2
Final Head Values

344.84	342.93	274.30	272.24				
346.53	338.23	328.03	317.83	307.63	297.43	287.23	277.03
346.33	338.03	327.84	317.64	307.44	297.23	287.03	276.84
346.21	337.92	327.72	317.52	307.32	297.12	286.92	276.72
346.17	337.88	327.68	317.48	307.28	297.08	286.88	276.68

346.21 337.92 327.72 317.52 307.32 297.12 286.92 276.72

Number of days = 950.00 Number of iterations = 2
Final Head Values
353.74 352.16 283.58 281.05
354.98 347.62 337.43 327.22 317.02 306.82 296.62 286.42
354.78 347.42 337.23 327.03 316.83 306.63 296.43 286.22
354.66 347.30 337.11 326.91 316.71 306.51 296.31 286.11
354.62 347.27 337.08 326.87 316.67 306.47 296.27 286.07
354.66 347.30 337.11 326.91 316.71 306.51 296.31 286.11

Number of days =1300.00 Number of iterations = 2
Final Head Values
359.40 357.98 289.30 286.16
360.50 353.58 343.40 333.20 323.00 312.80 302.60 292.35
360.30 353.39 343.21 333.01 322.81 312.60 302.40 292.16
360.19 353.27 343.09 332.89 322.69 312.49 302.29 292.04
360.15 353.23 343.05 332.85 322.65 312.45 302.25 292.00
360.19 353.27 343.09 332.89 322.69 312.49 302.29 292.04

Model 1, Simulation 3
Storativity = .050

Horizontal Hydraulic Conductivity Array
.113000 .113000 .113000 .113000 .113000 .113000
.113000 .113000 .113000 .113000 .113000 .113000
.113000 .113000 .113000 .113000 .113000 .113000
.113000 .113000 .113000 .113000 .113000 .113000
.113000 .113000 .113000 .113000 .113000 .113000

Vertical Hydraulic Conductivity Array
.113000 .113000 .113000 .113000 .113000 .113000
.113000 .113000 .113000 .113000 .113000 .113000
.113000 .113000 .113000 .113000 .113000 .113000
.113000 .113000 .113000 .113000 .113000 .113000
.113000 .113000 .113000 .113000 .113000 .113000

Initial head values
338.28 334.60 267.48 266.75
341.86 331.66 321.46 311.26 301.06 290.86 280.66 270.46
341.33 331.13 320.93 310.73 300.53 290.33 280.13 269.93
341.33 331.13 320.93 310.73 300.53 290.33 280.13 269.93

341.33 331.13 320.93 310.73 300.53 290.33 280.13 269.93
341.33 331.13 320.93 310.73 300.53 290.33 280.13 269.93

Number of days = 400.00 Number of iterations = 2
Final Head Values
345.65 343.60 274.96 272.94
348.11 339.21 329.01 318.81 308.61 298.41 288.21 278.01
347.59 338.70 328.50 318.30 308.10 297.90 287.70 277.50
347.28 338.39 328.19 317.99 307.79 297.59 287.39 277.19
347.18 338.29 328.09 317.89 307.69 297.49 287.29 277.09
347.28 338.39 328.19 317.99 307.79 297.59 287.39 277.19

Number of days = 950.00 Number of iterations = 2
Final Head Values
355.63 353.73 285.09 283.00
357.63 349.35 339.15 328.95 318.75 308.55 298.35 288.15
357.11 348.84 338.64 328.44 318.24 308.04 297.84 287.64
356.81 348.53 338.33 328.13 317.93 307.73 297.53 287.33
356.70 348.43 338.23 328.03 317.83 307.63 297.43 287.23
356.81 348.53 338.33 328.13 317.93 307.73 297.53 287.33

Number of days =1300.00 Number of iterations = 2
Final Head Values
361.95 360.15 291.52 289.27
363.78 355.80 345.60 335.40 325.20 315.00 304.80 294.60
363.26 355.29 345.09 334.89 324.69 314.49 304.29 294.09
362.96 354.98 344.78 334.58 324.38 314.18 303.98 293.78
362.85 354.88 344.68 334.48 324.28 314.08 303.88 293.68
362.96 354.98 344.78 334.58 324.38 314.18 303.98 293.78

Appendix F
Conceptual Model 2: Program and Results

```
C ***************************************************************
C * Solving 2-D finite difference transient state flow model of
C * the resaturation of a reclaimed lignite mine.
C * Modeling Project for Master's Thesis
C * Program by Karen E. Jarocki
C ***************************************************************
C * This finite difference model simulates the resaturation of
C * shallow spoil aquifers at a reclaimed lignite mine.  The
C * model uses a node centered finite difference grid consisting
C * 6 rows and 240 columns.  The nodes are spaced at 25 feet
C * along the X and Z axes.  Hydraulic conductivity can decrease
C * with depth due to compaction.  Recharge can vary spatially
C * in the X direction.
C ***************************************************************

C * Defining variables and grid
C * HCX= horizontal hydraulic conductivity (ft/day)
C * HCZ= vertical hydraulic conductivity (ft/day)
C * R1= high rate of recharge (ft/day)
C * R2= low rate of recharge (ft/day)
C * S= storativity (-)
C * DX= horizontal distance increment (ft)
C * DZ= vertical distance increment (ft)
C * DX=DZ=25 ft
C * DT= time increment (day)
C * HOLD= head at time step n
C * HNEW= head at time step n+1
C * REC= recharge rate (ft/day)
C * PER= percent of recharge rate used in field C-24
      DIMENSION HNEW(480,5),HOLD(480,5),HCX(480,5),HCZ(480,5)
      CHARACTER*12 OUTFILE
      S=0.05
      DX=25.0
      DT=1.0
      REC=0.0024
      PER=1.0

C * Opening output file
      WRITE (*,*) 'Enter the output file name.'
      READ (*,10) OUTFILE
10    FORMAT (A12)
      OPEN (UNIT=6,FILE=OUTFILE)

C * Initialize HCX and HCZ arrays with heterogeneous values
C * of hydraulic conductivity
      DO 20 J=1,5
        DO 20 I=1,480
```

```
            HCX(I,J)=0.099
            HCZ(I,J)=0.099
            IF (J.EQ.2) THEN
               HCX(I,J)=HCX(I,J)*5.0
               HCZ(I,J)=HCZ(I,J)*5.0
               ELSEIF (J.EQ.3) THEN
               HCX(I,J)=HCX(I,J)*2.0
               HCZ(I,J)=HCZ(I,J)*2.0
               ELSEIF (J.EQ.4) THEN
               HCX(I,J)=HCX(I,J)*0.5
               HCZ(I,J)=HCZ(I,J)*0.5
            ENDIF
20       CONTINUE

C * Begin writing output with storativity and hydraulic
C * conductivity
         WRITE (6,30) S
30       FORMAT (1X, 'Storativity = ', F4.3)
         WRITE (6,40)
40       FORMAT (/ 1X, 'Horizontal Hydraulic Conductivity Array')
         WRITE (6,50) ((HCX(I,J),I=1,480,80),J=1,5)
50       FORMAT (1X,6F10.6)
         WRITE (6,60)
60       FORMAT (/ 1X, 'Vertical Hydraulic Conductivity Array')
         WRITE (6,70) ((HCZ(I,J),I=1,480,80),J=1,5)
70       FORMAT (1X,6F10.6)

C * Initialize head values at all nodes.
         DO 80 J=1,5
            DO 80 I=1,480
               HOLD(I,J)=341.5-I*0.17
               HNEW(I,J)=341.5-I*0.17
80       CONTINUE

C * Initialize head values for known nodes
         HOLD(20,2)=338.28
         HOLD(32,2)=334.6
         HOLD(436,2)=267.48
         HOLD(448,2)=266.75
         HOLD(479,2)=260.0
         HNEW(20,2)=338.28
         HNEW(32,2)=334.60
         HNEW(436,2)=267.48
         HNEW(448,2)=266.75
         HNEW(479,2)=260.0

C * Initialize head values for top image nodes
```

```
      DO 90 I=1,480
         IF (I.LT.240) THEN
           HOLD(I,1)=HOLD(I,2)+REC*DX/HCZ(I,2)
           HNEW(I,1)=HNEW(I,2)+REC*DX/HCZ(I,2)
           ELSE
           HOLD(I,1)=HOLD(I,2)+REC*PER*DX/HCZ(I,2)
           HNEW(I,1)=HNEW(I,2)+REC*PER*DX/HCZ(I,2)
         ENDIF
90    CONTINUE

C * Write initial head values for the grid
      WRITE (6,120)
120   FORMAT (/ 1X, 'Initial head values')
      WRITE (6,130)
     +HOLD(20,2),HOLD(32,2),HOLD(436,2),HOLD(448,2)
130   FORMAT (1X, 4F9.2)
      WRITE (6,140) ((HOLD(I,J),I=1,480,60),J=1,5)
140   FORMAT (1X, 8F9.2)

C * Using the Crank-Nicolson approximation to iterate through
C * the nodes
      ALPHA=0.5
      TIME=0.0
      K=0
      NEND=1300
      DO 270 N=1,NEND
         NUMIT=0
         TIME=TIME+DT
180      AMAX=0.0
         NUMIT=NUMIT+1
         DO 200 J=2,4
            DO 190 I=2,479
               IF (I.EQ.479) GO TO 200
               OLDVAL=HNEW(I,J)
               H1=(HCX(I,J)*(HOLD(I-1,J)+HOLD(I+1,J))+HCZ(I,J)*
     +            (HOLD(I,J-1)+HOLD(I,J+1)))/2.0
               H2=(HCX(I,J)*(HNEW(I-1,J)+HNEW(I+1,J))+HCZ(I,J)*
     +            (HNEW(I,J-1)+HNEW(I,J+1)))/2.0
               F1=DX*S/(2.0*DT)
               F2=ALPHA*(HCX(I,J)+HCZ(I,J))
               F3=1/(F1+F2)
               HNEW(I,J)=F3*((F1*HOLD(I,J))+(1.0-ALPHA)*
     +          (H1-(HCX(I,J)+HCZ(I,J))*HOLD(I,J))+ALPHA*H2)
               ERR=ABS(HNEW(I,J)-OLDVAL)
               IF (ERR.GT.AMAX) AMAX=ERR
190         CONTINUE
200      CONTINUE
```

```
C * Assigning new values for left, right, and bottom image
C * points
         DO 210 J=1,5
            HNEW(1,J)=HNEW(3,J)
            HNEW(480,J)=HNEW(478,J)
210      CONTINUE
         DO 220 I=1,480
            HNEW(I,5)=HNEW(I,3)
220      CONTINUE
         IF (AMAX.GT.0.01) GO TO 180

C * Prepare for next time step
225      DO 230 I=1,480
            DO 230 J=1,5
               IF (J.EQ.1.AND.I.LE.240) THEN
                 HOLD(I,1)=HNEW(I,1)
                 HNEW(I,1)=HNEW(I,2)+REC*DX/HCZ(I,J)
                 ELSEIF (J.EQ.1.AND.I.GT.240) THEN
                 HOLD(I,1)=HNEW(I,1)
                 HNEW(I,1)=HNEW(I,2)+REC*PER*DX/HCZ(I,J)
                 ELSE
                 HOLD(I,J)=HNEW(I,J)
               ENDIF
230      CONTINUE

C * Output of final results
         K=K+1
         IF (K.EQ.400.OR.K.EQ.950.OR.K.EQ.1300) THEN
           WRITE (6,240) TIME, NUMIT
240        FORMAT (/ 1X,'Number of days =',F7.2, 5X,
     +             'Number of iterations =',I4)
           WRITE (6,250)
250        FORMAT (1X, 'Final Head Values')
           WRITE (6,255)
     +     HOLD(20,2),HOLD(32,2),HOLD(436,2),HOLD(448,2)
255        FORMAT (1X,4F9.2)
           WRITE (6,260) ((HOLD(I,J),I=1,480,60),J=1,5)
260        FORMAT (1X,8F9.2)
         ELSE
           K=K
         ENDIF
270    CONTINUE
1000   STOP
       END
```

Model 2, Simulation 1
Storativity = .050

Horizontal Hydraulic Conductivity Array

.099000	.099000	.099000	.099000	.099000	.099000
.495000	.495000	.495000	.495000	.495000	.495000
.198000	.198000	.198000	.198000	.198000	.198000
.049500	.049500	.049500	.049500	.049500	.049500
.099000	.099000	.099000	.099000	.099000	.099000

Vertical Hydraulic Conductivity Array

.099000	.099000	.099000	.099000	.099000	.099000
.495000	.495000	.495000	.495000	.495000	.495000
.198000	.198000	.198000	.198000	.198000	.198000
.049500	.049500	.049500	.049500	.049500	.049500
.099000	.099000	.099000	.099000	.099000	.099000

Initial head values

338.28	334.60	267.48	266.75				
341.45	331.25	321.05	310.85	300.65	290.45	280.25	270.05
341.33	331.13	320.93	310.73	300.53	290.33	280.13	269.93
341.33	331.13	320.93	310.73	300.53	290.33	280.13	269.93
341.33	331.13	320.93	310.73	300.53	290.33	280.13	269.93
341.33	331.13	320.93	310.73	300.53	290.33	280.13	269.93

Number of days = 400.00 Number of iterations = 2
Final Head Values

349.30	347.29	278.63	276.59				
351.68	342.95	332.75	322.55	312.35	302.15	291.95	281.75
351.10	342.37	332.17	321.97	311.77	301.57	291.37	281.17
350.60	341.86	331.66	321.46	311.26	301.06	290.86	280.66
350.28	341.52	331.32	321.12	310.92	300.73	290.53	280.33
350.60	341.86	331.66	321.46	311.26	301.06	290.86	280.66

Number of days = 950.00 Number of iterations = 2
Final Head Values

363.72	361.90	293.26	291.02				
365.64	357.59	347.39	337.19	327.00	316.80	306.60	296.40
365.06	357.01	346.81	336.62	326.42	316.22	306.02	295.82
364.56	356.51	346.31	336.11	325.91	315.71	305.51	295.31
364.23	356.17	345.97	335.77	325.57	315.37	305.17	294.97
364.56	356.51	346.31	336.11	325.91	315.71	305.51	295.31

Number of days =1300.00 Number of iterations = 2

Final Head Values

372.87	371.17	302.51	299.87				
374.63	366.91	356.71	346.51	336.32	326.12	315.92	305.71
374.05	366.33	356.13	345.94	335.74	325.54	315.34	305.13
373.54	365.82	355.63	345.43	335.23	325.03	314.83	304.63
373.21	365.49	355.29	345.09	334.89	324.69	314.49	304.29
373.54	365.82	355.63	345.43	335.23	325.03	314.83	304.63

Model 2, Simulation 2

Storativity = .050

Horizontal Hydraulic Conductivity Array

.142000	.142000	.142000	.142000	.142000	.142000
.710000	.710000	.710000	.710000	.710000	.710000
.284000	.284000	.284000	.284000	.284000	.284000
.071000	.071000	.071000	.071000	.071000	.071000
.142000	.142000	.142000	.142000	.142000	.142000

Vertical Hydraulic Conductivity Array

.142000	.142000	.142000	.142000	.142000	.142000
.710000	.710000	.710000	.710000	.710000	.710000
.284000	.284000	.284000	.284000	.284000	.284000
.071000	.071000	.071000	.071000	.071000	.071000
.142000	.142000	.142000	.142000	.142000	.142000

Initial head values

338.28	334.60	267.48	266.75				
341.41	331.21	321.01	310.81	300.61	290.41	280.21	270.01
341.33	331.13	320.93	310.73	300.53	290.33	280.13	269.93
341.33	331.13	320.93	310.73	300.53	290.33	280.13	269.93
341.33	331.13	320.93	310.73	300.53	290.33	280.13	269.93
341.33	331.13	320.93	310.73	300.53	290.33	280.13	269.93

Number of days = 400.00 Number of iterations = 2

Final Head Values

348.74	346.78	278.12	276.07				
350.77	342.26	332.06	321.86	311.66	301.46	291.26	281.06
350.37	341.87	331.67	321.47	311.27	301.07	290.87	280.67
350.03	341.52	331.32	321.12	310.92	300.72	290.52	280.32
349.81	341.29	331.09	320.89	310.69	300.49	290.29	280.09

350.03 341.52 331.32 321.12 310.92 300.72 290.52 280.32

Number of days = 950.00 Number of iterations = 2
Final Head Values

362.62	360.93	292.29	289.81				
364.18	356.50	346.30	336.10	325.90	315.70	305.50	295.29
363.79	356.10	345.90	335.70	325.50	315.30	305.10	294.90
363.45	355.75	345.55	335.35	325.15	314.95	304.75	294.55
363.22	355.52	345.33	335.13	324.93	314.73	304.53	294.32
363.45	355.75	345.55	335.35	325.15	314.95	304.75	294.55

Number of days =1300.00 Number of iterations = 2
Final Head Values

371.43	369.88	301.15	297.99				
372.85	365.55	355.35	345.15	334.95	324.75	314.55	304.33
372.45	365.15	354.96	344.76	334.56	324.36	314.16	303.93
372.11	364.81	354.61	344.41	334.21	324.01	313.81	303.59
371.88	364.58	354.38	344.18	333.98	323.78	313.58	303.36
372.11	364.81	354.61	344.41	334.21	324.01	313.81	303.59

Model 2, Simulation 3

Storativity = .050

Horizontal Hydraulic Conductivity Array

.057000	.057000	.057000	.057000	.057000	.057000
.285000	.285000	.285000	.285000	.285000	.285000
.114000	.114000	.114000	.114000	.114000	.114000
.028500	.028500	.028500	.028500	.028500	.028500
.057000	.057000	.057000	.057000	.057000	.057000

Vertical Hydraulic Conductivity Array

.057000	.057000	.057000	.057000	.057000	.057000
.285000	.285000	.285000	.285000	.285000	.285000
.114000	.114000	.114000	.114000	.114000	.114000
.028500	.028500	.028500	.028500	.028500	.028500
.057000	.057000	.057000	.057000	.057000	.057000

Initial head values

338.28	334.60	267.48	266.75				
341.54	331.34	321.14	310.94	300.74	290.54	280.34	270.14
341.33	331.13	320.93	310.73	300.53	290.33	280.13	269.93

341.33 331.13 320.93 310.73 300.53 290.33 280.13 269.93
341.33 331.13 320.93 310.73 300.53 290.33 280.13 269.93
341.33 331.13 320.93 310.73 300.53 290.33 280.13 269.93

Number of days = 400.00 Number of iterations = 2
Final Head Values
350.12 348.08 279.42 277.38
353.22 344.19 333.99 323.79 313.59 303.39 293.19 282.99
352.19 343.17 332.97 322.77 312.57 302.37 292.17 281.97
351.30 342.26 332.06 321.86 311.66 301.46 291.26 281.06
350.72 341.66 331.46 321.26 311.06 300.86 290.66 280.46
351.30 342.26 332.06 321.86 311.66 301.46 291.26 281.06

Number of days = 950.00 Number of iterations = 2
Final Head Values
365.09 363.13 294.47 292.40
367.74 359.25 349.05 338.85 328.65 318.45 308.25 298.05
366.72 358.22 348.02 337.82 327.62 317.42 307.22 297.02
365.82 357.32 347.12 336.92 326.72 316.52 306.32 296.12
365.23 356.72 346.52 336.32 326.12 315.92 305.72 295.52
365.82 357.32 347.12 336.92 326.72 316.52 306.32 296.12

Number of days =1300.00 Number of iterations = 2
Final Head Values
374.58 372.70 304.04 301.86
377.07 368.83 358.63 348.43 338.23 328.03 317.83 307.63
376.04 367.80 357.60 347.40 337.20 327.00 316.80 306.60
375.15 366.90 356.70 346.50 336.30 326.10 315.90 305.70
374.55 366.30 356.10 345.90 335.70 325.50 315.30 305.10
375.15 366.90 356.70 346.50 336.30 326.10 315.90 305.70

Appendix G
Conceptual Model 3: Program and Results

```
C ***************************************************************
C * Solving 2-D finite difference transient state flow model of
C * the resaturation of a reclaimed lignite mine.
C * Modeling Project for Master's Thesis
C * Program by Karen E. Jarocki
C ***************************************************************
C * This finite difference model simulates the resaturation of
C * shallow spoil aquifers at a reclaimed lignite mine.
C * The model uses a node centered finite difference grid
C * consisting 6 rows and 240 columns.  The nodes are spaced at
C * 25 feet along the X and Z axes.  Hydraulic conductivity can
C * decrease with depth due to compaction.  Recharge can vary
C * spatially in the X direction.
C ***************************************************************

C * Defining variables and grid
C * C13HCX=horizontal hydraulic conduct. (ft/day) for field C-13
C * C24HCZ=vertical hydraulic conduct. (ft/day) for field C-24
C * C24HCX=horizontal hydraulic conduct. (ft/day) for field C-13
C * C24HCZ=vertical hydraulic conduct. (ft/day) for field C-24
C * R1= high rate of recharge (ft/day)
C * R2= low rate of recharge (ft/day)
C * S= storativity (-)
C * DX= horizontal distance increment (ft)
C * DZ= vertical distance increment (ft)
C * DX=DZ=25 ft
C * DT= time increment (day)
C * HOLD= head at time step n
C * HNEW= head at time step n+1
C * REC= recharge rate (ft/day)
C * PER= percent of recharge rate used in field C-24
      DIMENSION HNEW(480,5),HOLD(480,5),HCX(480,5),HCZ(480,5)
      CHARACTER*12 OUTFILE
      S=0.05
      DX=25.0
      DT=1.0
      REC=0.0024
      PER=1.0
      C13HCX=0.0198
      C13HCZ=1.98
      C24HCX=1.98
      C24HCZ=0.0198

C * Opening output file
      WRITE (*,*) 'Enter the output file name.'
      READ (*,10) OUTFILE
10    FORMAT (A12)
```

```
      OPEN (UNIT=6,FILE=OUTFILE)

C * Initialize HCX and HCZ arrays with heterogeneous values
C * of hydraulic conductivity
      DO 20 J=1,5
        DO 20 I=1,480
         IF (I.LE.240) THEN
            HCX(I,J)=C13HCX
            HCZ(I,J)=C13HCZ
            ELSE
            HCX(I,J)=C24HCX
            HCZ(I,J)=C24HCZ
         ENDIF
         IF (J.EQ.2) THEN
            HCX(I,J)=HCX(I,J)*5.0
            HCZ(I,J)=HCZ(I,J)*5.0
            ELSEIF (J.EQ.3) THEN
            HCX(I,J)=HCX(I,J)*2.0
            HCZ(I,J)=HCZ(I,J)*2.0
            ELSEIF (J.EQ.4) THEN
            HCX(I,J)=HCX(I,J)*0.5
            HCZ(I,J)=HCZ(I,J)*0.5
         ENDIF

20    CONTINUE

C * Begin writing output with storativity and hydraulic
C * conductivity
      WRITE (6,30) S
30    FORMAT (1X, 'Storativity = ', F4.3)
      WRITE (6,40)
40    FORMAT (/ 1X, 'Horizontal Hydraulic Conductivity Array')
      WRITE (6,50) ((HCX(I,J),I=1,480,80),J=1,5)
50    FORMAT (1X,6F10.6)
      WRITE (6,60)
60    FORMAT (/ 1X, 'Vertical Hydraulic Conductivity Array')
      WRITE (6,70) ((HCZ(I,J),I=1,480,80),J=1,5)
70    FORMAT (1X,6F10.6)

C * Initialize head values at all nodes.
      DO 80 J=1,5
         DO 80 I=1,480
            HOLD(I,J)=341.5-I*0.17
            HNEW(I,J)=341.5-I*0.17
80    CONTINUE

C * Initialize head values for known nodes
```

```
      HOLD(20,2)=338.28
      HOLD(32,2)=334.6
      HOLD(436,2)=267.48
      HOLD(448,2)=266.75
      HOLD(479,2)=260.0
      HNEW(20,2)=338.28
      HNEW(32,2)=334.60
      HNEW(436,2)=267.48
      HNEW(448,2)=266.75
      HNEW(479,2)=260.0

C * Initialize head values for top image nodes
      DO 90 I=1,480
         IF (I.LT.240) THEN
           HOLD(I,1)=HOLD(I,2)+REC*DX/HCZ(I,2)
           HNEW(I,1)=HNEW(I,2)+REC*DX/HCZ(I,2)
           ELSE
           HOLD(I,1)=HOLD(I,2)+REC*PER*DX/HCZ(I,2)
           HNEW(I,1)=HNEW(I,2)+REC*PER*DX/HCZ(I,2)
         ENDIF
90    CONTINUE

C * Write initial head values for the grid
      WRITE (6,120)
120   FORMAT (/ 1X, 'Initial head values')
      WRITE (6,130)
     +HOLD(20,2),HOLD(32,2),HOLD(436,2),HOLD(448,2)
130   FORMAT (1X, 4F9.2)
      WRITE (6,140) ((HOLD(I,J),I=1,480,60),J=1,5)
140   FORMAT (1X, 8F9.2)

C * Using the Crank-Nicolson approximation to iterate through
C * the nodes
      ALPHA=0.5
      TIME=0.0
      K=0
      NEND=1300
      DO 270 N=1,NEND
         NUMIT=0
         TIME=TIME+DT
180      AMAX=0.0
         NUMIT=NUMIT+1
         DO 200 J=2,4
            DO 190 I=2,479
               IF (I.EQ.479) GO TO 200
               OLDVAL=HNEW(I,J)
               H1=(HCX(I,J)*(HOLD(I-1,J)+HOLD(I+1,J))+HCZ(I,J)*
```

```
     +            (HOLD(I,J-1)+HOLD(I,J+1)))/2.0
                H2=(HCX(I,J)*(HNEW(I-1,J)+HNEW(I+1,J))+HCZ(I,J)*
     +            (HNEW(I,J-1)+HNEW(I,J+1)))/2.0
                F1=DX*S/(2.0*DT)
                F2=ALPHA*(HCX(I,J)+HCZ(I,J))
                F3=1/(F1+F2)
                HNEW(I,J)=F3*((F1*HOLD(I,J))+(1.0-ALPHA)*
     +              (H1-(HCX(I,J)+HCZ(I,J))*HOLD(I,J))+ALPHA*H2)
                ERR=ABS(HNEW(I,J)-OLDVAL)
                IF (ERR.GT.AMAX) AMAX=ERR
190          CONTINUE
200       CONTINUE

C * Assigning new values for left, right, and bottom image
C * points
          DO 210 J=1,5
             HNEW(1,J)=HNEW(3,J)
             HNEW(480,J)=HNEW(478,J)
210       CONTINUE
          DO 220 I=1,480
             HNEW(I,5)=HNEW(I,3)
220       CONTINUE
          IF (AMAX.GT.0.01) GO TO 180

C * Prepare for next time step
225       DO 230 I=1,480
             DO 230 J=1,5
                IF (J.EQ.1.AND.I.LE.240) THEN
                  HOLD(I,1)=HNEW(I,1)
                  HNEW(I,1)=HNEW(I,2)+REC*DX/HCZ(I,J)
                  ELSEIF (J.EQ.1.AND.I.GT.240) THEN
                  HOLD(I,1)=HNEW(I,1)
                  HNEW(I,1)=HNEW(I,2)+REC*PER*DX/HCZ(I,J)
                  ELSE
                  HOLD(I,J)=HNEW(I,J)
                ENDIF
230       CONTINUE

C * Output of final results
          K=K+1
          IF (K.EQ.400.OR.K.EQ.950.OR.K.EQ.1300) THEN
            WRITE (6,240) TIME, NUMIT
240         FORMAT (/ 1X,'Number of days =',F7.2, 5X,
     +              'Number of iterations =',I4)
            WRITE (6,250)
250         FORMAT (1X, 'Final Head Values')
            WRITE (6,255)
```

```
     +      HOLD(20,2),HOLD(32,2),HOLD(436,2),HOLD(448,2)
255         FORMAT (1X,4F9.2)
            WRITE (6,260) ((HOLD(I,J),I=1,480,60),J=1,5)
260         FORMAT (1X,8F9.2)
          ELSE
            K=K
          ENDIF
270    CONTINUE
1000   STOP
       END
```

Model 3, Simulation 1
Storativity = .050

Horizontal Hydraulic Conductivity Array

.142000	.142000	.142000	.057000	.057000	.057000
.710000	.710000	.710000	.285000	.285000	.285000
.284000	.284000	.284000	.114000	.114000	.114000
.071000	.071000	.071000	.028500	.028500	.028500
.142000	.142000	.142000	.057000	.057000	.057000

Vertical Hydraulic Conductivity Array

.142000	.142000	.142000	.057000	.057000	.057000
.710000	.710000	.710000	.285000	.285000	.285000
.284000	.284000	.284000	.114000	.114000	.114000
.071000	.071000	.071000	.028500	.028500	.028500
.142000	.142000	.142000	.057000	.057000	.057000

Initial head values

338.28	334.60	267.48	266.75				
341.41	331.21	321.01	310.81	300.74	290.54	280.34	270.14
341.33	331.13	320.93	310.73	300.53	290.33	280.13	269.93
341.33	331.13	320.93	310.73	300.53	290.33	280.13	269.93
341.33	331.13	320.93	310.73	300.53	290.33	280.13	269.93
341.33	331.13	320.93	310.73	300.53	290.33	280.13	269.93

Number of days = 400.00 Number of iterations = 2
Final Head Values

348.75	346.78	279.42	277.38				
350.77	342.27	332.07	321.87	313.16	303.39	293.19	282.99
350.37	341.87	331.67	321.47	312.14	302.37	292.17	281.97
350.03	341.52	331.32	321.12	311.38	301.46	291.26	281.06
349.82	341.29	331.09	320.89	310.87	300.86	290.66	280.46
350.03	341.52	331.32	321.12	311.38	301.46	291.26	281.06

Number of days = 950.00 Number of iterations = 2
Final Head Values

362.62	360.93	294.47	292.40				
364.19	356.50	346.30	336.10	327.91	318.45	308.25	298.05
363.79	356.10	345.90	335.70	326.88	317.42	307.22	297.02
363.45	355.76	345.56	335.36	326.12	316.52	306.32	296.12
363.23	355.53	345.33	335.13	325.61	315.92	305.72	295.52
363.45	355.76	345.56	335.36	326.12	316.52	306.32	296.12

Number of days =1300.00 Number of iterations = 2

Final Head Values

371.44	369.88	304.04	301.86				
372.85	365.55	355.36	345.16	337.29	328.03	317.83	307.63
372.45	365.15	354.96	344.76	336.26	327.00	316.80	306.60
372.11	364.81	354.61	344.41	335.50	326.10	315.90	305.70
371.89	364.58	354.39	344.19	334.99	325.50	315.30	305.10
372.11	364.81	354.61	344.41	335.50	326.10	315.90	305.70

Model 3, Simulation 2

Storativity = .050

Horizontal Hydraulic Conductivity Array

.142000	.142000	.142000	2.000000	2.000000	2.000000
.710000	.710000	.710000	10.000000	10.000000	10.000000
.284000	.284000	.284000	4.000000	4.000000	4.000000
.071000	.071000	.071000	1.000000	1.000000	1.000000
.142000	.142000	.142000	2.000000	2.000000	2.000000

Vertical Hydraulic Conductivity Array

.142000	.142000	.142000	2.000000	2.000000	2.000000
.710000	.710000	.710000	10.000000	10.000000	10.000000
.284000	.284000	.284000	4.000000	4.000000	4.000000
.071000	.071000	.071000	1.000000	1.000000	1.000000
.142000	.142000	.142000	2.000000	2.000000	2.000000

Initial head values

338.28	334.60	267.48	266.75				
341.41	331.21	321.01	310.81	300.54	290.34	280.14	269.94
341.33	331.13	320.93	310.73	300.53	290.33	280.13	269.93
341.33	331.13	320.93	310.73	300.53	290.33	280.13	269.93
341.33	331.13	320.93	310.73	300.53	290.33	280.13	269.93
341.33	331.13	320.93	310.73	300.53	290.33	280.13	269.93

Number of days = 400.00 Number of iterations = 2

Final Head Values

348.76	346.80	271.34	269.03				
350.79	342.28	332.08	321.88	309.03	294.44	284.22	274.00
350.39	341.89	331.69	321.49	309.02	294.42	284.20	273.98
350.05	341.54	331.34	321.14	308.93	294.40	284.18	273.97

349.83 341.31 331.11 320.91 308.87 294.39 284.17 273.96
350.05 341.54 331.34 321.14 308.93 294.40 284.18 273.97

Number of days = 950.00 Number of iterations = 2
Final Head Values
362.64 360.95 275.71 272.57
364.20 356.52 346.32 336.12 320.54 300.33 289.67 278.99
363.81 356.12 345.92 335.72 320.53 300.31 289.65 278.97
363.47 355.77 345.57 335.37 320.44 300.30 289.63 278.96
363.24 355.54 345.35 335.15 320.38 300.29 289.62 278.95
363.47 355.77 345.57 335.37 320.44 300.30 289.63 278.96

Number of days =1300.00 Number of iterations = 2
Final Head Values
371.45 369.90 277.07 275.40
372.87 365.57 355.37 345.17 327.88 304.43 293.14 281.84
372.47 365.17 354.98 344.77 327.87 304.41 293.12 281.82
372.13 364.83 354.63 344.43 327.78 304.40 293.10 281.80
371.90 364.60 354.40 344.20 327.72 304.39 293.09 281.80
372.13 364.83 354.63 344.43 327.78 304.40 293.10 281.80

Model 3, Simulation 3
Storativity = .050

Horizontal Hydraulic Conductivity Array
.014200 .014200 .014200 1.420000 1.420000 1.420000
.071000 .071000 .071000 7.100000 7.100000 7.100000
.028400 .028400 .028400 2.840000 2.840000 2.840000
.007100 .007100 .007100 .710000 .710000 .710000
.014200 .014200 .014200 1.420000 1.420000 1.420000

Vertical Hydraulic Conductivity Array
1.420000 1.420000 1.420000 .014200 .014200 .014200
7.100000 7.100000 7.100000 .071000 .071000 .071000
2.840000 2.840000 2.840000 .028400 .028400 .028400
.710000 .710000 .710000 .007100 .007100 .007100
1.420000 1.420000 1.420000 .014200 .014200 .014200

Initial head values
338.28 334.60 267.48 266.75
341.34 331.14 320.94 310.74 301.38 291.18 280.98 270.78

341.33 331.13 320.93 310.73 300.53 290.33 280.13 269.93
341.33 331.13 320.93 310.73 300.53 290.33 280.13 269.93
341.33 331.13 320.93 310.73 300.53 290.33 280.13 269.93
341.33 331.13 320.93 310.73 300.53 290.33 280.13 269.93

Number of days = 400.00 Number of iterations = 2
Final Head Values
344.18 342.03 279.19 275.88
346.87 337.23 327.03 316.83 311.47 307.34 297.35 286.70
346.85 337.20 327.00 316.80 307.26 303.14 293.15 282.49
346.82 337.18 326.98 316.78 306.88 299.82 289.80 279.23
346.81 337.17 326.97 316.76 306.68 297.85 287.79 277.32
346.82 337.18 326.98 316.78 306.88 299.82 289.80 279.23

Number of days = 950.00 Number of iterations = 2
Final Head Values
352.27 350.16 287.12 282.02
354.78 345.33 335.13 324.93 319.89 318.49 309.12 296.29
354.75 345.30 335.10 324.90 315.68 314.29 304.92 292.08
354.73 345.28 335.08 324.88 315.30 311.00 301.59 288.94
354.72 345.26 335.06 324.86 315.11 309.09 299.61 287.22
354.73 345.28 335.08 324.88 315.30 311.00 301.59 288.94

Number of days =1300.00 Number of iterations = 2
Final Head Values
357.42 355.32 291.34 285.20
359.84 350.48 340.28 330.08 325.24 325.37 316.33 301.58
359.81 350.45 340.25 330.05 321.03 321.16 312.13 297.37
359.79 350.43 340.23 330.03 320.66 317.90 308.83 294.29
359.78 350.42 340.22 330.01 320.46 316.00 306.88 292.66
359.79 350.43 340.23 330.03 320.66 317.90 308.83 294.29

Model 3, Simulation 4
Storativity = .050

Horizontal Hydraulic Conductivity Array
1.420000 1.420000 1.420000 .014200 .014200 .014200
7.100000 7.100000 7.100000 .071000 .071000 .071000
2.840000 2.840000 2.840000 .028400 .028400 .028400
.710000 .710000 .710000 .007100 .007100 .007100
1.420000 1.420000 1.420000 .014200 .014200 .014200

Vertical Hydraulic Conductivity Array

.014200	.014200	.014200	1.420000	1.420000	1.420000
.071000	.071000	.071000	7.100000	7.100000	7.100000
.028400	.028400	.028400	2.840000	2.840000	2.840000
.007100	.007100	.007100	.710000	.710000	.710000
.014200	.014200	.014200	1.420000	1.420000	1.420000

Initial head values

338.28	334.60	267.48	266.75				
342.18	331.98	321.78	311.58	300.54	290.34	280.14	269.94
341.33	331.13	320.93	310.73	300.53	290.33	280.13	269.93
341.33	331.13	320.93	310.73	300.53	290.33	280.13	269.93
341.33	331.13	320.93	310.73	300.53	290.33	280.13	269.93
341.33	331.13	320.93	310.73	300.53	290.33	280.13	269.93

Number of days = 400.00 Number of iterations = 2

Final Head Values

348.80	347.76	273.46	271.51				
353.61	348.10	338.16	327.74	306.87	296.43	286.23	276.03
349.40	343.90	333.95	323.54	306.84	296.40	286.20	276.00
346.25	340.58	330.60	320.22	306.82	296.38	286.18	275.98
344.54	338.63	328.59	318.25	306.80	296.36	286.16	275.96
346.25	340.58	330.60	320.22	306.82	296.38	286.18	275.98

Number of days = 950.00 Number of iterations = 2

Final Head Values

358.72	357.99	281.55	279.57				
363.33	359.21	350.00	338.88	315.24	304.52	294.32	284.12
359.12	355.00	345.79	334.67	315.21	304.50	294.29	284.09
355.90	351.71	342.45	331.39	315.19	304.47	294.27	284.07
354.08	349.79	340.46	329.48	315.17	304.46	294.26	284.05
355.90	351.71	342.45	331.39	315.19	304.47	294.27	284.07

Number of days =1300.00 Number of iterations = 2

Final Head Values

365.28	364.65	286.70	284.71				
369.83	366.19	357.39	345.75	320.57	309.68	299.47	289.27
365.62	361.99	353.19	341.54	320.54	309.65	299.45	289.24
362.38	358.70	349.86	338.28	320.51	309.63	299.42	289.22
360.54	356.79	347.88	336.39	320.50	309.61	299.41	289.20
362.38	358.70	349.86	338.28	320.51	309.63	299.42	289.22

Model 3, Simulation 5
Storativity = .050

Horizontal Hydraulic Conductivity Array

1.420000	1.420000	1.420000	.027500	.027500	.027500
7.100000	7.100000	7.100000	.137500	.137500	.137500
2.840000	2.840000	2.840000	.055000	.055000	.055000
.710000	.710000	.710000	.013750	.013750	.013750
1.420000	1.420000	1.420000	.027500	.027500	.027500

Vertical Hydraulic Conductivity Array

.014200	.014200	.014200	2.750000	2.750000	2.750000
.071000	.071000	.071000	13.750000	13.750000	13.750000
.028400	.028400	.028400	5.500000	5.500000	5.500000
.007100	.007100	.007100	1.375000	1.375000	1.375000
.014200	.014200	.014200	2.750000	2.750000	2.750000

Initial head values

338.28	334.60	267.48	266.75				
342.18	331.98	321.78	311.58	300.53	290.33	280.13	269.93
341.33	331.13	320.93	310.73	300.53	290.33	280.13	269.93
341.33	331.13	320.93	310.73	300.53	290.33	280.13	269.93
341.33	331.13	320.93	310.73	300.53	290.33	280.13	269.93
341.33	331.13	320.93	310.73	300.53	290.33	280.13	269.93

Number of days = 400.00 Number of iterations = 2
Final Head Values

348.80	347.76	271.50	269.57				
353.61	348.10	338.16	327.69	305.07	294.46	284.26	274.06
349.40	343.90	333.95	323.49	305.06	294.45	284.25	274.05
346.25	340.58	330.60	320.18	305.05	294.44	284.24	274.04
344.54	338.63	328.59	318.23	305.04	294.43	284.23	274.03
346.25	340.58	330.60	320.18	305.05	294.44	284.24	274.04

Number of days = 950.00 Number of iterations = 2
Final Head Values

358.72	357.99	276.93	274.95				
363.33	359.21	349.98	338.44	311.01	299.88	289.68	279.48
359.12	355.00	345.77	334.23	311.00	299.87	289.67	279.47
355.90	351.71	342.44	330.99	310.99	299.86	289.66	279.46
354.08	349.79	340.45	329.12	310.98	299.85	289.65	279.45
355.90	351.71	342.44	330.99	310.99	299.86	289.66	279.46

Number of days =1300.00 Number of iterations = 2
Final Head Values

365.28	364.65	280.38	278.39				
369.83	366.19	357.32	344.89	314.79	303.33	293.13	282.93
365.62	361.99	353.12	340.69	314.78	303.32	293.12	282.92
362.38	358.70	349.80	337.47	314.77	303.31	293.11	282.91
360.54	356.78	347.83	335.65	314.77	303.31	293.10	282.90
362.38	358.70	349.80	337.47	314.77	303.31	293.11	282.91

Model 3, Simulation 6

Storativity = .050

Horizontal Hydraulic Conductivity Array

1.420000	1.420000	1.420000	.030000	.030000	.030000
7.100000	7.100000	7.100000	.150000	.150000	.150000
2.840000	2.840000	2.840000	.060000	.060000	.060000
.710000	.710000	.710000	.015000	.015000	.015000
1.420000	1.420000	1.420000	.030000	.030000	.030000

Vertical Hydraulic Conductivity Array

.014200	.014200	.014200	3.000000	3.000000	3.000000
.071000	.071000	.071000	15.000000	15.000000	15.000000
.028400	.028400	.028400	6.000000	6.000000	6.000000
.007100	.007100	.007100	1.500000	1.500000	1.500000
.014200	.014200	.014200	3.000000	3.000000	3.000000

Initial head values

338.28	334.60	267.48	266.75				
342.18	331.98	321.78	311.58	300.53	290.33	280.13	269.93
341.33	331.13	320.93	310.73	300.53	290.33	280.13	269.93
341.33	331.13	320.93	310.73	300.53	290.33	280.13	269.93
341.33	331.13	320.93	310.73	300.53	290.33	280.13	269.93
341.33	331.13	320.93	310.73	300.53	290.33	280.13	269.93

Number of days = 400.00 Number of iterations = 2
Final Head Values

348.80	347.76	271.26	269.33				
353.61	348.10	338.16	327.69	304.85	294.21	284.01	273.81
349.40	343.90	333.95	323.48	304.84	294.20	284.00	273.80
346.25	340.58	330.60	320.18	304.83	294.19	283.99	273.79
344.54	338.63	328.59	318.23	304.82	294.19	283.99	273.79

346.25 340.58 330.60 320.18 304.83 294.19 283.99 273.79

Number of days = 950.00 Number of iterations = 2
Final Head Values
358.72 357.99 276.35 274.38
363.33 359.21 349.97 338.39 310.49 299.31 289.10 278.90
359.12 355.00 345.77 334.18 310.48 299.29 289.09 278.89
355.90 351.71 342.44 330.94 310.47 299.29 289.09 278.89
354.08 349.79 340.45 329.08 310.46 299.28 289.08 278.88
355.90 351.71 342.44 330.94 310.47 299.29 289.09 278.89

Number of days =1300.00 Number of iterations = 2
Final Head Values
365.28 364.65 279.60 277.61
369.83 366.19 357.32 344.79 314.09 302.55 292.35 282.15
365.62 361.98 353.11 340.58 314.08 302.54 292.34 282.13
362.38 358.70 349.79 337.37 314.07 302.53 292.33 282.13
360.54 356.78 347.83 335.55 314.06 302.52 292.32 282.12
362.38 358.70 349.79 337.37 314.07 302.53 292.33 282.13

Model 3, Simulation 7
Storativity = .050

Horizontal Hydraulic Conductivity Array
.019800 .019800 .019800 1.980000 1.980000 1.980000
.099000 .099000 .099000 9.900000 9.900000 9.900000
.039600 .039600 .039600 3.960000 3.960000 3.960000
.009900 .009900 .009900 .990000 .990000 .990000
.019800 .019800 .019800 1.980000 1.980000 1.980000

Vertical Hydraulic Conductivity Array
1.980000 1.980000 1.980000 .019800 .019800 .019800
9.900000 9.900000 9.900000 .099000 .099000 .099000
3.960000 3.960000 3.960000 .039600 .039600 .039600
.990000 .990000 .990000 .009900 .009900 .009900
1.980000 1.980000 1.980000 .019800 .019800 .019800

Initial head values
338.28 334.60 267.48 266.75
341.34 331.14 320.94 310.74 301.14 290.94 280.74 270.54
341.33 331.13 320.93 310.73 300.53 290.33 280.13 269.93

341.33 331.13 320.93 310.73 300.53 290.33 280.13 269.93
341.33 331.13 320.93 310.73 300.53 290.33 280.13 269.93
341.33 331.13 320.93 310.73 300.53 290.33 280.13 269.93

Number of days = 400.00 Number of iterations = 3
Final Head Values
343.21 341.05 277.11 273.90
345.86 336.24 326.04 315.84 309.19 304.12 294.16 283.43
345.85 336.23 326.03 315.83 306.17 301.11 291.16 280.42
345.83 336.21 326.01 315.81 305.91 298.78 288.80 278.14
345.82 336.20 326.00 315.80 305.78 297.45 287.42 276.86
345.83 336.21 326.01 315.81 305.91 298.78 288.80 278.14

Number of days = 950.00 Number of iterations = 2
Final Head Values
350.09 347.97 283.95 279.13
352.54 343.13 332.93 322.73 316.43 314.26 304.98 291.85
352.53 343.12 332.92 322.72 313.40 311.25 301.97 288.84
352.51 343.10 332.90 322.70 313.14 308.96 299.65 286.65
352.50 343.09 332.89 322.69 313.02 307.67 298.31 285.52
352.51 343.10 332.90 322.70 313.14 308.96 299.65 286.65

Number of days =1300.00 Number of iterations = 3
Final Head Values
354.47 352.36 287.51 281.78
356.82 347.51 337.31 327.11 321.00 320.40 311.44 296.37
356.80 347.49 337.29 327.09 318.00 317.39 308.43 293.36
356.79 347.48 337.28 327.08 317.73 315.12 306.13 291.21
356.78 347.47 337.27 327.07 317.61 313.85 304.84 290.13
356.79 347.48 337.28 327.08 317.73 315.12 306.13 291.21

Appendix H
Conceptual Model 4: Program and Results

```
C ***************************************************************
C * Solving 2-D finite difference transient state flow model of
the resaturation of a reclaimed lignite mine.
C * Modeling Project for Master's Thesis
C * Program by Karen E. Jarocki
C ***************************************************************
C * This finite difference model simulates the resaturation of
C * shallow spoil aquifers at a reclaimed lignite mine.  The
C * model uses a node centered finite difference grid consisting
C * 6 rows and 240 columns.  The nodes are spaced at 25 feet
C * along the X and Z axes.  Hydraulic conductivity can decrease
C * with depth due to compaction.  Recharge can vary spatially
C * in the X direction.
C ***************************************************************

C * Defining variables and grid
C * HCX= horizontal hydraulic conductivity (ft/day)
C * HCZ= vertical hydraulic conductivity (ft/day)
C * R1= high rate of recharge (ft/day)
C * R2= low rate of recharge (ft/day)
C * S= storativity (-)
C * DX= horizontal distance increment (ft)
C * DZ= vertical distance increment (ft)
C * DX=DZ=25 ft
C * DT= time increment (day)
C * HOLD= head at time step n
C * HNEW= head at time step n+1
C * REC= recharge rate (ft/day)
C * PER= percent of recharge rate used in field C-24
      DIMENSION HNEW(480,5),HOLD(480,5),HCX(480,5),HCZ(480,5)
      CHARACTER*12 OUTFILE
      S=0.05
      DX=25.0
      DT=1.0
      REC=0.0024
      PER=0.50

C * Opening output file
      WRITE (*,*) 'Enter the output file name.'
      READ (*,10) OUTFILE
10    FORMAT (A12)
      OPEN (UNIT=6,FILE=OUTFILE)

C * Initialize HCX and HCZ arrays with heterogeneous values
C * of hydraulic conductivity
      DO 20 J=1,5
        DO 20 I=1,480
```

```
            HCX(I,J)=0.099
            HCZ(I,J)=0.099
            IF (J.EQ.2) THEN
               HCX(I,J)=HCX(I,J)*5.0
               HCZ(I,J)=HCZ(I,J)*5.0
               ELSEIF (J.EQ.3) THEN
               HCX(I,J)=HCX(I,J)*2.0
               HCZ(I,J)=HCZ(I,J)*2.0
               ELSEIF (J.EQ.4) THEN
               HCX(I,J)=HCX(I,J)*0.5
               HCZ(I,J)=HCZ(I,J)*0.5
            ENDIF
20       CONTINUE

C * Begin writing output with storativity and hydraulic
C * conductivity
         PERRECH=PER*100
         WRITE (6,30) S, PERRECH
30       FORMAT (1X, 'Storativity = ', F4.3, 10X, 'C-24 Percent
        +Recharge =', F4.1)
         WRITE (6,40)
40       FORMAT (/ 1X, 'Horizontal Hydraulic Conductivity Array')
         WRITE (6,50) ((HCX(I,J),I=1,480,80),J=1,5)
50       FORMAT (1X,6F10.6)
         WRITE (6,60)
60       FORMAT (/ 1X, 'Vertical Hydraulic Conductivity Array')
         WRITE (6,70) ((HCZ(I,J),I=1,480,80),J=1,5)
70       FORMAT (1X,6F10.6)

C * Initialize head values at all nodes.
         DO 80 J=1,5
            DO 80 I=1,480
               HOLD(I,J)=341.5-I*0.17
               HNEW(I,J)=341.5-I*0.17
80       CONTINUE

C * Initialize head values for known nodes
         HOLD(20,2)=338.28
         HOLD(32,2)=334.6
         HOLD(436,2)=267.48
         HOLD(448,2)=266.75
         HOLD(479,2)=260.0
         HNEW(20,2)=338.28
         HNEW(32,2)=334.60
         HNEW(436,2)=267.48
         HNEW(448,2)=266.75
         HNEW(479,2)=260.0
```

```
C * Initialize head values for top image nodes
      DO 90 I=1,480
         IF (I.LT.240) THEN
           HOLD(I,1)=HOLD(I,2)+REC*DX/HCZ(I,2)
           HNEW(I,1)=HNEW(I,2)+REC*DX/HCZ(I,2)
           ELSE
           HOLD(I,1)=HOLD(I,2)+REC*PER*DX/HCZ(I,2)
           HNEW(I,1)=HNEW(I,2)+REC*PER*DX/HCZ(I,2)
         ENDIF
90    CONTINUE

C * Write initial head values for the grid
      WRITE (6,120)
120   FORMAT (/ 1X, 'Initial head values')
      WRITE (6,130)
     +HOLD(20,2),HOLD(32,2),HOLD(436,2),HOLD(448,2)
130   FORMAT (1X, 4F9.2)
      WRITE (6,140) ((HOLD(I,J),I=1,480,60),J=1,5)
140   FORMAT (1X, 8F9.2)

C * Using the Crank-Nicolson approximation to iterate through
C * the nodes
      ALPHA=0.5
      TIME=0.0
      K=0
      NEND=1300
      DO 270 N=1,NEND
         NUMIT=0
         TIME=TIME+DT
180      AMAX=0.0
         NUMIT=NUMIT+1
         DO 200 J=2,4
            DO 190 I=2,479
               IF (I.EQ.479) GO TO 200
               OLDVAL=HNEW(I,J)
               H1=(HCX(I,J)*(HOLD(I-1,J)+HOLD(I+1,J))+HCZ(I,J)*
     +            (HOLD(I,J-1)+HOLD(I,J+1)))/2.0
               H2=(HCX(I,J)*(HNEW(I-1,J)+HNEW(I+1,J))+HCZ(I,J)*
     +            (HNEW(I,J-1)+HNEW(I,J+1)))/2.0
               F1=DX*S/(2.0*DT)
               F2=ALPHA*(HCX(I,J)+HCZ(I,J))
               F3=1/(F1+F2)
               HNEW(I,J)=F3*((F1*HOLD(I,J))+(1.0-ALPHA)*
     +              (H1-(HCX(I,J)+HCZ(I,J))*HOLD(I,J))+ALPHA*H2)
               ERR=ABS(HNEW(I,J)-OLDVAL)
               IF (ERR.GT.AMAX) AMAX=ERR
```

```
190         CONTINUE
200      CONTINUE

C * Assigning new values for left, right, and bottom image
C * points
         DO 210 J=1,5
            HNEW(1,J)=HNEW(3,J)
            HNEW(480,J)=HNEW(478,J)
210      CONTINUE
         DO 220 I=1,480
            HNEW(I,5)=HNEW(I,3)
220      CONTINUE
         IF (AMAX.GT.0.01) GO TO 180

C * Prepare for next time step
225      DO 230 I=1,480
            DO 230 J=1,5
               IF (J.EQ.1.AND.I.LE.240) THEN
                 HOLD(I,1)=HNEW(I,1)
                 HNEW(I,1)=HNEW(I,2)+REC*DX/HCZ(I,J)
                 ELSEIF (J.EQ.1.AND.I.GT.240) THEN
                 HOLD(I,1)=HNEW(I,1)
                 HNEW(I,1)=HNEW(I,2)+REC*PER*DX/HCZ(I,J)
                 ELSE
                 HOLD(I,J)=HNEW(I,J)
               ENDIF
230      CONTINUE

C * Output of final results
         K=K+1
         IF (K.EQ.400.OR.K.EQ.950.OR.K.EQ.1300) THEN
           WRITE (6,240) TIME, NUMIT
240        FORMAT (/ 1X,'Number of days =',F7.2, 5X,
     +              'Number of iterations =',I4)
           WRITE (6,250)
250        FORMAT (1X, 'Final Head Values')
           WRITE (6,255)
     +     HOLD(20,2),HOLD(32,2),HOLD(436,2),HOLD(448,2)
255        FORMAT (1X,4F9.2)
           WRITE (6,260) ((HOLD(I,J),I=1,480,60),J=1,5)
260        FORMAT (1X,8F9.2)
         ELSE
           K=K
         ENDIF
270   CONTINUE
1000  STOP
      END
```

Model 4, Simulation 1

Storativity = .050 C-24 Percent Recharge = 25.0

Horizontal Hydraulic Conductivity Array

.099000	.099000	.099000	.099000	.099000	.099000
.495000	.495000	.495000	.495000	.495000	.495000
.198000	.198000	.198000	.198000	.198000	.198000
.049500	.049500	.049500	.049500	.049500	.049500
.099000	.099000	.099000	.099000	.099000	.099000

Vertical Hydraulic Conductivity Array

.099000	.099000	.099000	.099000	.099000	.099000
.495000	.495000	.495000	.495000	.495000	.495000
.198000	.198000	.198000	.198000	.198000	.198000
.049500	.049500	.049500	.049500	.049500	.049500
.099000	.099000	.099000	.099000	.099000	.099000

Initial head values

338.28	334.60	267.48	266.75				
341.45	331.25	321.05	310.85	300.56	290.36	280.16	269.96
341.33	331.13	320.93	310.73	300.53	290.33	280.13	269.93
341.33	331.13	320.93	310.73	300.53	290.33	280.13	269.93
341.33	331.13	320.93	310.73	300.53	290.33	280.13	269.93
341.33	331.13	320.93	310.73	300.53	290.33	280.13	269.93

Number of days = 400.00 Number of iterations = 2

Final Head Values

349.30	347.29	270.19	268.16				
351.68	342.95	332.75	322.55	307.30	293.28	283.08	272.88
351.10	342.37	332.17	321.97	307.17	293.14	282.94	272.74
350.60	341.86	331.66	321.46	306.92	293.01	282.81	272.61
350.28	341.52	331.32	321.12	306.73	292.93	282.73	272.53
350.60	341.86	331.66	321.46	306.92	293.01	282.81	272.61

Number of days = 950.00 Number of iterations = 2

Final Head Values

363.72	361.90	273.85	271.76				
365.64	357.59	347.39	337.19	316.28	296.94	286.74	276.54
365.06	357.01	346.81	336.61	316.14	296.80	286.60	276.40
364.56	356.51	346.31	336.11	315.90	296.67	286.47	276.27
364.23	356.17	345.97	335.77	315.71	296.59	286.39	276.19
364.56	356.51	346.31	336.11	315.90	296.67	286.47	276.27

Number of days =1300.00 Number of iterations = 2

Final Head Values

372.87	371.17	276.16	273.97				
374.63	366.91	356.71	346.51	322.01	299.27	289.07	278.87
374.05	366.33	356.13	345.93	321.88	299.13	288.93	278.73
373.54	365.82	355.63	345.42	321.63	299.00	288.80	278.60
373.21	365.49	355.29	345.09	321.44	298.92	288.71	278.51
373.54	365.82	355.63	345.42	321.63	299.00	288.80	278.60

Model 4, Simulation 2

Storativity = .050 C-24 Percent Recharge = 50.0

Horizontal Hydraulic Conductivity Array

.099000	.099000	.099000	.099000	.099000	.099000
.495000	.495000	.495000	.495000	.495000	.495000
.198000	.198000	.198000	.198000	.198000	.198000
.049500	.049500	.049500	.049500	.049500	.049500
.099000	.099000	.099000	.099000	.099000	.099000

Vertical Hydraulic Conductivity Array

.099000	.099000	.099000	.099000	.099000	.099000
.495000	.495000	.495000	.495000	.495000	.495000
.198000	.198000	.198000	.198000	.198000	.198000
.049500	.049500	.049500	.049500	.049500	.049500
.099000	.099000	.099000	.099000	.099000	.099000

Initial head values

338.28	334.60	267.48	266.75				
341.45	331.25	321.05	310.85	300.59	290.39	280.19	269.99
341.33	331.13	320.93	310.73	300.53	290.33	280.13	269.93
341.33	331.13	320.93	310.73	300.53	290.33	280.13	269.93
341.33	331.13	320.93	310.73	300.53	290.33	280.13	269.93
341.33	331.13	320.93	310.73	300.53	290.33	280.13	269.93

Number of days = 400.00 Number of iterations = 2

Final Head Values

349.30	347.29	273.00	270.97				
351.68	342.95	332.75	322.55	308.98	296.24	286.04	275.84
351.10	342.37	332.17	321.97	308.70	295.95	285.75	275.55
350.60	341.86	331.66	321.46	308.37	295.69	285.49	275.29
350.28	341.52	331.32	321.12	308.13	295.52	285.32	275.12
350.60	341.86	331.66	321.46	308.37	295.69	285.49	275.29

Number of days = 950.00 Number of iterations = 2
Final Head Values

363.72	361.90	280.32	278.18				
365.64	357.59	347.39	337.19	319.85	303.55	293.35	283.16
365.06	357.01	346.81	336.61	319.57	303.27	293.07	282.87
364.56	356.51	346.31	336.11	319.23	303.01	292.81	282.61
364.23	356.17	345.97	335.77	318.99	302.84	292.64	282.44
364.56	356.51	346.31	336.11	319.23	303.01	292.81	282.61

Number of days =1300.00 Number of iterations = 2
Final Head Values

372.87	371.17	284.94	282.60				
374.63	366.91	356.71	346.51	326.78	308.21	298.01	287.81
374.05	366.33	356.13	345.93	326.50	307.92	297.72	287.52
373.54	365.82	355.63	345.43	326.16	307.67	297.47	287.27
373.21	365.49	355.29	345.09	325.93	307.50	297.30	287.10
373.54	365.82	355.63	345.43	326.16	307.67	297.47	287.27

Model 4, Simulation 3
Storativity = .050 C-24 Percent Recharge = 28.0

Horizontal Hydraulic Conductivity Array

.099000	.099000	.099000	.099000	.099000	.099000
.495000	.495000	.495000	.495000	.495000	.495000
.198000	.198000	.198000	.198000	.198000	.198000
.049500	.049500	.049500	.049500	.049500	.049500
.099000	.099000	.099000	.099000	.099000	.099000

Vertical Hydraulic Conductivity Array

.099000	.099000	.099000	.099000	.099000	.099000
.495000	.495000	.495000	.495000	.495000	.495000
.198000	.198000	.198000	.198000	.198000	.198000
.049500	.049500	.049500	.049500	.049500	.049500
.099000	.099000	.099000	.099000	.099000	.099000

Initial head values

338.28	334.60	267.48	266.75				
341.45	331.25	321.05	310.85	300.56	290.36	280.16	269.96
341.33	331.13	320.93	310.73	300.53	290.33	280.13	269.93
341.33	331.13	320.93	310.73	300.53	290.33	280.13	269.93
341.33	331.13	320.93	310.73	300.53	290.33	280.13	269.93
341.33	331.13	320.93	310.73	300.53	290.33	280.13	269.93

Number of days = 400.00 Number of iterations = 2
Final Head Values

349.30	347.29	270.53	268.50				
351.68	342.95	332.75	322.55	307.50	293.64	283.44	273.24
351.10	342.37	332.17	321.97	307.35	293.47	283.27	273.07
350.60	341.86	331.66	321.46	307.10	293.33	283.13	272.93
350.28	341.52	331.32	321.12	306.90	293.24	283.04	272.84
350.60	341.86	331.66	321.46	307.10	293.33	283.13	272.93

Number of days = 950.00 Number of iterations = 2
Final Head Values

363.72	361.90	274.62	272.53				
365.64	357.59	347.39	337.19	316.70	297.73	287.53	277.33
365.06	357.01	346.81	336.61	316.55	297.57	287.37	277.17
364.56	356.51	346.31	336.11	316.30	297.43	287.23	277.03
364.23	356.17	345.97	335.77	316.10	297.33	287.13	276.93
364.56	356.51	346.31	336.11	316.30	297.43	287.23	277.03

Number of days =1300.00 Number of iterations = 2
Final Head Values

372.87	371.17	277.21	275.01				
374.63	366.91	356.71	346.51	322.58	300.34	290.14	279.94
374.05	366.33	356.13	345.93	322.43	300.18	289.98	279.78
373.54	365.82	355.63	345.42	322.18	300.04	289.83	279.64
373.21	365.49	355.29	345.09	321.98	299.94	289.74	279.54
373.54	365.82	355.63	345.42	322.18	300.04	289.83	279.64

Model 4, Simulation 4

Storativity = .050 C-24 Percent Recharge = 30.0

Horizontal Hydraulic Conductivity Array

.142000	.142000	.142000	.142000	.142000	.142000
.710000	.710000	.710000	.710000	.710000	.710000
.284000	.284000	.284000	.284000	.284000	.284000
.071000	.071000	.071000	.071000	.071000	.071000
.142000	.142000	.142000	.142000	.142000	.142000

Vertical Hydraulic Conductivity Array

.142000	.142000	.142000	.142000	.142000	.142000
.710000	.710000	.710000	.710000	.710000	.710000
.284000	.284000	.284000	.284000	.284000	.284000
.071000	.071000	.071000	.071000	.071000	.071000
.142000	.142000	.142000	.142000	.142000	.142000

Initial head values

338.28	334.60	267.48	266.75				
341.41	331.21	321.01	310.81	300.56	290.36	280.16	269.96
341.33	331.13	320.93	310.73	300.53	290.33	280.13	269.93
341.33	331.13	320.93	310.73	300.53	290.33	280.13	269.93
341.33	331.13	320.93	310.73	300.53	290.33	280.13	269.93
341.33	331.13	320.93	310.73	300.53	290.33	280.13	269.93

Number of days = 400.00 Number of iterations = 2

Final Head Values

348.74	346.78	270.61	268.57				
350.77	342.26	332.06	321.86	307.33	293.68	283.48	273.28
350.37	341.87	331.67	321.47	307.22	293.56	283.36	273.16
350.03	341.52	331.32	321.12	307.04	293.45	283.25	273.05
349.81	341.29	331.09	320.89	306.91	293.38	283.18	272.99
350.03	341.52	331.32	321.12	307.04	293.45	283.25	273.05

Number of days = 950.00 Number of iterations = 2

Final Head Values

362.62	360.93	274.87	272.69				
364.18	356.50	346.30	336.10	316.45	297.96	287.75	277.55
363.79	356.10	345.90	335.70	316.34	297.84	287.63	277.43
363.45	355.75	345.55	335.35	316.16	297.73	287.53	277.33
363.22	355.52	345.33	335.12	316.02	297.66	287.46	277.26
363.45	355.75	345.55	335.35	316.16	297.73	287.53	277.33

Number of days =1300.00 Number of iterations = 2

Final Head Values

371.43	369.88	277.53	275.15				
372.85	365.55	355.35	345.15	322.27	300.68	290.48	280.27
372.45	365.15	354.96	344.75	322.16	300.56	290.36	280.15
372.11	364.81	354.61	344.41	321.98	300.46	290.25	280.04
371.88	364.58	354.38	344.18	321.85	300.39	290.18	279.97
372.11	364.81	354.61	344.41	321.98	300.46	290.25	280.04

Model 4, Simulation 5

Storativity = .050 C-24 Percent Recharge = 32.0

Horizontal Hydraulic Conductivity Array

.142000	.142000	.142000	.142000	.142000	.142000
.710000	.710000	.710000	.710000	.710000	.710000
.284000	.284000	.284000	.284000	.284000	.284000
.071000	.071000	.071000	.071000	.071000	.071000
.142000	.142000	.142000	.142000	.142000	.142000

Vertical Hydraulic Conductivity Array

.142000	.142000	.142000	.142000	.142000	.142000
.710000	.710000	.710000	.710000	.710000	.710000
.284000	.284000	.284000	.284000	.284000	.284000
.071000	.071000	.071000	.071000	.071000	.071000
.142000	.142000	.142000	.142000	.142000	.142000

Initial head values

338.28	334.60	267.48	266.75				
341.41	331.21	321.01	310.81	300.56	290.36	280.16	269.96
341.33	331.13	320.93	310.73	300.53	290.33	280.13	269.93
341.33	331.13	320.93	310.73	300.53	290.33	280.13	269.93
341.33	331.13	320.93	310.73	300.53	290.33	280.13	269.93
341.33	331.13	320.93	310.73	300.53	290.33	280.13	269.93

Number of days = 400.00 Number of iterations = 2

Final Head Values

348.74	346.78	270.82	268.78				
350.77	342.26	332.06	321.86	307.46	293.90	283.70	273.50
350.37	341.87	331.67	321.47	307.34	293.77	283.57	273.37
350.03	341.52	331.32	321.12	307.16	293.66	283.46	273.26
349.81	341.29	331.09	320.89	307.02	293.59	283.39	273.19
350.03	341.52	331.32	321.12	307.16	293.66	283.46	273.26

Number of days = 950.00 Number of iterations = 2

Final Head Values

362.62	360.93	275.36	273.18				
364.18	356.50	346.30	336.10	316.72	298.46	288.26	278.06
363.79	356.10	345.90	335.70	316.60	298.33	288.13	277.93
363.45	355.75	345.55	335.35	316.42	298.22	288.02	277.82
363.22	355.52	345.33	335.12	316.28	298.15	287.95	277.75
363.45	355.75	345.55	335.35	316.42	298.22	288.02	277.82

Number of days =1300.00 Number of iterations = 2

Final Head Values

371.43	369.88	277.20	275.80				
372.85	365.55	355.35	345.15	322.63	301.37	291.16	280.95
372.45	365.15	354.96	344.75	322.51	301.24	291.04	280.83
372.11	364.81	354.61	344.41	322.33	301.13	290.93	280.72
371.88	364.58	354.38	344.18	322.19	301.06	290.85	280.64
372.11	364.81	354.61	344.41	322.33	301.13	290.93	280.72

References

Albrecht, K.A., B.L. Hertzog, L.R. Follmer, I.G. Krapac, R.A. Griffin, and K. Cartwright, 1989, Excavation of an Instrumented Earthen Liner: Inspection of Dyed Flow Paths and Morphology. Hazardous Waste and Hazardous Materials, vol. 6, no. 3, p. 269-279.

Armstrong, S.C., 1987, Engineering Geologic Analysis of Reclaimed Spoil at a Southeast Texas Gulf Coast Lignite Mine. M.S. Thesis, Texas A&M University, 179 p.

Borbely, E.S., 1988, Development and Chemical Quality of a Ground-water System in the Cast Overburden at the Gibbons Creek Lignite Mine. M.S. Thesis, Texas A&M University, 199 p.

Bowman, R.S. and D.B. Stephens, 1991, Field Study of Multidimensional Flow and Transport in the Vadose Zone. New Mexico Water Resources Research Institute, Technical Completion Report No. 262, 132 p.

Butters, G.L., W.A. Jury, and F.F. Ernst, 1989, Field Scale Transport of Bromide in an Unsaturated Soil 1. Experimental Methodology and Results. Water Resources Research. vol. 25, no. 7, p. 1575-1581.

Canarache, A., E. Motoc, and R. Dumitriu, 1968, Infiltration Rates as Related to Hydraulic Conductivity, Moisture Content and Other Soil Properties. In Water in the Unsaturated Zone, D.E. Rijtena and H. Wassink (eds.), IAHS Publication 82(1), p. 392-410.

Clarke, J.V. and P.J. Vincent, 1974, A new technique using insoluble dyestuffs for the study of water movements in soil. Journal of Biogeography, vol. 1, p. 247-252.

Corey, J.C., 1968, Evaluation of dyes for tracing water movement in acid soils. Soil Science, vol. 106, no. 3, p. 182-187.

Day, P.R., *et al.*, 1956, Report of the Committee on Physical Analyses, 1954-1955. Soil Science Society of America Proceedings, vol. 20, p. 167-169.

Dixon, R.M., 1975, Design and Use of Closed-top Infiltrometers. Soil Science Society of America Proceedings, vol. 39, p. 755-763.

Dutton, A.R., 1982, Hydrogeochemistry of the Unsaturated Zone at Big Brown Lignite Mine, East Texas. Dissertation, University of Texas, Austin, 239 p.

Fisher, W.L. and J.H. McGowen, 1967, Depositional Systems in the Wilcox Group of Texas and Their Relationship to the Occurrence of Oil and Gas. Gulf Coast Association Geological Society Transactions, v. 17, p. 102-126.

French, L.N., 1979, Hydrogeologic Aspects of Lignite Strip Mines near Fairfield, Texas. M.A. Thesis, University of Texas at Austin, 105 p.

Ghodrati, M. and W.A. Jury, 1990, A Field Study Using Dyes to Characterize Preferential Flow of Water. Soil Science Society of America Journal, vol. 54, p. 1558-1563.

Grube, W.E., R.M. Smith, and J.T. Ammons, 1982, Mineralogical Alterations that Affect Pedogenesis in Mine Soils from Bituminous Coal Overburdens. in Acid Sulfate Weathering. Soil Science Society of America, vol. 46 , p. 209-223.

Guebert, M.D. and T.W. Gardner, 1992, Soil Macropores: Control on Infiltration, Hillslope and Surface Hydrology on a Reclaimed Surface-Mined Watershed. GSA Annual Meeting, Abstracts and Programs, p. 69.

Guyton, W.F. and Associates, 1972, Groundwater Conditions in Anderson, Cherokee, Freestone, and Henderson Counties, Texas. Texas Water Development Board Report 150, 335 p.

Hall, W.D., D.R. Frick, G.J. Berger, A. Turner, and S.G. Brand, 1985, Big Brown: Geology and Ground Water. Hall Southwest Water Consultants, Inc., Unpublished.

Henry, C.D. and J.M. Basciano, 1979, Environmental Geology of the Wilcox Group Lignite Belt, East Texas. Bureau of Economic Geology, Report of Investigation, No. 98, University of Texas at Austin, 28 p.

Henry, C.D., J.M. Basciano, and T.W. Duex, 1980, Hydrology and Water Quality of the Eocene Wilcox Group: Significance for Lignite Development in East Texas. Bureau of Economic Geology, Geological Circular 80-3, University of Texas at Austin, 9 p.

Heuvelman, W.J., K.J. McInness, L.P. Wilding and C.T. Hallmark, 1993, Water and Solute Flow in a Highly-Structured Soil. Texas Water Resources Institute, Texas A&M University, Technical Report No. 161, 43 p.

Hewitt, Charles D., 1990, Hydraulic Properties of the Saturated Zone of a Reclaimed Lignite Surface Mine, East Texas. M.A. Thesis, University of Texas at Austin, 151 p.

Holzmer, Frederick J., 1992, Redevelopment of the Groundwater System at a Reclaimed Lignite Surface Mine, East Texas. M.A. Thesis, University of Texas at Austin, 193 p.

Horton, Robert E., 1940, An Approach Toward a Physical Interpretation of Infiltration Capacity. Soil Science Society of America Proceedings 5, p. 399-417.

Imeson, A.C., 1977, A Simple Field Portable Rainfall Simulator for Difficult Terrain. Earth Surface Processes, vol. 2, p. 431-436.

Jabro, J.D., E.G. Loste, K.E. Simmons and D.E. Baker, 1991, A Field Study of Macropore Flow Under Saturated Conditions Using a Bromide Tracer. Journal of Soil and Water Conservation, Sept.-Oct., p. 376-380.

Jarvis, N.J., P.B. Leeds-Harrison and J.M. Dosser, 1987, The Use of Tension Infiltrometers to Assess Routes and Rates of Infiltration in a Clay Soil. Journal of Soil Science, vol. 38, p. 633-640.

Jorgensen, D.W. and T.W. Gardner, 1987, Infiltration Capacity of Disturbed Soils: Temporal Change and Lithologic Control. Water Resources Bulletin, vol. 23, no. 6, p. 1161-1172.

Kaiser, W.R., W.B. Ayers, and L.W. LaBrie, 1980, Lignite Resources in Texas. University of Texas at Austin, Bureau of Economic Geology Report of Investigation, No. 104, 52 p.

Kaiser, W.R., 1974, Texas Lignite: Near-surface and Deep Basin. Bureau of Economic Geology, Report of Investigation, No. 79, University of Texas at Austin, 70 p.

Kaiser, W.R., J.E. Johnson, and W.N. Bach, 1978, Sand-Body Geometry and the Occurrence of Lignite in the Eocene of Texas. Bureau of Economic Geology, Geological Circular 78-4, University of Texas at Austin, 19 p.

Levy, B.S. and R.M. Chambers, 1987, Bromide as a Conservative Tracer for Soil-water Studies. Hydrological Processes, vol. 1, p. 385-389.

Lynch, F.L., 1994, Effects of Depositional Environment and Formation Water Chemistry on the Diagensis of Frio (Oligocene) Sandstones and Shales, Aransas, Nueces, and San Patricio Counties, Texas. Dissertation, University of Texas at Austin, 303 p.

McLaughlin, M.J., 1982, A review of the use of dyes as soil water tracers. Water S.A., vol. 8, no. 4, p. 196-201.

Munn, J.R. and G.L. Huntington, 1976, A Portable Rainfall Simulator for Erodibility and Infiltration Measurements of Rugged Terrain. Soil Science Society of America Journal, vol. 40, p. 622-624.

Munsell Soil Color Charts, 1973 edition, McBeth Division of the Kollpmorgen Corporation, Baltimore, Maryland.

Mutchler, C.K. and L.F. Hermsmeier, 1965, A Review of Rainfall Simulators. Transactions of the ASAE, vol. 8, p. 67-68.

Omoti, U. and A. Wild, 1979, Use of fluorescent dyes to mark the pathways of solute movement through soils under leaching conditions: 2 field experiments. Soil Science, vol. 128, no. 2, p. 98-104.

Peterson, A.E. and G.D. Bubenzer, 1986, Intake Rate: Sprinkler Infiltrometer. In Methods of Soil Analysis, Part 1. Physical and Mineralogical Methods - Agronomy Monograph No. 9, 2nd edition, p. 845-870.

Pollock, C.R., 1982, Ground-water Hydrogeology and Geochemistry of a Reclaimed Lignite Surface Mine. M.S. Thesis, Texas A&M University, 152 p.

Ritter, J.B. and T.W. Gardner, 1993, Hydrologic Evolution of Drainage Basins by Disturbed Surface Mining, Central Pennsylvania. Geological Society of America Bulletin, vol. 105, p. 101-115.

Schneider, W.J., 1977, Analysis of the Densification of Reclaimed Surface Mined Land. M.S. Thesis, Texas A&M University, 125 p.

Shiau, Ben and David A. Sabatini, 1992, Sorption of Rhodamine WT as Affected by Molecular Properties. in Tracer Hydrology, Hotzl and Werner (eds.), Balkema, Rotterdam, p. 57-64.

Simpson, T.W. and R.L. Cunningham, 1982, The occurrence of flow channels in soils. Journal of Environmental Quality, vol. 11, no. 1, p. 29-30.

Smith, Lonnie C., 1986, A Report on the Bucket Wheel Excavator/Cross-Pit Spreader System at Big Brown Mine, Texas. Texas Utilities Mining Company, 13 p.

Soil Moisture Equipment Company, 1986, Guelph Permeameter: Model 2800 KI Operating Instructions. Santa Barbara, California, 28 p.

Stephens, D.B., E. Hicks, and T. Stein, 1991, Field Analysis on the Role of Three-Dimensional Moisture Flow in Groundwater Recharge and Evapotranspiration. New Mexico Water Resources Research Institute, Technical Completion Report No. 260, 67 p.

Thomas, David and Ivan Jansen, 1985, Soil Development in Coal Mine Spoils. Journal of Soil and Water Conservation, Sept.-Oct., p. 439-442.

Thomas, G.W. and R.E. Phillips, 1979, Consequences of water movement in macropores. Journal of Environmental Quality, vol. 8, no. 2, p. 149-152.

Thomas, G.W. and R.E. Phillips, 1991, The Transient Instability of Tensiometer Readings During Infiltration. Soil Science, vol. 152, no. 3, p. 231-235.

Toth, J., 1962, A theory of groundwater motion in small drainage basins in Central Alberta, Canada. Journal of Geophysical Research, vol. 67, no. 11, p. 4375-4387.

Tucker, Maurice, 1982, The Field Description of Sedimentary Rocks. Geological Society of London Handbook, Open University Press, New York, 112 p.

Varela, C., C. Vazquez, M.V. Gonzalez-Sangregorio, M.C. Leiros, and F. Gil-Sotres, 1993, Chemical and Physical Properties of Opencast Lignite Minesoils. Soil Science, vol. 156, no. 3, p. 193-203.

Wang, H.F., and M.P. Anderson, 1982, Introduction to Groundwater Modeling, Finite Difference and Finite Element methods. W.H. Freeman and Co.. 237 p.

Wendt, C.W., O.C. Wilke, and L.L. New, 1978, Use of Methanol-water Solutions for Freeze Protection of Tensiometers. Agronomy Journal, vol. 70, p. 890-891.

White, Richard L., 1978, Land Reclamation in Texas-An Opportunity. In Kaiser, W.R. (editor), Proceedings Gulf Coast Lignite Conference: Geology, Utilization, and Environmental Aspects. Bureau of Economic Geology, Report of Investigation #90, University of Texas at Austin, p. 218-227.

Wu, L., J.B. Swan, J.L. Nieber, and R.R. Allmaras, 1993, Soil-macropore and layer influences on saturated hydraulic conductivity measured with borehole permeameters. Soil Science Society of America Journal, vol. 57, p. 917-923.

Yao, Li, 1994, Effects of Compaction on Reclamation of Surface Mined Lands in East Texas. Dissertation, Texas A&M University, 134 p.

This digitized document does not include the vita page from the original.